UNIVERSITY OF CALIFORNIA
RIVERSIDE

Engineering Smart Thermal Properties in Metal-Organic-Frameworks

A Dissertation submitted in partial satisfaction
of the requirements for the degree of

Doctor of Philosophy

in

Mechanical Engineering

by

Luping Han

March 2018

Dissertation Committee:

Prof. P. Alex Greaney, Chairperson
Prof. Chen Li
Prof. Bryan Wong

The Dissertation of Luping Han is approved:

Committee Chairperson

University of California, Riverside

Acknowledgments

First and foremost I want to thank my advisor Professor P. Alex Greaney. It has been an honor to be the first student in our Computational Materials Science (CMS) Group. His guidance helped me in all the time of research and writing of this thesis. I appreciate all his contributions of time, ideas, and funding completing my Ph.D.. He is always full of passion for our research which was motivational to me even during tough times in these years. I could not imagine having a better advisor and mentor for my Ph.D. pursuit.

The members of the CMS group have contributed a lot to my personal and Ph.D. pursuit at both Oregon State University and U.C. Riverside. I am grateful to the members of our research group: Laura de Sousa Oliveira and Agnieszka Truszkowska. The collaboration and friendships in our group are helpful to my Ph.D. study. Laura and I collaborated a project on "Thermal Conductivity Transition in the Breathing Metal-Organic Framework MIL-53", in which, Laura contributed immensely and helped me a lot. Agnieszka helped me immensely on reviewing my proposal and thesis. Other past and present group members that I have had the pleasure to work with are graduate students: Saranam Venkata Rajesh, Kritsa Chinadanon, CongCong Hu, ZhiChao Yu, Jude De Unic and a lot of summer session undergraduate students who have come through the group.

Last but not the least, I would like to thank my family: my parents for supporting me spiritually throughout writing this thesis and my my life in general.

ABSTRACT OF THE DISSERTATION

Engineering Smart Thermal Properties in Metal-Organic-Frameworks

by

Luping Han

Doctor of Philosophy, Graduate Program in Mechanical Engineering
University of California, Riverside, March 2018
Prof. P. Alex Greaney, Chairperson

Metal-organic-framework (MOFs) are the most porous materials known to humanity, and thus they attract intensive interest for their huge potential. Hydrogen storage is one of their most important applications. MOFs are promising materials for gas storage and absorption refrigerators–reducing the overall size of the absorption bed. Central to the performance of the MOF is its ability to withdraw heat from the absorbed working gas. The poor thermal conductivity of MOFs limits the refueling time of hydrogen storage because of the removal of latent heat shown in Fig. 0.1. Currently, to meet DoE's performance targets for H_2 storage, at least a fivefold increase in thermal conductivity is required. However, their thermal properties have received limited attention. We use molecular dynamics (MD) simulations to study MOFs' thermal transport properties and to identify how they can be exploited to create new materials with smart thermal properties. We "measure" the thermal conductivities of MOFs to test mechanisms for externally tuning the thermal conductivities, and determine if changes in thermal properties of MOFs could be used for chemical recognition. These were performed for the purpose of establishing design principles that

can be used in the development of new MOFs with tailored thermal conductivity.

The structure of metal-organic-frameworks (MOFs) is radically different from that of conventional fully-dense crystals and their vibrational behavior differs correspondingly. There are thousands of known MOFs that encompass a wide spectrum of topologies and symmetries. These structures open avenues for engineering materials with entirely new thermal properties. Advancing our theoretical understanding of thermal conduction in these materials, and with it our control over the transport of heat, has a huge potential to impact the way we use and think about heat. More than letting us use heat more efficiently, it will enable us to use heat differently. For example, creating materials in which the thermal conductivity can be externally tuned, and materials that use heat to carry chemical information for chemical recognition.

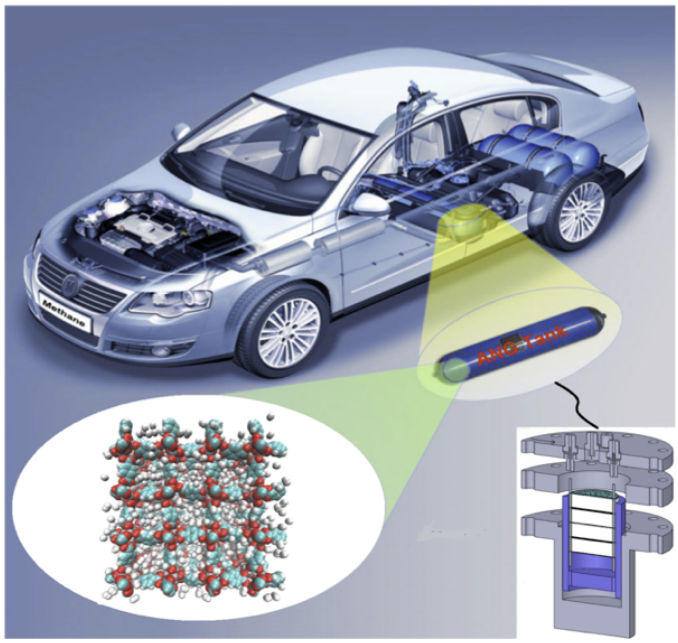

Figure 0.1: An illustration of MOF-5 that is used as adsorption bed in the hydrogen adsorption tank in hydrogen vehicles. The tank is under development at Oregon State University. [583, 132]

Contents

List of Figures

List of Tables

Chapter 1

Introduction

The goal of this research project is to obtain theoretical understanding of heat transport mechanisms in MOFs, and to identify how they can be exploited to create new materials with smart thermal properties. To accomplish the objectives, we apply computational methods to test mechanisms for externally tuning the thermal conductivity of MOFs, and determine if changes in thermal properties of MOFs could be used for chemical recognition.

This thesis mainly contains three parts: Introduction, Manuscripts and Conclusion. The manuscripts has four chapters that are my four journal papers [215, 217, 123, 218] (published or submitted), respectively.

In this chapter, I will introduce each chapter, respectively. Chapter 2 is the comprehensive background of MOFs and the method to compute thermal properties of MOFs. Chapter 3 interprets the relationship between the heat transfer and the structure of MOF-5. The three approaches to study the fundamental thermal transport mechanism of MOFs are

used (shown in Fig. 1.1): (a) computing the MOFs with systematically increasing linker length in Chapter 4, (b) computing MOFs with articulated network geometry in Chapter 5 and (c) computing MOFs filled with things (MOFs and gases) in Chapter **??**.

The objective is accomplished using a combination of theory and molecular dynamics simulation to identify competing transport processes, and systematically map their behavior to architectural features in MOFs.

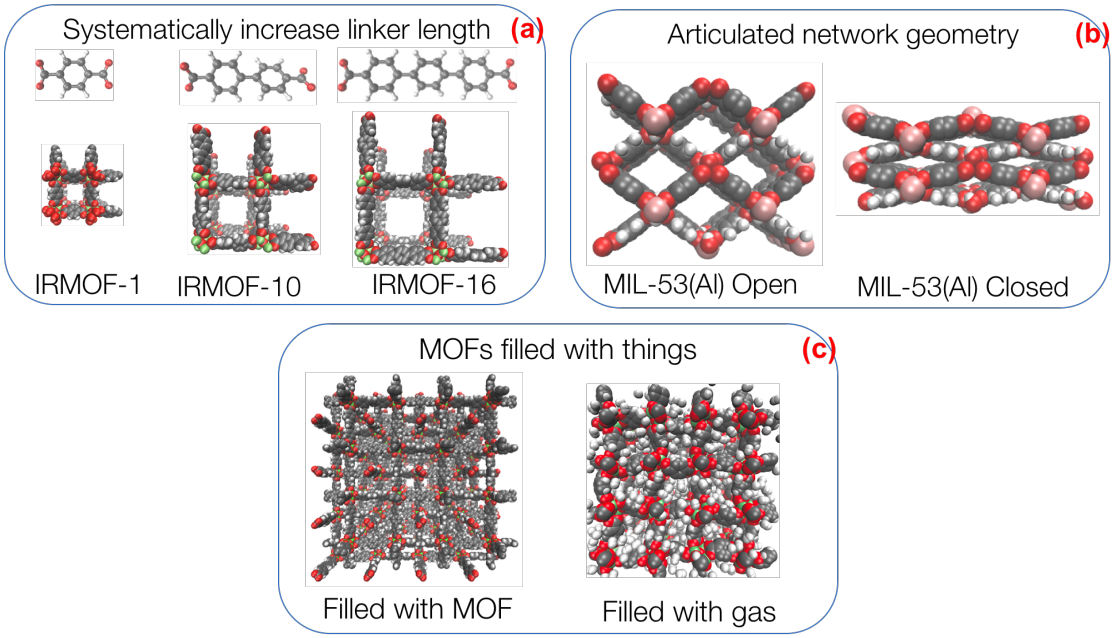

Figure 1.1: There are three approaches for understanding the heat transport in MOFs. Figure (a) shows the idea to compute the MOFs with systematically increasing linker length. Figure (b) shows the idea to compute MOFs with articulated network geometry. Figure (c) shows the idea to compute MOFs filled with things (MOFs and gases).

Chapter 2

Background

2.1 MOFs

The metal-organic frameworks (MOFs) are a type of porous polymeric material [262], comprising of metal-organic nodal units connected together by organic bridging linkers [247, 262]. MOFs are the most porous materials known to humanity and have a large surface to mass ratios [672]. Compared to other nanoporous crystals with inorganic host frameworks, MOFs have these advantages: three-dimensional hybrid frameworks [251], and highly designable frameworks such as pore shape and pore size [247, 262, 156, 465, 599, 549, 417]. Because of the wide choice of metal and ligand (organic linker), MOF family contains abundant members, which gives a wide range of structural, magnetic, electrical, optical, thermal and catalytic properties that may be embodied by such materials [262, 465, 599, 549, 417]. MOFs are currently attracting high fundamental and industrial interest because of their high adsorption surface area and large free cage volume [251, 516], which are the reasons of their high sorption capacities [262], shown in Table 2.1. However, the outstanding ar-

chitecture also gives a poor thermal conductivity that directly impacts the performance of the material in applications such as gas storage and gas separation. Although thermal transport properties of MOFs in these applications are both unusual and important, their thermal properties have received limited attention, and thus warrant detailed research.

In this thesis, our goal is to understand the heat transfer mechanisms in MOFs theoretically. In addition, understand how to use heat transfer mechanisms of MOFs to design and engineer new materials. Specifically, advance scientific and theoretical understanding of heat transport in gas laden MOFs to enable the advancement of materials for key energy applications. Apply computational methods to test mechanisms for externally tuning the thermal conductivity of MOFs, and determine if changes in thermal properties of MOFs could be used for chemical recognition. [200]

2.2 Thermal Properties of MOFs

Large number of MOFs have been identified including 1-, 2-, and 3-dimensional frameworks [668] due to the highly designable structure of MOFs, since Tomic stated MOFs in 1965, especially during the last decade. The self-assembled metal ions which act as nodal units connected by organic linker arms makes an open space-frame structure. Because of the highest porosity and the ultrahigh surface area, MOFs have many critical energy related applications, including gas storage [189, 532, 346] and gas separation [689, 360]. However, the network architecture also gives rise to unusual and exotic thermal properties [367, 370], properties that can be intimately tied to gas absorption. The various structures with different thermal properties can help us to learn theoretical thermal conduction in MOFs,

MOF-5	Conditions		Surface area/m^2 g^{-1}		H_2 storage		Ref.
(IRMOF-1)	P/bar	T/K	BET	Langmuir	Excess/wt%	Vol./gL^{-1}	
	1	20.4			10.96	71	[285]
	1	77	950	1250			[253]
	1	77		2900			[345]
	1	77	1450		4.5	27.99	[507]
	1	77			2.1	12.46	[336]
	1	77	1794		2.0	11.81	[138]
	1	77	3362		1.32	7.41	[509]
	1	77			1.32	7.41	[694]
	1	77	2885		1.15	6.31	[514]
	10	77			1.6	9.49	[456]
	30	77			4.3	25.5	[694]
	30	77		3080	4.3	25.5	[579]
	30	77		3080	4.3	25.5	[120]
	40	77	3800	4400	7.1	42.1	[285]
	45.4	77	3534	4171	4.95	30.8	[650]
	50	77	2296	3840	4.7	29.29	[457]
	100	77			10.0	66	[285]
	170	77			11.5	77	[285]
	60	200			0.9	4.67	[457]
	48	298			1.65	9.9	[454]
	60	298			0.45	1.78	[579]
	65	298			0.28	0.67	[457]
	67	298	572	1014	0.2	1.19	[456]
	100	298			0.57	2.55	[285]

Table 2.1: Surface area, hydrogen storage and nitrogen storage under different conditions for MOF-5 (IRMOF-1).

and further to control the transport of heat.

Understanding the mechanism of thermal transport in MOFs is technologically beneficial. Adsorption refrigeration [580] and hydrogen storage [663] are applications of gas adsorption properties of MOFs. Both of the applications are strongly thermal conductivity dependent. For hydrogen storage, the poor thermal conductivity of the MOF-5 (0.31 W/mK, similar to concrete) adsorption bed limits the rate at which latent heat can be removed, with the refueling time limited [686, 485]. DOE's performance targets for H_2 storage are: a capacity of 45 g/L, a refuelling time of 3 min, and an ability to operate within the temperature range -30 to 50 °C [83, 3]. To meet the targets, at least a fivefold

increase in thermal conductivity is required. To design new materials that mitigate the thermal transport bottleneck it is imperative to understand the limiting processes of heat transport.

Although MOFs are widely attracting intense scrutiny for their merit of gas storage and gas separation, their thermal properties are limited understood. However, detailed research is required, since the thermal transport properties of MOFs are both unusual and important. Heat transport in MOFs (with and without gases) is unusual because it straddles two domains: heat transport by crystal lattice modes (like in a crystalline solid); and heat transport between localized molecular modes by communication between localized oscillators as in the case of amorphous polymers. Kaviany et al. have performed an outstanding computational research of thermal transport in empty MOF-5, characterizing the transport mechanisms and determining that the molecular-mode and lattice-mode heat currents contribute roughly equally to the thermal conductivity [251]. Wilmer et al. have studied mechanisms of heat transfer with adsorbed gases in MOFs, which have reported that thermal conductivity of MOFs decreases as increased concentration of adsorbed gases [33]. Wilmer et al. have reported that the reason (for decreasing thermal conductivity with increasing concentration of adsorbed gases) is because of MOF–gases phonon scattering, however, MOF–MOF phonon scattering still dominates the thermal conductivity [33]. These works have been instrumental for identifying key heat transport processes in MOFs, but have not systematically addressed the dependence of these processes on the framework architecture. In this work we elucidate the role that MOFs' architecture plays in governing the interplay and dominance of molecular and lattice modes [215]. Rather than examine an

individual MOF or an idealized MOFs we examine trends in heat transport across a family of isoreticular MOFs (IRMOFs) examining processes of heat transport and analyzing the family's adherence or deviation form elementary heat transport models.

2.3 Molecular Dynamics

2.3.1 Introduction to Molecular Dynamics

With the rapid improvement of computer and software performance [95], computer simulations are widely used in science and engineering such as physics, astrophysics, chemistry, biology, economics and psychology etc. There are two main families of molecular computer simulation technique: molecular dynamics (MD) and Monte Carlo (MC) [428]. MD simulations combined with electron density-function theory (DFT) and discrete approaches such as cellular automata and the lattice-Boltzmann method, and MC simulations are based on quantum techniques involving path-integral and Monte Carlo methods [499, p.3]. The advantage of MD over MC is that MC can only be used to study systems in equilibrium and MD gives a route to properties of the dynamical system: transport coefficients, time-dependent responses to perturbations, rheological properties and spectra [428, 499, p.6].

In this thesis, MD simulations are mainly introduced. Molecular dynamics (MD) simulations have been widely used for computing the equilibrium and transport properties of a classical, many-body system that is modelled at the atomic or some coarse-grained level [12, 467, 125]. MD is a complement to usual experiments [428]. It helps to understand the properties of molecules in terms of their structure and the dynamical interactions between

them at microscopic level [12, 428].

There are two main families of MD: the classical MD simulation and the quantum or first-principles MD simulation [467]. The quantum MD simulations are precisely based on the quantum nature of the chemical bond and formulate to characterize the distribution of electrons and nuclei [303, 467]. Although classical MD simulations are widely used, there are a few molecular processes operations which are beyond the limits of the classical MD simulations, such as proton transfer and tunneling which can be simulated by quantum MD simulations [526]. The classical MD simulations are based on the approximation that motion of particle is defined by the laws of classical mechanics [12, 467, 37]. The molecules are treated as classical entities, i.e. ones that have position and momentum [629]. The classical MD simulations are widely used for studying the thermodynamic properties of liquids and solids [14], because classical MD simulations have an advantage that is the equations of motion can be solved simply, even for a large complicated system [37]. In this proposal, the classical MD will simply be referred to as MD.

Fig. 2.1 summarizes a typical MD approach. The force field and force calculations are the most important parts in MD, and we will discuss these parts in 2.3.2 and 2.3.3.

2.3.2 Force Field and Periodic Boundary Conditions

The atomic force field model is an empirical potential energy that describes a physical system of atoms kept together by interatomic forces [393, 500, 467]. Depending on the Lagrange equation of motion, assuming identical mass of particles, Newton's second

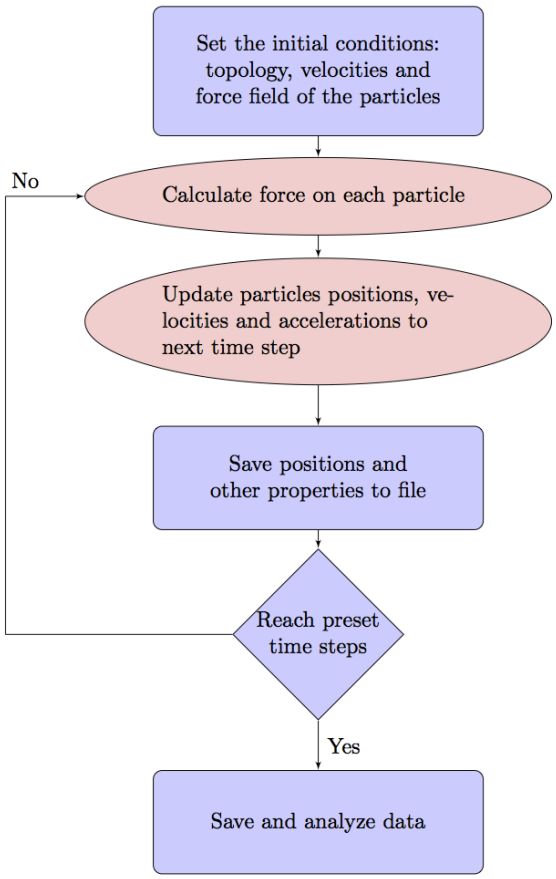

Figure 2.1: Schematic flowchart of a classical MD simulation.

law for a simple atomic system can be written as

$$m\ddot{q}_i = -\frac{\partial U}{\partial q_i} = f_i \tag{2.1}$$

where m is the identical mass of atoms, q_i is the component of the Cartesian coordinates for atom i, U is the potential energy of atom i and f_i is the corresponding force component [499]. Therefore, in order to calculate the atomic forces, we should specify the potential energy function $U(r^N)$. $U(r_1, ..., r_N)$ represents the potential energy of N interacting atoms in terms of their positions $r_i = (x_i, y_i, z_i)$ [467]. The potential energy U is constituted by

bonded interactions and nonbonded interactions that are depend on the specific bonds of the structure and the distance between the atoms respectively [393].

$$\begin{aligned} U &= U_{bonded} + U_{nonbonded}, \\ U_{bonded} &= U_{bond} + U_{bend} + U_{torsion} + U_{inversion}, \\ U_{nonbonded} &= U_{vdw} + U_{electrostatic}. \end{aligned} \tag{2.2}$$

The bonded interactions consist of bond stretch (U_{bond}, two-body), bond-angle bend (U_{bend}, three-body), dihedral angle torsion ($U_{torsion}$, four-body), and inversion terms ($U_{inversion}$, four-body). The nonbonded interactions consist of van der Waals (U_{vdw}) terms and electrostatic ($U_{electrostatic}$) terms. [393, 500] The simplest and typical force field used in MD takes the form shown in Eq. (2.3).

$$U(r_1, \cdots, r_N) = \sum_{bond} \frac{1}{2} k_{jk}(r_{jk} - r_0)^2 \tag{2.3a}$$

$$+ \sum_{bend} \frac{1}{2} k_{ijk}(\theta_{ijk} - \theta_0)^2 \tag{2.3b}$$

$$+ \sum_{torsion} k_{ijkl}(1 + cos(n\phi_{ijkl} - \phi_0)) \tag{2.3c}$$

$$+ \sum_{inversion} \frac{1}{2} k_{ijkl}(\xi_{ijkl} - \xi_0)^2 \tag{2.3d}$$

$$+ \sum_{vdw} 4\epsilon_{ij}[(\frac{\sigma_{ij}}{r_{ij}})^{12} - (\frac{\sigma_{ij}}{r_{ij}})^6] \tag{2.3e}$$

$$+ \sum_{electrostatic} \frac{q_i q_j}{4\pi\epsilon_0 r_{ij}} \tag{2.3f}$$

In Eq. (2.3a, 2.3b, 2.3c, 2.3d) (bonded interactions), summation indices represent all the bonds, angle bends, dihedral torsions and inversions. In Eq. (2.3a, 2.3b, 2.3c, 2.3d), k is the stiffness of different types of bonding interactions, r is the bond distance, θ is the value of the angle, ϕ_{ijkl} is the proper dihedral angle, ξ_{ijkl} is the improper dihedral angle, and the terms with a subscript of zero are the equilibrium values of the bonds, angles, dihedrals and impropers, respectively. The geometry of Eq. (2.3a, 2.3b, 2.3c) are illustrated in Fig. 2.2(a), and the geometry of Eq. (2.3d) is also shown in Fig. 2.2(b). Eq. (2.3e) describes the van der Waals repulsive and attractive forces between particles in the Lennard-Jones 12-6 potential [276], where σ is the diameter, and ϵ is the well depth. This is shown in Fig. 2.3. Eq. (2.3f) is the Coulomb electrostatic potential, where q_i, q_j are the charges in electron units and ϵ_0 is the dielectric constant.

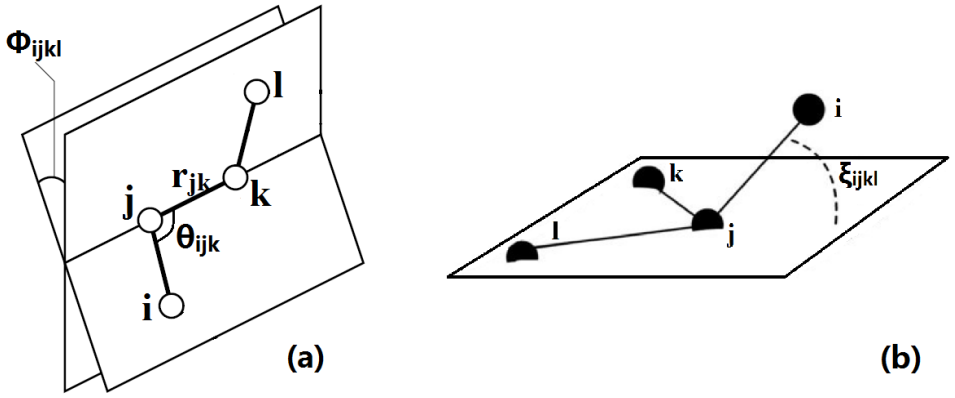

Figure 2.2: Geometry of a simple chain molecule, illustrating the definition of bonded interatomic interactions: (a) bond r_{jk}, angle θ_{ijk} and proper dihedral ϕ_{ijkl} (b) improper dihedral ξ_{ijkl}. [428]

Since the models of MD simulation are generally very small compared to the experimental substance, a suitable boundary conditions are important to a MD simulation

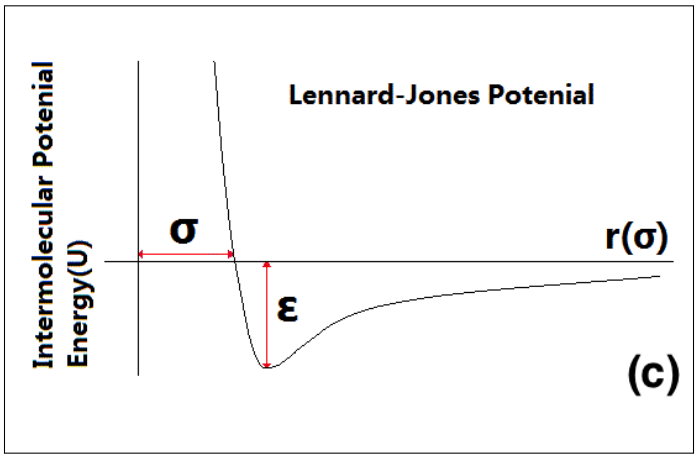

Figure 2.3: The standard non-bonded 12/6 Lennard-Jones style van der Waals interaction. [276]

[73]. Periodic boundary conditions (PBC) aim to replicate the primary cell (simulation volume or simulation cell) into an infinite, periodic array of replicas or images [73, 14]. The particles in the image cells move in exactly same way as the particles in primary cell [14]. If a particle leaves the primary cell, its images will enter the cell though the opposite face synchronously, because there are no walls at the boundary [14].

2.3.3 Integration of Trajectories

After computing all the forces between the particles, we can utilize the algorithm to integrate Newton's equations of motion [125, p.69]. The commonly used algorithms are the Verlet algorithm and the Gear predictor-corrector [14]. The Verlet algorithm contains three different algorithms: basic Verlet, leap-frog scheme and velocity Verlet [14]. The objective of the numerical integration of Newton's equation of motion is to find an expression that computes positions $r_i(t+\Delta t)$ as a function of the known positions $r_i(t)$ [467]. Derived from the Taylor expansion of the coordinates of a particle, the equation of the Verlet algorithm

[125] is:

$$r_i(t + \Delta t) \approx 2r_i(t) - r_i(t - \Delta t) + \frac{F_i(t)}{m_i}\Delta t^2 \tag{2.4}$$

where r_i is the postion of atom i at a certain time, F_i is the force acting on atom i, m_i is the mass of atom i and Δt is the time step. From Eq. (2.4), we know that the velocity is not used to compute the new position [125]. However, the velocities are important because kinetic energy and temperature are derived from velocities [125]. Therefore, we have to find a way to define the velocities. It can be derived from trajectories by using:

$$v_i(t) = \frac{r_i(t + \Delta t) - r_i(t - \Delta t)}{2\Delta t} + \varrho(\Delta t^2) \tag{2.5}$$

where $\varrho(\Delta t^2)$ is an error that is of the order Δt^2 in the velocity $v_i(t)$ [125].

The time step (Δt) is important to the integration algorithms. A big time step will make the motion of a molecule unstable because of the error in the integration, which may cause a deformation of molecules. Reversely, a small time step is not efficient for simulation [102].

2.3.4 Thermodynamic Ensembles

In this section, we briefly discuss different ensembles of molecular dynamics which are generally used. MD simulations can be used to compute macroscopic thermodynamic properties of a system. The identical macroscopic thermodynamic state have different microscopic states. An ensemble is the collection of all virtual copies of a system which has different microscopic states [150]. Since the thermal fluctuations are small, the utilization of ensembles at the macroscopic thermodynamic level for microscopic systems are convenient

[499]. There are three mainly used ensembles, and the number of particles are all conserved.

1. Microcanonical Ensemble (NVE): The NVE ensemble is defined by a fixed number of particles N, a fixed system volume V and a fixed total energy E. It is used to analyze an isolated thermodynamic system which has reached thermal equilibrium [150]. The advantage of this ensemble is that it allows to compute average of thermodynamic properties.

2. Canonical Ensemble (NVT): The NVT ensemble is characterized by a fixed number of particles N, a fixed system volume V and a fixed temperature T. It is used to analyze a Boltzmann's distribution of microscopic states of the system [74]. The Helmholtz free energy $A(N, V, T)$ of NVT ensemble can be derived from the entropy $S(N, V, E)$ of NVE ensemble by Legendre tranform [74].

3. Isobaric-Isothermal Ensemble (NPT): The NPT ensemble analyzes systems attached with a thermostat at temperature T and a bariostat at pressure P [74]. The system exchanges energy with the thermostat and exchanges volume with the bariostat [74].

2.4 Computing Thermal Conductivity κ

Heat travels by three mainly methods: radiation, conduction and convection. Fig. 2.4 shows the general idea of these three methods. Radiation is the electromagnetic waves, which can not be accurately investigated by MD simulations. However, MD is an effective tool to investigate conduction and convection. Conduction is the elastic impact of lattice (phonons) and convection is the movement of molecules from one part of fluid

to another. In conduction, both electrons and lattice vibrations can act as heat carriers. For heat transfer in non-metals, only phonons should be considered because there is no free electrons [498].

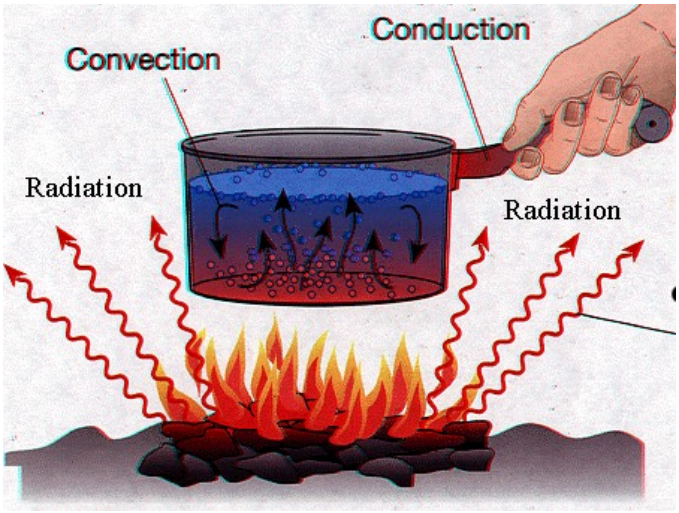

Figure 2.4: Discribe the three mainly methods of heat transfer. [330]

There are two common approaches to compute thermal conductivity by MD simulations: equilibrium MD (EMD) and nonequilibrium MD (NEMD) [535, 626, 329, 524, 400]. The common methods used for EMD and NEMD are the Green-Kubo method and the "direct method", respectively. The Green-Kubo method predicts the thermal conductivity in equilibrium by the fluctuation-dissipation theorem [211, 313]. In comparison, the direct method is based on a temperature gradient across the simulation box [524]. The direct method has two main disadvantages: (1) it is intricate to determine the reference temperature, (2) temperature gradients errors appear in the neighbor of the interfaces, because the boundary conditions influence the phonon distribution [626]. By contrast, the Green-Kubo method provides extra analytical data (e.g., the heat current autocorrelation function) [329].

Therefore, in most of the planned computer experiments we utilize the Green-Kubo method, equilibrium MD, to predict the thermal conductivity of Metal-Organic Frameworks and use the "direct method" as a secondary comparison.

2.4.1 Equilibrium Molecular Dynamics

The Green-Kubo method [211, 313] represents an Equilibrium Molecular Dynamics technique to investigate complex susceptibility of magnetic or electric polarization and complex conductivity in terms of integrals of time correlation functions. The thermal properties of abundant dielectric materials have been investigated by the Green-Kubo method. Since MOFs are dielectric materials, mostly we use the Green-Kubo method to predict thermal conductivity. The Green-Kubo method predicts the thermal conductivity in equilibrium by the fluctuation-dissipation theorem. The system is in the linear-response relation, because there is no imposed driving force in equilibrium. The thermal conductivity κ is proportional to the integral of the autocorrelation function (ACF) of fluctuations in the instantaneous heat flux:

$$\kappa = \frac{1}{V k_B T^2} \int_0^\infty \langle J(t) \cdot J(t+\tau) \rangle \, d\tau, \tag{2.6}$$

where V is the system volume, k_B is the Boltzmann constant, T is the system temperature , J is the heat current and $\langle J(t) \cdot J(t+\tau) \rangle$ is the heat current autocorrelation function. The common definition of the heat current J is

$$J(t) = \sum_i \mathbf{v}_i \varepsilon_i + \frac{1}{2} \sum_{ij \;\; i \neq j} \mathbf{r}_{ij} (\mathbf{F}_{ij} \cdot \mathbf{v}_i), \tag{2.7}$$

where $\mathbf{v}_i$, ε_i, $\mathbf{r}_{ij}$ and $\mathbf{F}_{ij}$ are the velocity, energy of atom i, the instantaneous interacting separation vectors, and the force between atom i and its neighbor j, respectively [405].

Note that the Green-Kubo method can be linked to "measuring" the thermal conductivity from a computer simulation, rather than a mechanism based prediction of κ as one obtains using Boltzmann transport theory. The thermal conductivity is predicted from the different modes of phonons in lattice dynamics by Boltzmann transport equation. This method is not useful for new model because of a lack of understanding of multiphonon interactions [400].

Khodadadi et al. [32] has done a great job to proof that the micro-convection has a minor role in some circumstances in Green-Kubo method. They considered that some high thermal conductivities that were computed by Green-Kubo method (EMD) were wrong. The critical technical reason was the subtraction of the average enthalpy of each atom type from the convective term in the heat flux J in Equ. 2.7, which should be re-written as

$$J = \sum_i \mathbf{v}_i \varepsilon_i + \frac{1}{2} \sum_{ij \;\; i \neq j} \mathbf{r}_{ij} (\mathbf{F}_{ij} \cdot \mathbf{v}_i) - \frac{1}{\mathbf{V}} \sum_\alpha \bar{\mathbf{v}}_\alpha \bar{\mathbf{h}}_\alpha, \tag{2.8}$$

where the last subtracted term is the partial micro-convection enthalpy term. In Equ. 2.8, α is each type of atom in the system, $\bar{\mathbf{v}}_\alpha$ denotes the average velocity of atom type α and $\bar{\mathbf{h}}_\alpha$ denotes the average partial enthalpy of atom type α which can be written as:

$$\bar{\mathbf{h}}_\alpha = \frac{\sum_{i=1}^{N_\alpha} [K_i + P_i + \frac{1}{3}(\mathbf{m}_i \mathbf{v}_i + \frac{1}{2} \sum_{j=1}^{N} \mathbf{r}_{ij} \cdot \mathbf{F}_{ij})]}{N_\alpha} \tag{2.9}$$

where K_i and P_i are the time-averaged kinetic and potential energies of particles of atom

type α, respectively. In Equ. 2.8, 2.9, $\mathbf{V}$, N and N_α are system volume, total number of atoms and total number of atom types, respectively.

We have computed the heat current by Equ. 2.8 for each simulation to compare with the one computed by Equ. 2.7. Results showed that the partial micro-convection enthalpy terms in Equ. 2.8 were relatively small that can be neglected. Fig. shows an example whose....

2.4.2 Non-Equilibrium Molecular Dynamics

Non-equilibrium molecular dynamics is the most intuitive computational method for predicting thermal conductivity. The κ is the ratio of heat flux to the temperature gradient, where the heat flux is defined as the energy transferred in unit time perpendicularly across a surface. One of common non-equilibrium molecular dynamics methods is Muller-Plathe algorithm [muller1997]. Muller-Plathe algorithm has the following advantages: 1, suitable for periodic boundary conditions, 2, accurate κ with small temperature gradient, 3, no thermostat problem and suitable for chosen ensemble, 4, converges quickly.

Fig. 2.5 A shows the schematic periodic simulation box divided by N slabs along the z direction, where slab 1 is the cool slab and slab N/2+1 is the hot slab. The velocities of the hottest atom in slab 1 and the coolest atom in slab N/2+1 are exchanged. Relative to center of mass motion of the two atoms will be exchanged, if the masses are not same plimpton1995. This mechanism provides an energy transfer from the cool slab to the hot slab. A temperature difference is generated between the cool and the hot slab. After

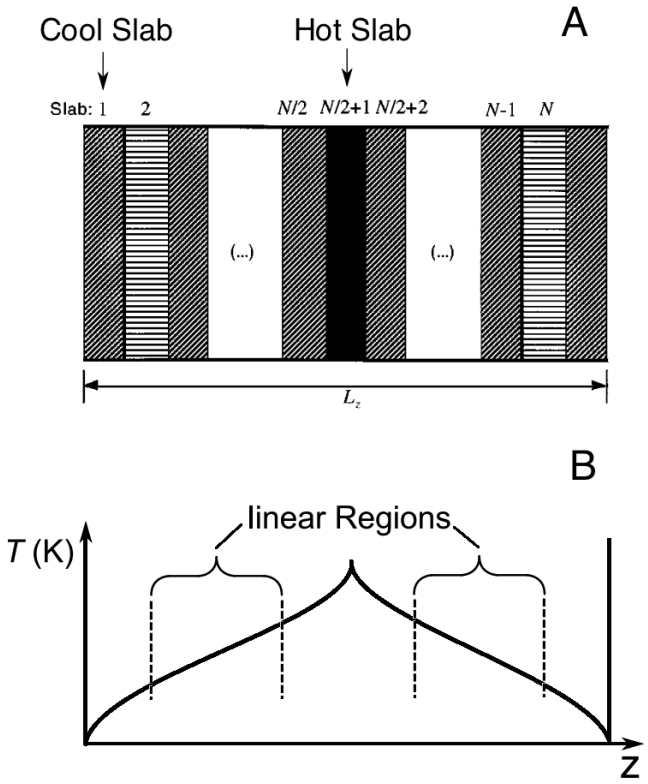

Figure 2.5: (A) Dividing the periodic simulation cell into N slabs. Slab N/2+1 is the middle slab. Slab 1 is the cool slab, slab N/2+1 is the hot slab. This should be a symmetric temperature profile since the cool slab and hot slab are separated by the same distance in both directions in a periodic boundary conditions. By exchanging the velocities of the hottest atom in slab 1 and the coolest atom in slab N/2+1, kinetic energy transfers from the cool to the hot slab in two directions. (B) The temperature profile is computed by determining the temperatures in the intervening slabs ($2 \sim N/2$ and $N/2+2 \sim N$). The energy of heat flux divided by the slope of the temperature profile is proportional to the thermal conductivity based on Eq. (2.10).

reaching steady state, the temperature gradient shows up. The thermal conductivity is

$$\kappa = \frac{\sum\limits_{exchange} \frac{m}{2}(v_h^2 - v_c^2)}{2tL_xL_y\left\langle \frac{\partial T}{\partial z} \right\rangle} \tag{2.10}$$

where m is the mass of the atoms, v_h and v_c are the velocities of hottest and coolest atoms, L_xL_y is the area through heat transport. The equation is summing all of the

velocities exchanging events during the simulation time t. The heat flux is moving in two directions because of the periodic boundary conditions.

Chapter 3

Relationship between thermal conductivity and framework architecture in MOF-5

Metal-organic-framework materials (MOFs) are the most porous materials known to humanity and thus are promising materials for gas storage and absorption refrigerators—reducing the overall size of the absorption bed. Central to the performance of the MOF is its ability to withdraw heat from the absorbed working gas. Here we use a suite of molecular dynamics simulations to relate structural features of the MOF-5 framework to its thermal transport properties. These were performed for the purpose of establishing design principles that can be used in the development of new MOFs with tailored thermal conductivity. The last part of the paper examines thermal transport in MOF-5 when loaded with hydrogen and deuterium which increases thermal conductivity.

3.1 Introduction

Metal-organic frameworks (MOFs) are the most porous materials known to humanity, comprised of organic linker molecules assembled into an open network structure through metallo-organic connections to nodal junctions. [377] Although metal-organic frameworks are currently attracting intense scrutiny for their exciting potential for gas storage and gas separation, their thermal properties have received limited attention. However, the thermal transport properties of MOFs are both unusual and important, and thus warrant detailed research. Since gas storage and separation processes involve exothermic and endothermic operations [687] the ability to transport heat into or out of the adsorption media can be the limiting factor in the performance of MOFs used in these applications. One beneficial application of MOFs is as the adsorption bed in adsorption chillers. [581] These are cooling systems that are driven by a heat source and use a cycle of evaporation and condensation to pump heat. The use of MOFs as the adsorption bed provides a huge reduction in size that makes chillers practicable for vehicular use when they can be powered by waste engine heat. The motivation for our research on heat transport is a second important application of MOFs—hydrogen storage in MOF-5.

Hydrogen storage devices using powder compacts of MOF-5 crystals as the adsorption bed are under development as part of the US Department of Energy's (DoE) Hydrogen Fuel Cell Program. These tanks are liquid nitrogen cooled and pressurized to 100 bar, and under these conditions can store 7% excess wt% of H which amounts to 215 H_2 dimers per unit cell of the MOF, or an average of 26.9 dimers per framework cage.[687] This yields comparable storage density to liquefied H_2, but at a more practicable temperature. The

limitations for these devices is not capacity but the refueling time. MOF-5 has poor thermal conductivity (0.31 W/m.K [252], similar to concrete) and this impedes the removal of latent heat of adsorption. [687, 486] Currently, to meet DoE's performance targets for H_2 storage, at least a fivefold increase in thermal conductivity is required. [82, 4]

Heat transport in MOF-5 is unusual. Heat is carried by both transfer between localized molecular modes (like in an amorphous polymer) and by propagating lattice-modes (like in a crystalline solid). Kaviany and co-workers have performed an excellent computational study of thermal transport in MOF-5, characterizing the transport mechanisms and determining that the molecular-mode and lattice-mode heat currents contribute roughly equally to the thermal conductivity.[248]

In this research, our goal is to establish design principles that will guide the development of new gas storage MOFs with improved thermal conductivity. Thus, we extend the work of Kaviany *et al.* to examine strategies for changing the MOF architecture. To design MOFs that mitigate the thermal transport bottleneck it is imperative to understand the relationship between the structure of the framework and *both* of the heat transport mechanisms. In this manuscript we report the results of a systematic molecular dynamics study on the sensitivity of thermal conductivity to variations in the MOF architecture. We also present a new approach to obtaining mechanistic information by spatially decomposing the heat current. The remainder of the article is organized as follows: After a brief description of the simulation methods and philosophy, we present and discuss the simulation results for empty MOFs. We then discuss simulations of MOF-5 filled with H_2. The article finishes with a summary and conclusions.

3.2 Method

Thermal conductivity, κ, of MOFs was computed from equilibrium classical molecular dynamics (MD) simulations in the microcanonical ensemble using the Green-Kubo method.[210, 314] This is a well established method based on the fluctuation dissipation theorem that relates the thermal conductivity to the integral of the autocorrelation function (ACF) of the instantaneous heat flux.

$$\kappa = \frac{V}{3k_B T^2} \int_0^\infty d\tau \left\langle \boldsymbol{J}(t) \cdot \boldsymbol{J}(t+\tau) \right\rangle , \tag{3.1}$$

This can be likened to "measuring" the thermal conductivity from a computer simulation, rather than a mechanism based prediction of κ as one obtains using Boltzmann transport theory. Our approach is to use simulations as a computer experiment, in which we vary various aspects of the MOFs and determine the impact on κ. In these experiments we decompose the heat current $\boldsymbol{J}$ into different local contributions,

$$\boldsymbol{J} = \sum_i \boldsymbol{J}_i \tag{3.2}$$

where $\boldsymbol{J}_i$ is the instantaneous heat current in region i. The contributions of the regional autocorrelations and the inter-regional cross-correlation to κ,

$$\left\langle \boldsymbol{J}(t) \cdot \boldsymbol{J}(t+\tau) \right\rangle = \sum_{ij} \left\langle \boldsymbol{J_i}(t) \cdot \boldsymbol{J_j}(t+\tau) \right\rangle , \tag{3.3}$$

are used to infer mechanistic changes to the heat transport processes. We have recently successfully used a similar spatial decomposition of $\boldsymbol{J}$ to map heat transport around defects in graphite. [5]

All simulations are performed on a $2 \times 2 \times 2$ super cells with periodic boundary conditions. (A single unit cell of the frameworks and their components is shown in Fig.3.1.) For the empty MOF-5 calculations this is a cubic compute cell with ~ 52 Å edges containing

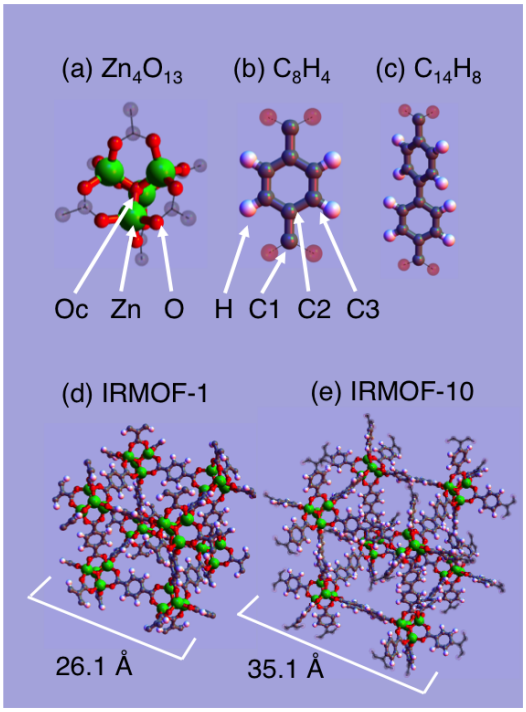

Figure 3.1: (a-c) shows the components of the IRMOF-1 (also called MOF-5) and IRMOF-10 frameworks. (a) shows the Zn_4O_{13} nodal units, (b) the C_8H_4 (1,4 phenyl dicarboxylate) linkers in IRMOR-1, and (c) the $C_{14}H_8$ (4,4 biphenyl dicarboxylate) linkers in IRMOF-10. (d & e) show a single unit cell of each framework. Note that along each direction the orientation of the nodes alternates and so there are 8 nodes per unit cell. This alternating structure means there are two types of interstitial cage.

3392 atoms. The previous work by Kaviany *et al.* has shown that a $2 \times 2 \times 2$ super cell is sufficiently large to obtain converged predictions for κ, and in this research we have

independently corroborated this. For their study of MOF-5, Kaviany *et al.* developed a set of empirical interatomic potentials for modeling the Zn, O, and C atoms in the framework (H they included indirectly by increasing the mass of the carbon with attached H atoms). We have tested these potentials against the Hessian matrix for MOF-5 computed from first principles. (The Hessian was computed using the SIESTA density functional theory package [566] with a DZP or better basis using the PBE generalized gradient exchange correlation energy functional.[462] Calculations were performed with a 700 Rydberg energy cutoff and the structure relaxed to minimize forces to a tolerance of 0.01 eV/Å^2.)

To correctly simulate the MOF interacting with gases intercalated into the framework we must model the H in the framework explicitly. Thus, we have augmented Kaviany's potentials with a set of bonding, angular, and dihedral terms for the H. These are listed in the table 3.1. Additionally, Kaviany's potential set does not include a C-C-O angular interaction at the end of the linkers. This means the framework has no resistance to in-plane bending of the linkers at the node-linker bridge, making the framework overly soft in shear along the (110) directions. We have included a C-C-O angular term. For most of the simulations we have kept this turned off in order to compare our work with that of Kaviany *et al.*. However, we have also computed κ with the extra angular stiffness turned on—the results are described in the next section. The non-bonded potentials for H were those used in the code Autodock and the added bonding terms were chden to match the full hessian matrix of MOF-5 that was computed from first principles.

All simulations were performed at 300 K. The simulation procedure was as follows: The empty MOF structure was optimized at 0 K. The $2 \times 2 \times 2$ supercell was created and

simulated in the NPT ensemble under zero pressure with the cell free to change volume but not shape. The temperature was ramped slowly to 400 K. From this simulation a fit was performed to obtain the thermal expansion coefficient for the potentials used (which is negative [371, 368]). For each simulation the $2 \times 2 \times 2$ super cell was scaled to its mean volume at 300 K and then heated to 300 K in the NVT ensemble, before being allowed to equilibrate by simulation for 100 ps in the NVE ensemble. After equilibration, NVE simulation was continued for a further 500 ps during which the heat flux was computed and its autocorrelation function averaged. The auto correlation was computed out to 10 ps or longer, and at least 40 simulations with different starting configurations were averaged to obtain each datum.

In simulations with gas atoms in the framework, the gas molecules were placed randomly in the framework interstices with random orientation (any randomly chosen positions that would have placed atoms too close together were rejected). The gas loaded framework was optimized and annealed prior to the NVT heating step to 300 K described above. Note that when we added the gas we did not alter the volume of the framework. At 300 K the gas condenses onto the framework and is not mobile across the voids within the framework. As a result, the gas put the framework under small *tensile* pressure as the gas acts to slightly contract the framework. Simulations were performed using the LAMMPS molecular dynamics simulation package [473]. Trajectories were integrated using the velocity verlet method with a time step of 0.2 fs, which was sufficient to minimize total energy fluctuations during NVE simulation to less than 10^{-5} of the thermal energy.

3.3 Dependence of κ on Framework Architecture

To a establish a set of design principles that can be used in the development of new gas storage MOFs with improved thermal transport properties we must understand how aspects of the framework structure impact heat transport by both molecular modes and by lattice modes. We consider four separate factors: The acoustic mismatch between the nodes and linker arms; the stiffness of the framework in shear; the effect of putting the system in tension; and the effect of the linker arm length.

3.3.1 Node-Linker Acoustic Mismatch

Heat transport by molecular modes is passed between localized molecular vibrations. To move through the MOF the heat must be passed from modes in the linkers to modes in the nodes. The node is much heavier than the linker. The nodes and linkers are acoustically mismatched creating a bottleneck for the molecular-mode heat transport. We have tuned the acoustic mismatch by scaling the mass of atoms in either the nodes (Zn, O and Oc) or the linkers (C1, C2, C3 and H). The thermal conductivity with mass scaling is shown in Fig.3.2. Sweeping the mass of the nodal atoms through a four-fold scaling from half to twice their normal mass increases the acoustic mismatch between the linkers and nodes and produces nearly a two-fold reduction in thermal conductivity (discernable even though the error bars are large). Reducing the mass of the node atoms reduces the frequency of the nodes' internal molecular modes, and so reduces the acoustic mismatch with the linker. Increasing the mass of the linker atoms should also reduce the acoustic mismatch; however, as is shown in Fig.3.2 this results in very little change in κ discernable

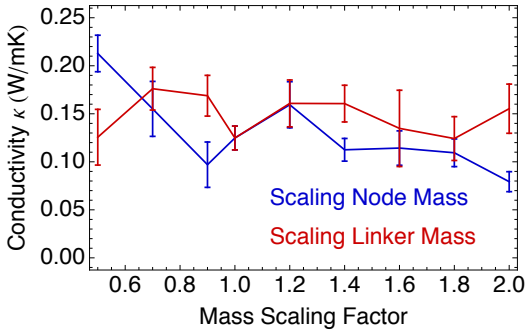

Figure 3.2: Thermal conductivity of MOF-5 as a function of scaling the mass of selected components of the lattice. The blue plot shows scaling the mass of nodes (atoms Oc, Zn, & O). The red plot shows scaling the mass of the linker atoms (C1, C2, C3, & H).

above the noise in the error bars.

It is clear from the mass scaling calculations that node-linker acoustic mismatch is only one factor affecting heat transport. We have computed the eigenvalues of the mass weighted Hessian matrix as a function of scaling the node or linker masses. It was found that as the nodes are much heavier than the linkers the mass of the node atoms have a strong influence on the lattice mode dispersion. Increasing the node mass affects both the molecular-mode and lattice mode heat current adversely. Increasing the linker mass improves molecular mode thermal conductivity but degrades the lattice mode thermal conductivity, and although κ changes little the spectral make up of the heat current ACF is different as can be seen in Fig.3.3. It can be seen in Fig. 3.3.(c) that changing the mass of the node or linker atoms has a large impact on the high frequency component of the heat current, however the high frequency fluctuations carry little heat. The relative importance of lattice and molecular modes is determined by fitting an approximate form of the ACF,

C_f, in fourrier space with the sum of decaying oscillatory processes:

$$C_f(t) = \sum_i A_i \cos(2\pi\nu_i t)\, e^{-t/\tau_i},$$

with amplitudes A, frequencies ν, and decay times τ as fitting parameters. In this approximation each process contributes

$$\kappa_i = \frac{V}{3k_B T^2} \frac{A_i \tau_i}{1 + (2\pi\nu_i\tau_i)^2}$$

to the total thermal conductivity. As heat current fluctuation processes are all underdamped, increasing the lifetime — that is, sharpening the peak in the power spectrum — reduces the contribution to thermal conductivity.

3.3.2 Framework Shear Stiffness

Simulations were performed to measure κ of MOF-5 with and without the angular O-C1-C2 interaction at the node-linker bridge. The angular interaction stiffens the shear modulus of the framework, but surprisingly does little to change κ. While net κ is altered, the angular interaction changes the nature of the thermal fluctuations—resulting in different spectral make-up and slower convergence of the heat current ACF shown in Figs.3.3.(a–c). The angular interaction also makes a small, but statistically significant, change to the cross-correlation of the linker and node heat flux. As can be seen in Fig.3.5, turning on this extra angular stiffness makes the node-linker cross-correlation have a positive rather than negative impact on the thermal conductivity.

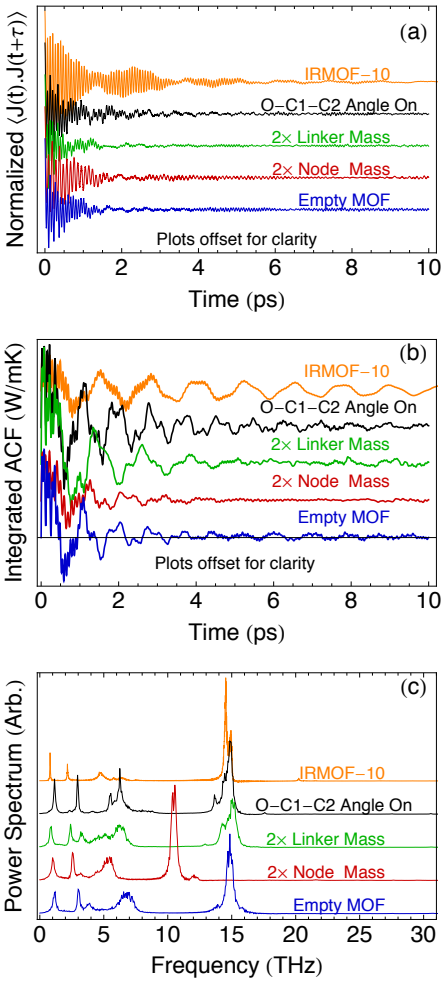

Figure 3.3: Plot (a) shows the averaged heat flux ACF for different MOFs. Plot (b) shows the integration of the ACF as a function of the integration duration. Plot (c) shows the power spectrum of heat current. In all plots (a–c) the curves are normalized and offset for clarity. The blue, red, green, black and orange traces are for: empty MOF-5, MOF-5 with heavy nodes; MOF-5 with heavy linkers; MOF-5 with the O-C1-C2 angular interaction turned on; and for IRMOF-10.

3.3.3 Effect of Strain on κ

We have measured (*in silico*) the effect of homogeneous strain on the thermal transport. Strains can arise from many sources; MOF-5 thermally contracts, and gas storage applications put MOFs under pressure—the working pressure for the MOF-5 based H_2

storage device is 100 bar. Moreover, we have found that MOF-5 contracts with the uptake of gas. The gas molecules bind to the framework preferentially at the "oxter"[1] where the linkers come together at a node and the gas molecules can interact with several linkers simultaneously. This interaction pinches the junctions causing contraction of the framework. Thermal contraction is due to activation of soft buckling modes in the linker arms [371, 368], and thus one might anticipate that—like tuning a guitar string—putting the linkers in tension would increase the lattice-mode thermal conductivity. In this reasoning the effect of strain would be asymmetric due to linker buckling under compression. Surprisingly, we observe only small systematic change in κ due to strain with tension reducing the ease of heat transport, as shown in Fig.3.4.

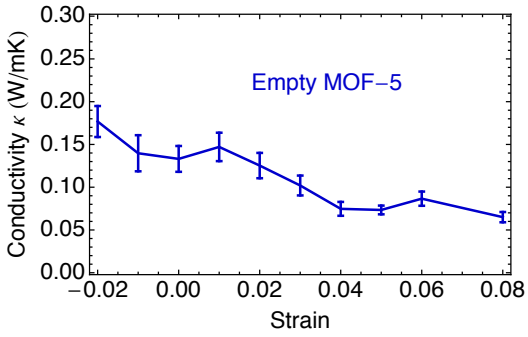

Figure 3.4: κ of MOF-5 computed as a function of strain.

3.3.4 Expanding Linker Arm Length

The topology of the framework proscribes that heat transported by molecular-modes must flow through the thermally resistive bridge between nodes and linkers. We exploit this to probe the interplay of molecular-mode and lattice-mode heat transport. If

[1] an old Scottish word for armpit

the resistance to molecular-mode heat transport is dominated by linker-node acoustic mismatch, then extending the length of linkers will increase the molecular-mode conductivity along a chain of links by reducing the number of resistive interfaces along each linker direction. However, increasing the linker length also reduces the areal density of linkers cutting through any cross-section of the framework. The density of heat conducting channels goes down faster than their thermal conductivity rises, and so one obtains a net reduction in the molecular mode thermal conductivity κ_M that scales with the framework's lattice parameter, a, as $\kappa_M \sim a^{-1}$. The beautiful modular chemistry of MOFs permits us to change a by inserting longer linker arms while maintaining the topology, symmetry, and nodal chemistry. We have simulated IRMOF-10 (isoreticular-MOF) in which phenyl groups are substituted with biphenyl. [144] (MOF-5 is the first in IRMOF series and is also called IRMOF-1. [145]) Simulating IRMOF-10 requires three new dihedral terms which are included in table 3.1.

The heat flux ACF and the resulting thermal conductivity value for IRMOF-10 are shown in Figs.3.2&3.5. The heat current ACF and its integral contains long slow oscillations that are slow to die out. To obtain converged results it was necessary to compute the ACF for IRMOF-10 out to 50 ps. The thermal conductivity of IRMOF-10 was less than one quarter of that of MOF-5. The lattice parameter of MOF-5 is only 0.75 times smaller than that of IRMOF-10, and so the reduction in κ can not be explained by the density of node-linker thermal bottlenecks alone (although it is possible that the phenyl-to-phenyl link at the center of the biphenyl linkers also introduces a thermal bottleneck for molecular modes). The longer lived fluctuations have a slower decay rate (as indicated by the sharper peaks in fig.3.3(c)), and as these are in the under damped limit increasing the fluctuation

lifetime reduces the contribution to heat transport (Eq.3.4).

3.3.5 Decomposition of $\boldsymbol{J}$

We analyse equilibrium MD simulations by decomposing the heat current, $\boldsymbol{J} = \boldsymbol{J}_N + \boldsymbol{J}_L$, into contributions from the nodes, $\boldsymbol{J}_N$, and contributions from the linkers, $\boldsymbol{J}_L$, and integrating the correlation functions (see Fig.3.5). A number of interesting observations

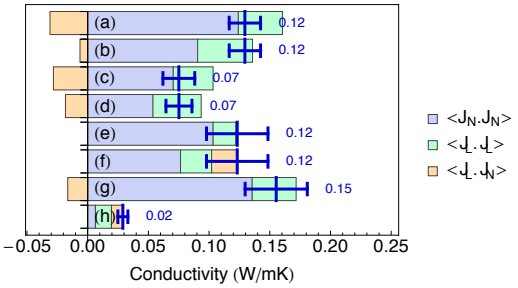

Figure 3.5: Bar chart of the thermal conductivity of frameworks, including the contributions from the autocorrelation of the heat current in nodes and linkers, and the node-linker heat current cross-correlation. (a & b) are for empty MOF-5, (c & d) are for MOF-5 with the mass of the Oc, Zn and O atoms doubled, and (e & f) are for MOF-5 with the O-C1-C2 angular interaction turned on. In (a, c, &, e) the O atoms are included in the calculation of $\boldsymbol{J}_N$, and in (b, d, & f) it is included in $\boldsymbol{J}_L$. Plot (g) is for MOF-5 with the mass of C1, C2, C3, and H doubled (and O included in $\boldsymbol{J}_N$). Plot (h) is for IRMOF-10 with O included in $\boldsymbol{J}_L$. The dark blue line indicates the total thermal conductivity for the framework with error bars.

arise from the contribution of these integrated correlation functions to κ.

- Increasing the mass of node atoms reduces the contribution of $\langle \boldsymbol{J}_N \cdot \boldsymbol{J}_N \rangle$ to κ.

- The cross-correlation in Figs.3.5.(a, b, c, d, & g) is negative. This implies that there is considerable reflection of heat current fluctuations at the interface between nodes and linkers.

- For MOF-5 the cross-correlation is most negative when O is considered part of the

linker. This indicates that most of the reflection occurs at the interface between O and Zn. This interface also has the largest mass difference.

- Increasing the linker length from MOF-5 to IRMOF-10 greatly reduces κ and changes the relative contributions of $\langle \boldsymbol{J}_N \cdot \boldsymbol{J}_N \rangle$, $\langle \boldsymbol{J}_L \cdot \boldsymbol{J}_L \rangle$, and $\langle \boldsymbol{J}_N \cdot \boldsymbol{J}_L \rangle$.

- Turning on the O-C1-C2 angular interaction does not change κ (at least within the resolution of the error bars), however Fig.3.5.(b & f) show a statistically significant change in the contribution from the cross-correlation $\langle \boldsymbol{J}_N \cdot \boldsymbol{J}_L \rangle$. This result illustrates an important difficulty for validation of computational prediction of thermal conductivity—namely that κ is an integral property and so it is possible to obtain the correct answer for the wrong reasons. Simply predicting a value of κ that matches experiment is insufficient to demonstrate the validity of the model that made the prediction.

3.4 Gas Filled Framework

MOFs used for gas storage will, by definition, be filled with gas. As it is the removal of latent heat of adsorption that limits gas uptake, it is important to determine the role that framework guests play in thermal transport. Simulations were performed of MOF-5 at 300 K, loaded with hydrogen and deuterium, up to an average 14 dimers per framework cage. Under these conditions the gas is bound to the framework and while the dimers migrate along the linker arms, there is little free motion across the voids of the framework. A typical simulation system is shown in Fig.3.6 along with the plot of κ as a function of gas concentration. Adding H_2 causes a modest increase in κ, along with a

small tensile stress. The surprising negative response to strain in Fig.3.4 indicates that this increase in κ is not due to stress. Furthermore, we have computed $\boldsymbol{J}_G$, the heat current involving gas atoms, and find correlations involving $\boldsymbol{J}_G$ make a negligible contribution to κ.

Adding deuterium to the system instead of H_2 gives a larger increase in κ, showing that the mass of the gas is important. Gas in the framework adds disorder to the system increasing scattering of lattice modes. However, as the gas binds preferentially to the oxter of the linkers, we attribute the increase in κ to the gas providing additional channels for heat transfer from nodes to linkers.

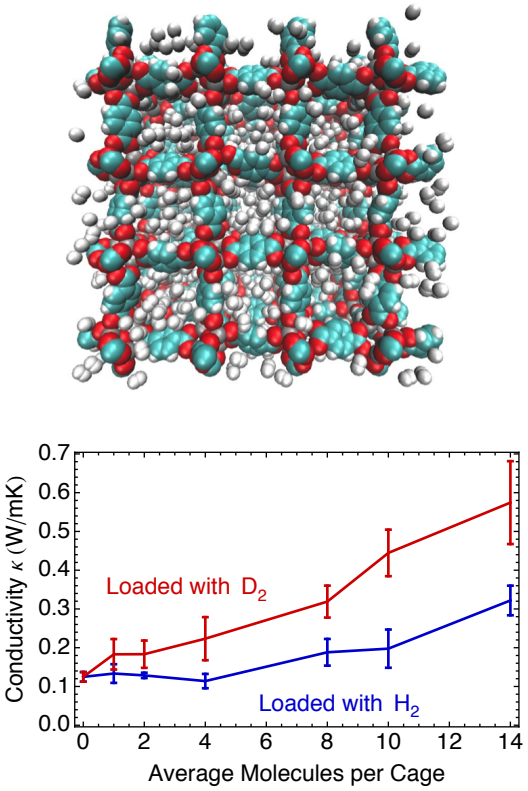

Figure 3.6: (top) Example of the 2x2x2 supercell structure of MOF-5 loaded with H_2 molecules (image is prior to annealing). (bottom) Plot of thermal conductivity of MOF-5 as a function of loading with hydrogen and deuterium.

3.5 Conclusions and Summary

In this paper we have presented a systematic study of the interplay of MOF architecture with heat transport mechanisms. It was found that many aspects of the framework impact both the molecular-mode and lattice-mode transport processes. Specifically, changing the linker mass and increasing the shear stiffness through the O-C1-C2 angular interaction produce little change in κ. In both of these cases simulations show very different dynamics in the heat current fluctuations. We thus conclude that changes to κ are buffered, because the linker mass and the O-C1-C2 angle affect the lattice and molecular modes in opposite directions. To engineer a substantial net change in κ it is necessary to identify parameters that change both heat transport mechanisms in the same direction. In this work we have found two such parameters: the node mass, and the linker arm length. The lattice-mode and molecular-mode thermal conductivity are both reduced by increasing the mass of nodes and the lengthening linker arms.

We have presented a new approach to analyzing equilibrium molecular dynamics simulations to obtain insight into heat transport mechanisms. This approach is based on the Green-Kubo method and involves spatially decomposing the instantaneous heat current, and computing the regional autocorrelations and cross-correlations separately. The sign of the cross-correlation reveals information about heat transfer between regions.

Finally, it was found that the thermal conductivity is increased by loading MOF-5 with gas, with κ increasing with both the concentration and mass of the adsorbed gas. This result is beneficial for many gas adsorption applications where the rate of adsorption is limited by the removal of latent heat. A more complete understanding of the mechanisms of

adsorbate-enhanced thermal transport will facilitate design of MOFs with desired thermal properties, and so this is an area of continued research.

Type	Potential	Parameters
	— Atom Labels —	
H2	Hydrogen (or duterium) in H_2 (D_2) dimer guest molecules	
Oc	O in node center	
Zn	Zinc in node	
O	Node-linker bridging Oxygen	
C1	Terminal carbon	
C2	C-C_3 in phenyl	
C3	C-C_2H in phenyl	
H	Hydrogen in phenyl ring	
	— Bonds —	
H2-H2	$E = K(r - r_o)^2$	K=1.85 eV $\cdot$ $\mathring{A}^{-2}$, r_o=0.74 $\mathring{A}$
C3-H	$E = K(r - r_o)^2$	K= 17.04 eV $\cdot$ $\mathring{A}^{-2}$, r_o=1.10 $\mathring{A}$
	— Angles —	
C2/3-C3-H	$E = K(\theta - \theta_o)^2$	K=1.6 eV, θ_o=120°
O-C1-C2	$E = K(\theta - \theta_o)^2$	K=3.0 eV, θ_o=120° (when turned on)
	— Dihedrals —	
C3-C2-C2-C3	$E = K[1 + d\cos(n\phi)]$	K=0.434 eV, d=-1, n=2
C2-C2-C3-H	$E = K[1 + d\cos(n\phi)]$	K=0.130 eV, d=-1, n=1
C2-C2-C3-C3	$E = K[1 + d\cos(n\phi)]$	K=1.735 eV, d=1, n=1
	— Non-Bonded Interations —	
H2-H2	$E = 4\varepsilon\left(\left(\frac{r_o}{r}\right)^{12} - \left(\frac{r_o}{r}\right)^{6}\right)$	ε= 0.00087 eV, r_o=2 $\mathring{A}$
H2-Oc	$E = 4\varepsilon\left(\left(\frac{r_o}{r}\right)^{12} - \left(\frac{r_o}{r}\right)^{6}\right)$	ε= 0.00750 eV, r_o=3.6 $\mathring{A}$
H2-Zn	$E = 4\varepsilon\left(\left(\frac{r_o}{r}\right)^{12} - \left(\frac{r_o}{r}\right)^{6}\right)$	ε= 0 eV, r_o=0 $\mathring{A}$
H2-O	$E = 4\varepsilon\left(\left(\frac{r_o}{r}\right)^{12} - \left(\frac{r_o}{r}\right)^{6}\right)$	ε= 0.00750 eV, r_o=3.6 $\mathring{A}$
H2-C1	$E = 4\varepsilon\left(\left(\frac{r_o}{r}\right)^{12} - \left(\frac{r_o}{r}\right)^{6}\right)$	ε= 0.01089 eV, r_o=4.0 $\mathring{A}$
H2-C2	$E = 4\varepsilon\left(\left(\frac{r_o}{r}\right)^{12} - \left(\frac{r_o}{r}\right)^{6}\right)$	ε= 0.01089 eV, r_o=4.0 $\mathring{A}$
H2-C3	$E = 4\varepsilon\left(\left(\frac{r_o}{r}\right)^{12} - \left(\frac{r_o}{r}\right)^{6}\right)$	ε= 0.01089 eV, r_o=4.0 $\mathring{A}$
H2-H	$E = 4\varepsilon\left(\left(\frac{r_o}{r}\right)^{12} - \left(\frac{r_o}{r}\right)^{6}\right)$	ε= 0.00390 eV, r_o=3.0 $\mathring{A}$

Table 3.1: Augmented interatomic potentials used to simulate MOF-5 and IRMOF-10. The cutoff of non-bonded interations is 10 $\mathring{A}$.

Chapter 4

Non systematic variation of thermal conductivity across the isoreticular family of metal-organic–frameworks

4.1 Introduction

Metal-organic frameworks (MOFs) are the most porous materials known to humanity. Advantages of MOFs such as 3-D hybrid frameworks, highly designable frameworks for pore shape and pore size attract intense scrutiny for their merit of gas storage and gas separation. Although MOFs are widely attracting intense scrutiny for their merit of gas storage and gas separation, their thermal properties are limited understood. Thus detailed

research is required, since the thermal transport properties of MOFs are both unusual and important.

Heat transport in MOFs is unusual because it straddles two domains: heat transport by crystal lattice modes (like in a crystalline solid); and heat transport between localized molecular modes by communication between localized oscillators as in the case of amorphous polymers. The problem is that thermal conductivities of MOFs are low (E.g. κ of MOF-5 is 0.31 W/m K,[251] close to that of concrete), because the heat transport by phonon in MOFs is insulated. The poor thermal conductivity of MOFs limits the refueling time of hydrogen storage because of the removal of latent heat of adsorption. However, MOFs' thermal properties have received such limited attention even under the booming interest of their exciting potential for gas storage and gas separation. Kaviany et al. have performed a research of thermal transport in empty MOF-5, characterizing the transport mechanisms and determining that the molecular-mode and lattice-mode heat currents contribute roughly equally to the thermal conductivity.[247] Zhang et al. have also computed the contributions of lattice-mode heat currents quantitatively.[689] Wilmer et al. and Grayson et al. have measured thermal conductivity of MOFs filled with gases computationally and experimentally, respectively.[33, 116] Wilmer et al. have reported that the reason of decreasing thermal conductivity of MOFs as increased concentration of adsorbed gases is because of MOF–gases phonon scattering, however, MOF–MOF phonon scattering still dominates the thermal conductivity. We have elucidated the role that MOFs' architecture plays in governing the interplay and dominance of molecular and lattice modes.[215]

Thus, we examine trends in heat transport across a family of MOFs with sys-

tematically vary architecture, rather than examine an individual MOF or idealized MOFs. Specifically we examine the subset of isoreticular MOFs (IRMOF) with linkers composed of benzene chains, that are IRMOF-1, -10 and -16. All three of these come with interpenetrated variants called IRMOFs-0, -9, and -15, respectively. Our approach is that systematically varying IRMOFs, examining processes of heat transport and analyzing the family's adherence or deviation from elementary heat transport models. The remainder of this article is laid out as follows: In the next section the simulation approach is described and section 4.3 describes a simple network model of heat transport. We then discuss the heat transport in the family of IRMOFs and their corresponding interpenetrated variants. The article finishes with a summary and conclusions.

4.2 Methods

We have simulated IRMOF-1, -10 and -16 whose linkers are phenyl, biphenyl and terphenyl, respectively, shown in Table 4.1. The family of IRMOFs is nicely and systematically in varying the linker length. Base on the network model in Fig. 4.1, molecular-mode heat transport must flow through the heat resisters between the heat carriers. The resistance of molecular-mode heat transport is mainly dominated by two factors: (1) linker-node acoustic mismatch, and (2) the areal density of linkers cutting through any cross-section of the framework.[215] Extending the length of linkers will not only increase the molecular-mode conductivity along a chain of links, but also reduce the areal density of linkers cutting through any cross-section of the framework. The network model provides a net reduced relationship with the molecular mode thermal conductivity κ_M and the lattice parameter

of the framework, a, as $\kappa_M \sim a^{-1}$.

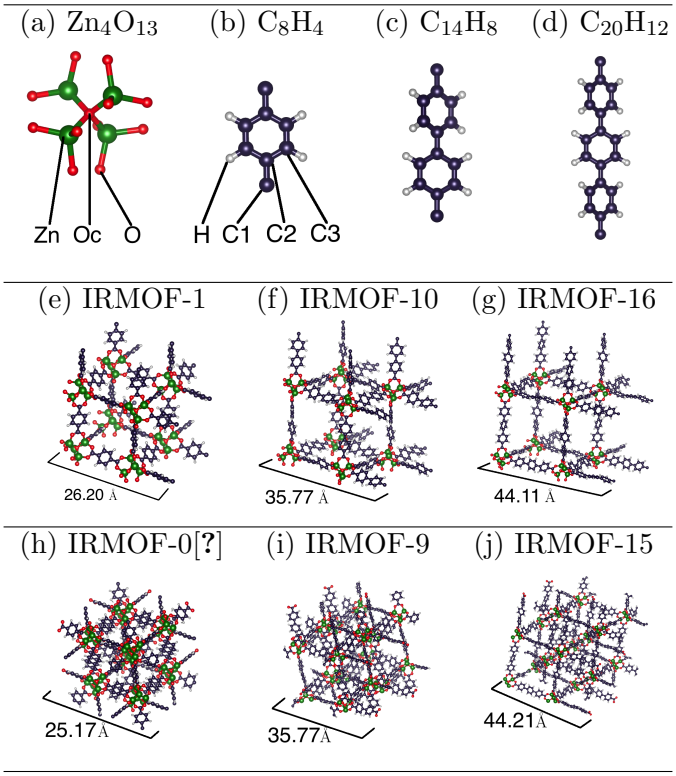

Table 4.1: (Table IRMOFs-table) (a-d) Shows the components of the IRMOF-1 (the first in IRMOF series and is also called MOF-5), IRMOF-10 and IRMOF-16. (a) Shows the Zn_4O_{13} nodal units, (b) the C_8H_4 (1,4 phenyl dicarboxylate) linkers in IRMOF-1, (c) the $C_{14}H_8$ (4,4 biphenyl dicarboxylate) linkers in IRMOF-10 and (d) the $C_{20}H_{12}$ (p-terphenyl 4,4 dicarboxylate) linkers in IRMOF-16. (e-g) Show a single unit cell of each framework. (h-j) Show a single unit cell of each interpenetrated framework, respectively.

Thermal conductivity, κ, of MOFs was predicted from equilibrium classical molecular dynamics (MD) simulations in the microcanonical ensemble (NVE) using the Green-Kubo formalism, which is based on the fluctuation dissipation theorem.[313, 211] The Green-Kubo method computes the thermal conductivity by the integral of the auto-correlation

function (ACF) of the instantaneous heat flux.

$$\kappa = \frac{V}{3k_B T^2} \int_0^\infty \langle J(t) \cdot J(t+\tau) \rangle \, d\tau, \tag{4.1}$$

where $J(t)$ is the instantaneous heat flux, and $\langle J(t) \cdot J(t+\tau) \rangle$ is the heat current auto-correlation function. The heat current J is decomposed into different contributions,

$$J = \sum_i J_i \tag{4.2}$$

where J_i is the instantaneous heat current of species i. In these multi-component systems the instantaneous heat current J_i is computed following the method of enthalpy correction.[32] The auto-correlations and the inter-species cross-correlations are determining the mechanism of the heat transport process.

The potentials of MOF-5 (IRMOF-1) are extracted from Han et al.,[215] which are augmented from Kaviany's[251] MOF-5 potential set. Compared to MOF-5, IRMOF-10, 9, 16 and 15 contain the additional C2-C2 bonds, C2-C3-C3 angles and C2-C3-C3-C2 dihedrals in linkers between the adjacent 1,4-dichlorobenzene rings, which are shown in Table 4.1. All simulations were performed on 2×2×2 supercells with periodic boundary conditions at 300 K. In order to simulate each 2×2×2 supercell with correct volume at 300 K, all of the supercells were generated and performed in the isothermal-isobaric ensemble (NPT) under zero pressure with the cell free to change volume but not shape. Each system was heated up to 400 K from 0 K slowly, and the negative thermal expansion coefficients of each IRMOFs were computed by slopes of the linear fits. Each 2×2×2 supercell was

Type	Potential	Parameters
Atom labels		
Oc	Oxygen in node center	
Zn	Zinc in node	
O	Node-linker bridging oxygen	
C1	Terminal carbon	
C2	$C - C_3$ in phenyl	
C3	$C - C_2H$ in phenyl	
H	Hydrogen in phenyl ring	
Bonds		
O-C1	$U = D\{[1 - e^{-\alpha(r-r_0)}]^2 - 1\}$	$D = 4.624\ eV,\ \alpha = 2.337\ \text{Å}^{-1},\ r_0 = 1.28\ \text{Å}$
C1/2-C2	$U = D\{[1 - e^{-\alpha(r-r_0)}]^2 - 1\}$	$D = 5.439\ eV,\ \alpha = 1.669\ \text{Å}^{-1},\ r_0 = 1.482\ \text{Å}$
C2/3-C2/3	$U = D\{[1 - e^{-\alpha(r-r_0)}]^2 - 1\}$	$D = 8.196\ eV,\ \alpha = 1.680\ \text{Å}^{-1},\ r_0 = 1.388\ \text{Å}$
C3-H	$U = K(r - r_0)^2$	$K = 17.04\ eV\ \text{Å}^{-2},\ r_0 = 1.10\ \text{Å}$
Angles		
C2/3-C2/3-C2/3	$U = K(cos\ \theta - cos\ \theta_0)^2$	$K = 5.866\ eV,\ \theta_0 = 120^\circ$
O-C1-O	$U = K(cos\ \theta - cos\ \theta_0)^2$	$K = 5.5\ eV,\ \theta_0 = 120^\circ$
C1/2-C2-C3	$U = K(cos\ \theta - cos\ \theta_0)^2$	$K = 4.799\ eV,\ \theta_0 = 120^\circ$
Zn-O-C1	$U = K(cos\ \theta - cos\ \theta_0)^2$	$K = 5.5\ eV,\ \theta_0 = 132.3^\circ$
C2/3-C3-H	$U = K(\theta - \theta_0)^2$	$K = 1.6\ eV,\ \theta_0 = 120^\circ$
O-C1-C2	$U = K(\theta - \theta_0)^2$	$K = 3.0\ eV,\ \theta_0 = 120^\circ$
Dihedrals		
C2/3-C2/3-C2/3-C2/3	$U = K[1 - cos(\phi - \phi_0)]$	$K = 1.735\ eV,\ \phi_0 = 0^\circ$
O-C1-C2-C3	$U = K[1 - cos(\phi - \phi_0)]$	$K = 1.587\ eV,\ \phi_0 = 0^\circ$
O-C1-O-Zn	$U = K[1 - cos(\phi - \phi_0)]$	$K = 1.732\ eV,\ \phi_0 = 0^\circ$
C3-C2-C2-C3	$U = K[1 + d\ cos(n\phi)]$	$K = 0.434\ eV,\ d = -1,\ n = 2$
C2-C2-C3-H	$U = K[1 + d\ cos(n\phi)]$	$K = 0.130\ eV,\ d = -1,\ n = 1$
C2-C2-C3-C3	$U = K[1 + d\ cos(n\phi)]$	$K = 1.735\ eV,\ d = 1,\ n = 1$
Non-bonded interactions		
Oc-Zn	$U = \frac{1}{r} q_{Oc} q_{Zn} + Ae^{-r/\rho} - Cr^{-6}$	$A = 770.127\ eV,\ \rho = 0.357\ \text{Å},\ C = 0.00088\ eV\ \text{Å}^6$
Oc-O	$U = \frac{1}{r} q_{Oc} q_O$	
O-Zn	$U = \frac{1}{r} q_O q_{Zn} + Ae^{-r/\rho} - Cr^{-6}$	$A = 529.7\ eV,\ \rho = 0.352\ \text{Å},\ C = 0.0\ eV\ \text{Å}^6$
Zn-Zn	$U = \frac{1}{r} q_{Zn} q_{Zn}$	
O-O	$U = \frac{1}{r} q_O q_O$	

Table 4.2: Interatomic potentials of the family of IRMOFs. The cutoff of non-bonded interactions is 10 Å.

scaled to its mean volume at 300 K. The canonical ensemble (NVT) is performed at 300 K for 100 ps to equilibration. And then the heat flux was computed and its auto- and cross-correlation functions are averaged during the 500 ps microcanonical ensemble (NVE).

The auto- and cross-correlation functions were computed out to 50 ps, and 40 simulations with different starting configurations were averaged to obtain each thermal conductivity and error bar. The LAMMPS MD simulation package[474] was used to perform velocity–Verlet time integration with a time step of 0.2 fs which was sufficient to minimize total energy fluctuations during NVE simulation to less than 10^{-5} of the thermal energy.

4.3 The network model

In order to guide the understanding and interpretation of heat transfer, a network model is used as a simple thermal transportation model for both IRMOFs family and breathing MOFs.[123] The models like this are quite good for understanding other properties of MOFs, like folding mechanical behavior, stiffness and so on. The network model is derived from the thermal resistance of the nodes and linkers, which are unknowns, R_{Node} and R_{Linker}. Although we don't know them, we know when are they constant. We should be able to untangle what is the node and linker effect to thermal conductivity. Since IRMOFs are isotropic, the heat transfer rate, $\dot{Q}$, flow along the node-linker network due to a temperature difference (unit of [K]), ΔT, which have a relationship as $\dot{Q} = \Delta T \cdot (R_{Node} + R_{Linker})^{-1}$. The negative temperature gradient, ∇T, (unit of $[K \cdot m^{-1}]$) is the time averaged temperature difference between the ends along one direction, which can be written as $\nabla T = -\langle \partial T / \partial x \rangle$. Fourier's Law of cooling provides the relationship between heat flux and thermal conductivity, $J = -\kappa \cdot \nabla T$. The thermal conductance C is the reciprocal of thermal resistances R. Then the heat flux is derived by Equ. 4.3a, where A, L are area of heat conducting channel and lattice parameter of IRMOFs, respectively. The thermal

conductivity of IRMOFs is written by Equ. 4.3b.

The thermal conductance of linker can be written as $C_{Linker} = \kappa_{Linker} \cdot L_{Linker}$. The thermal conductivity of IRMOFs is further derived as Equ. 4.3c. The thermal conductivities of linkers (shown in Table 4.1, b-d) is computed by Green-Kubo method.

$$J = \frac{\dot{Q}}{A} = \frac{\Delta T}{(R_{Nd} + R_{Lk})\, A} = -\frac{\nabla T}{(R_{Nd} + R_{Lk})\, L} \tag{4.3a}$$

$$\kappa = \frac{C_{Nd} \cdot C_{Lk}}{(C_{Nd} + C_{Lk})\, L} \tag{4.3b}$$

$$= \frac{C_{Nd} \cdot k_{Lk}}{(C_{Nd} L_{Lk} + k_{Lk}) L}. \tag{4.3c}$$

Increasing the linker length will reduce the areal density of linkers cutting through any cross-section of MOF. Thermal conductivity of Molecular modes is proportional to the reciprocal of lattice parameter. The density of heat conducting channels decrease faster than their thermal conductivity increase.

4.4 Results

4.4.1 Non-interpenetrated MOFs

Based on the network model Equ. 4.3c, thermal conductivity is determined by three parameters: C_{Node}, γ and L, in which C_{Node} is independent in linker length and L is increasing linearly. The family of isoreticular MOFs (IRMOF-1, 10, and 16) in Table 4.1 is nicely and systematically in varying the linker length. The solid red line in Fig. 4.3

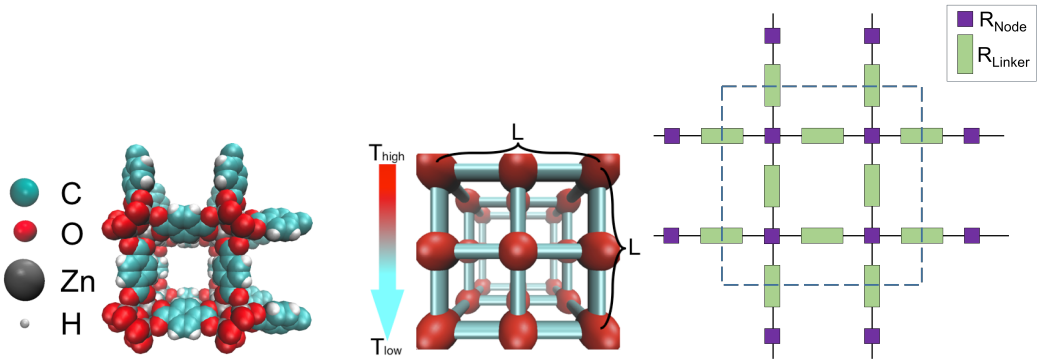

Figure 4.1: (Fig. Network) Nodes can be treated as heat carriers (red spheres) and linkers can be treated as heat resisters (blue sticks). Since nodes carry much more heat than the linkers. Left is the simplest member of IRMOFs, MOF-5 (IRMOF-1),

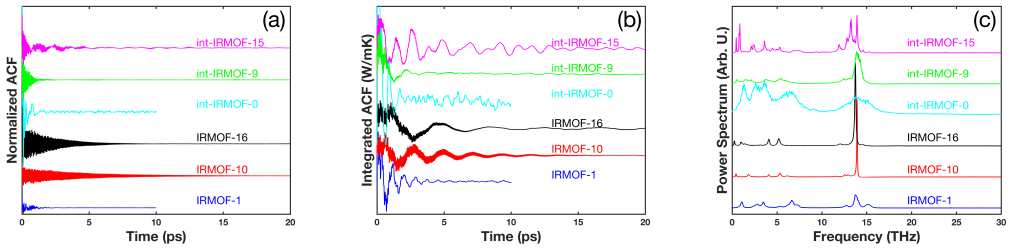

Figure 4.2: Plot (a) shows the averaged heat flux ACF for different MOFs. Plot (b) shows the integration of the ACF as a function of the integration duration. Plot (c) shows the power spectrum of heat current. In all plots (a-c) the curves are normalized and offset for clarity. The blue, red, black, cyan, green and magenta traces are for: IRMOF-1, -10, -16, and Interpenetrated IRMOF-0, -9, -15, respectively.

corresponds to the thermal conductivities computed by MD simulations. The three dashed lines are the thermal conductivities predicted by the network model, depending on the three thermal conductivities computed by MD simulations, respectively. The network model has a decreasing trend, but does not accurately match the MD thermal conductivities. γ is unknown, however, the thermal conductivities of different length of linkers (like shown in Table 4.1 [b-d]) can be computed by MD simulations, which are the values of γ. Subplot of Fig. 4.3 shows the value of γ of nude linkers with different linker length oscillating around 170 W$\cdot$m/K, which is also independent in linker length. Therefore the thermal conductivities of IRMOFs are only determined by C_{Node}. Depending on Equ. 4.3c, C_{Node} can be computed by three different κ (IRMOF-1, 10 and 16). With three different values of C_{Node}, the predicted network model is computed and plotted in dashed lines in Fig. 4.3.

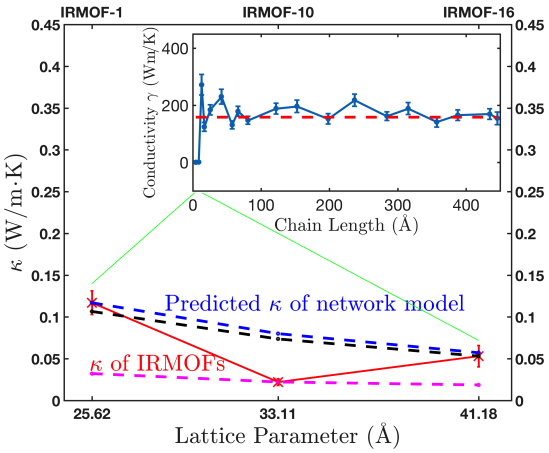

Figure 4.3: Thermal conductivity as a function of lattice parameter of IRMOF-1, -10 and -16. The blue plot is the thermal conductivity predicted by the network model. The red plot corresponds to the thermal conductivity computed by MD simulations. The subplot shows the parameter γ in network model as a function of linker length.

The nodes carry much more heat than the linkers, however, the linkers and the

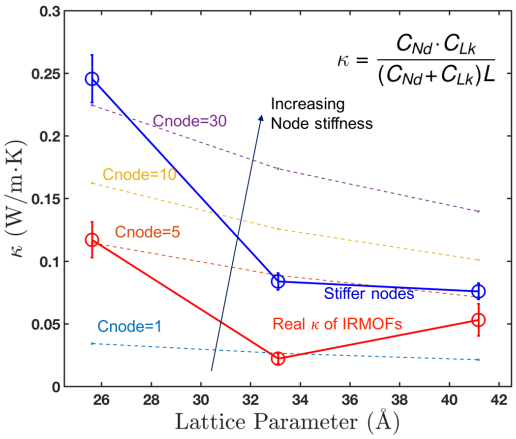

Figure 4.4: The solid red line is same as the one in Fig.4.3, which is the thermal conductivity as a function of lattice parameter of IRMOF-1, -10 and -16. The solid blue line is the thermal conductivity of IRMOF-1, -10 and -16 with stiffer nodes, which is compared with the dotted lines with different values of C_{Node} computed by the network model.

soft heavy nodes create an acoustically mismatched bottleneck for the molecular-mode heat transport.[215] We have stiffened the nodes by changing the non-bonded interactions of nodes into bonded interactions (details in support information). The thermal conductivity with stiffer nodes is the solid blue line shown in Fig. 4.4. In this case, C_{Linker} is independent in stiffness of nodes. Dashed lines are the network model predicted thermal conductivity based on different values of C_{Node}. Obviously, stiffer nodes increase C_{Node} and sequentially increase thermal conductivity.

The network model predicts a decreasing trend, however, κ of IRMOF-16 is higher than that of IRMOF-10. In long range, γ is independent in linker length. Nonetheless, in the range of linker length of IRMOF-1, -10 and -16 (referred to lattice parameters are from 25.62 Å to 41.18 Å shown in Fig. 4.3), γ of IRMOF-16 increases drastically than that of IRMOF-1 and -10. That is the reason why κ of IRMOF-16 does not follow the network model.

Fig. 4.2 (a) presents the heat current ACF of IRMOF-1, -10 and -16, in which -10 and -16 show long oscillations that decay slowly. The long decaying fluctuations are indicated by the sharper peaks in Fig. 4.2 (c). This is because there are numerous extra phonon scattering.

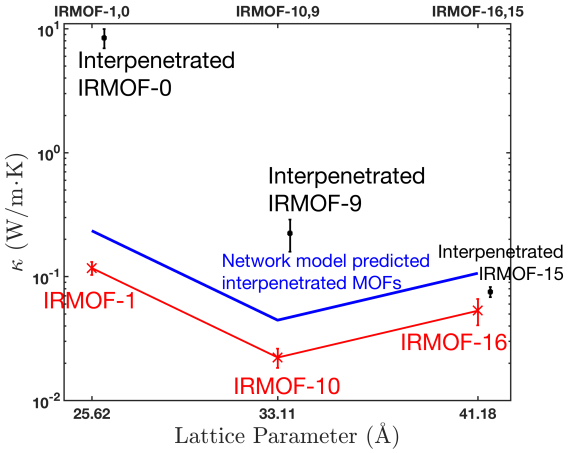

Figure 4.5: Red error bars show the thermal conductivity of non-interpenetrated frameworks, IRMOF-1, -10 and -16 as a comparison to interpenetrated frameworks IRMOF-0, -9 and -15 (black error bars). Blue line shows the thermal conductivity of interpenetrated frameworks predicted by the network model.

4.4.2 Interpenetrated MOFs

The non-interpenetrated IRMOF-1, -10 and -16 are isomers of doubly-interpenetrated IRMOF-0, -9 and -15, respectively. In the network model, IRMOF-0, -9 or -15 can be treated as an IRMOF-1, -10 or -16 assembled together with another identical IRMOF-1, -10 or -16, shown in Table 4.1 (e,h, and f,i and g,j). The thermal conductivities of interpenetrated IRMOFs are shown in Fig. 4.5 (black).

If the resistance to molecular-mode heat transport is only computed by the network model, the thermal conductivities of interpenetrated IRMOFs should be doubled (as

shown in blue Fig. 4.5), since the density of heat conducting channels is doubled. However, increasing the density of heat conducting channels also increases the numbers of resistance and linker-node acoustic mismatch. Therefore, κ of interpenetrated IRMOF-15 is lower than the one predicted. From a topological point of view, both IRMOF-9 and -15 are doubled interpenetrated frameworks, however, the orientation of the two isomers are different. The structure of IRMOF-9 is orthorhombic, while that of IRMOF-15 is cubic. The two isomers of IRMOF-9 are favoured to stay close to each other compared to IRMOF-15 whose one isomer evenly resides within the other (so does IRMOF-1) and a co-facial inter-lattice linker distance of 10.8 Å. The framework resides near the nodes at the junction of the linkers of the other framework, base on the theory of "oxter", the framework binds with two or more linkers of the other framework simultaneously, which makes heat transfer from linker to linker much more easier. Consequently, κ of interpenetrated IRMOF-0 and -9 are much higher than the one predicted by the network model.

4.4.3 Cross-Correlations

We analyse equilibrium MD simulations by decomposing the heat current into contributions from each type of atoms, $J = \sum_i J_i$, where i is atom type, and integrating the correlation functions. We use color map to show the integral of each correlation functions instead of numbers (see Fig. 4.6). The colors that are referred to integral from high to low are from yellow to green to blue. We observe several interesting things:

- In the top row, compared to IRMOF-1 and -16, thermal conductivity of IRMOF-10 is much lower because of the negative cross-correlation of Zn–O and Zn–Oc. The

negative cross-correlation implies that there is considerable reflection of heat current fluctuations at the bond of Zn–O and Zn–Oc.

- Increasing the linker length from interpenetrated IRMOF-0, -9 to -15, which is shown in the bottom row, keeps the pattern. The trend is that the contribution to thermal conductivity from auto-correlation of Zn becomes progressively dominating.

- In the left and middle column, both interpenetrations keep the pattern. For IRMOF-1 and -0, auto-correlation of O contributes to thermal conductivity mainly, in addition, auto-correlation of Zn becomes important after interpenetration. For IRMOF-10 and 9, auto-correlation of O contributes to thermal conductivity mainly, in addition, auto-correlation of C1 becomes important after interpenetration.

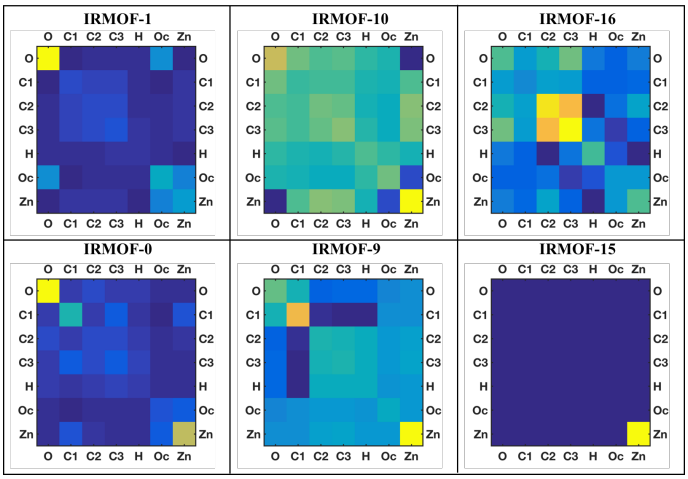

Figure 4.6: An illustration of the correlation color map for each two types of atoms of IRMOFs. Each color pixel illustrates the integral of the auto- or cross-correlation of the two types of atoms. The colors that are referred to integral of correlation functions from high to low are from yellow to green to blue. The IRMOFs in the top row are IRMOF-1, -10, -16 and the ones in bottom row are the corresponding interpenetrated IRMOF-0, -9, -15, respectively.

Chapter 5

Phonon-focusing and rattler-mode interference in thermal conductivity transitions of the breathing metal-organic–framework MIL-53

Laura de Sousa Oliveira, Luping Han, Agnieszka Truszkowska, Wenxi Huang, Brady J. Gibbons and P. Alex Greaney

In this research, Oliveira and I contributed most of the work. MIL-53 behaves like a concertina between open and closed pore cases under different pressures, which is shown

in Fig 5.1. My work was focused on computing thermal conductivities of MIL-53 by Green-Kubo method that were analyzed with that computed by the geometric network model under different pressures. Oliveira's work was focused on performing the first principles calculations of MIL-53 and on building geometric network model of thermal conductivity.

The metal-organic–framework (MOF) MIL-53 has a framework geometry with an unconstrained winerack mode that enables it to concertina between open and closed structures either under pressure or with the uptake of adsorbates. Here we show that in these breathing MOFs the thermal conductivity — an important property for gas sorption in high surface area materials — also changes significantly between open and closed conformations. We present a very simple geometric network model of conductivity in these materials that underpins the base trend and a second rattler model that provides a mechanistic understanding of the deviations from it.

5.1 Introduction

The metal organic framework (MOF) MIL-53 is the holotype for a series of geometrically hinged MOFs that can concertina between open and closed pore structures through a so called "wine rack" deformation [539, 363, 378, 437]. The transition between open and closed configurations can be driven by the uptake of gas or by pressure leading to intense exploration of these flexible MOFs for uses in gas storage and gas separation applications [539, 610, 427, 641]. An important auxiliary factor in the gas sorption performance of MOFs is thermal conductivity, which is often a bottleneck for delivering or dissipating latent heat of adsorption [249, 487, 216]. In this letter we have examined how the ther-

mal conductivity of MIL-53 changes as it switches from open to closed. Importantly, we find that the thermal conductivity changes significantly, but not as dramatically as would be expected based on the geometric change in the network. We find that the anisotropy in the thermal conductivity stems from a phonon focusing effect tempered by scattering from non-propagating "rattler" modes. Phonon focusing is a phenomenon of considerable technological interest in the phonon transport community and has been proposed as the mechanism that enables materials with ultra low thermal conductivity — materials with thermal conductivity that along one direction exceeds the theoretical lower limit for heat conduction in amorphous materials [100]. In our present work on MIL-53 we find the first example of a material in which the phonon focusing can be tuned as the structure switches, providing important insights on how to engineer phonon focusing materials. The transition in phonon focusing in MIL-53 explains the deviation in thermal conductivity from the purely geometric effects, and our analysis of the rattler modes provides key insights into why the framework architecture of MOFs makes MOFs, as a materials class, fundamentally poor at conducting heat.

5.2 Methods

5.2.1 Thermal Conductivity

The MIL-53(Al) thermal conductivities, κ, were computed using the well-established Green-Kubo formalism [210, 314]:

$$\kappa = \frac{V}{3k_B T^2} \int_0^\infty \langle \mathbf{J}(t)\mathbf{J}(t+\tau) \rangle \; d\tau, \tag{5.1}$$

where k_B, T and V are the Boltzmann's constant, the temperature, and the volume of the simulated region respectively. $\mathbf{J}$ is the heat-flux, and $\langle \mathbf{J}(t)\mathbf{J}(t+\tau)\rangle$ is the non-normalized heat current autocorrelation function (HCACF). The Green-Kubo expression (Eqn. 5.1), based on the fluctuation-dissipation theorem, relates instantaneous fluctuations in the system heat-flux to thermal transport, and it allows thermal conductivity calculations from equilibrium classical molecular dynamics simulations. Classical molecular dynamics simulations were performed with the large-scale atomic/molecular massively parallel simulator (LAMMPS) software [475]. Simulations were performed for 3×3×3 and 2×5×2 supercells, with 2,052, and 1,520 atoms respectively, and periodic boundary conditions. We found that while κ in the a, and c directions is converged with 3 unit cell lengths, a larger cell size (5× the lattice parameter) is needed to converge κ along b, the channel direction. By contrast, thermal conductivity studies of MOF-5 have shown a 2×2×2 supercell size to yield converged κ values [216, 249]. Molecular dynamics simulations require the specification of an appropriate set of interatomic potentials. In this paper we use the intramolecular and non-bonded force field parameters adjusted by Vanduyfhuys *et. al.* along with the atomic partial charges resultant from Vanduyfhuys *et al.*'s DFT Mulliken population analysis [619] to explore the host-independent pressure behavior of the MIL-53(Al) framework. To compute the lattice parameter of the MIL-53 at 300 K, the MIl-53 supercells were optimized at 0 K. In the isothermal–isobaric ensemble (NPT) with the cell free to change volume, the temperature was increased slowly to 1,000 K and cooled down back to 0 K. The negative expansion coefficient was obtained by fitting to the simulation. The supercells were scaled to its mean volume at 300 K. In addition to a SCHEME minimization, to find the most

energetically favorable configuration, the 3×3×3 and 2×5×2 MIL-53 supercells were annealed to 300 K for 5 ns from 0 MPa to 300 MPa and back to 0 MPa for another 5 ns in NPT, relaxing the atomic structure as well as supercell shape and size. After relaxing the atomic structure, along with the size of the compute cell, all systems were given a thermal energy equivalent to 300 K and equilibrated in the microcanonical ensemble (NVE) for 50 ps before starting to record the HCACF. The simulations were then performed for an additional 5 ns with 1 fs time step and periodic boundary conditions. Throughout the period in NVE the average temperature remained at approximately 300 K, the HCACF was computed out to 50 ps, and 40 simulations with different starting configurations were averaged to obtain each datum.

5.2.2 Phonon properties

Phonon properties for both op and cp MIL-53(Al) were computed with a self-consistent-charge density functional tight binding (SCC-DFTB) approach [148], using the DFTB+ software package [22]. The parameter sets, or Slater Koster files, used for the calculations are provided by the developers [170] and can be downloaded from the DFTB+ website (under "matsci"). A comprehensive review of DFTB can be found in the literature [479, 534, 148]. Relaxation calculations were performed with a 76 atom unit cell obtained from a database of computation-ready MOF structures derived from experimental data, the CoRE (computation-ready, experimental) MOF database [106]. The atomic positions were optimized using the conjugate-gradient algorithm to near 5×10^{-7} eV/$\mathring{A}$ and the electronic optimization was within 3×10^{-7} eV. The Brillouin zone was sampled by a converged 2×2×2 Monkhorst-pack scheme k-point mesh [421, 450]. The hessian was com-

puted using a double-sided finite difference approach implemented through Phonopy [597] from the force constants obtained for a 2×2×1 supercell and a displacement amplitude of 0.01 $\mathring{A}$ for each one-sided atomic displacement. Periodic boundary conditions were enforced in all directions.

Group velocities, $\mathbf{v}_g$, were calculated for the acoustic bands, i.e. $\nu = 1, 2, 3$, along the reciprocal wave vectors, $\mathbf{k}$, corresponding to the a, b, c, and linker directions, using the Phonopy software package [597], as

$$\mathbf{v}_g(\mathbf{k}\nu) = \nabla_{\mathbf{k}}\omega(\mathbf{k}\nu). \tag{5.2}$$

The number of phonon states at a given frequency, ω, wave vector, $\mathbf{k}$, and temperature, T, can be approximated by the Bose–Einstein distribution, $f(\omega, T)$. We define phonon flux at a given wave vector, $\mathbf{k}$, frequency and temperature, $\phi(\mathbf{k}, \omega, T)$, as

$$\phi(\mathbf{k}, \omega, T) = \mathbf{v}_g(\mathbf{k}, \omega)\hbar\omega(\mathbf{k})D(\mathbf{k}, \omega)f(\omega, T), \tag{5.3}$$

where $2\pi\hbar$ is Planck's constant, such that $E(\omega) = \hbar\omega$. In the above expression, the density of states, $D(\mathbf{k}, \omega)$, is the number of phonons at $\mathbf{k}$ of frequency ω per volume of the Brillouin zone considered. In the interest of performing a comparative quantitative analysis, we normalize the *phonon flux* with respect to the maximum flux of both the open- and closed-pore structures, such that any constants can be disregarded. Sorting the phonon branches can be a daunting task and we have, therefore, opted to consider the sum of the phonon

flux over multiple frequencies. Over all frequencies at a given $\mathbf{k}$, the sum is given by:

$$\phi_{\mathbf{k}}(T) = \sum_{m=\nu}^{3N} \phi_m(\mathbf{k}, T), \tag{5.4}$$

where N is the number of atoms in a unit cell, and $3N$ the total number of phonon branches.

Validation of DFTB+

Albeit less accurate than the more common density functional theory (DFT) approach, DFTB has been shown to perform well on various systems from molecules to periodic materials [148], and offers a significant reduction in computational costs. In addition to the DFTB calculations, we relaxed the op and cp MIL-53(Al) with DFT to compare the relaxed geometries obtained with both methods. For the DFT calculation, a unit cell was relaxed with the plane-wave Vienna *Ab-initio* Simulation Package (VASP) [309, 306, 307, 308], using the project-augmented wave (PAW) method [48, 310] in the local density approximation (LDA)[464]. Energy convergence to 0.1 eV was attained with a Γ-centered 4×4×4 irreducible Monkhorst-Pack k-point sampling of the Brillouin zone and a 800 eV kinetic energy cut-off. The structure, cell size and shape were relaxed with a Gaussian smearing approach, until ionic and electronic tolerances reached 0.05 eV/$\mathring{A}$ and 0.01 meV, respectively.

All bond lengths are within 0.01 $\mathring{A}$ of each other (see Table 5.1 in the Supporting Information). The lattice parameters, volume and angles are shown in Table 5.4 for the op and cp MIL-53(Al) structures. The DFTB calculations consistently overestimate b and c and underestimate a. Experimental measurements of thermally-actuated MIL-53(Al) [363] result in a monoclinic structure, not observed in either DFT or DFTB calculations. The

cp MIL-53 structure appears to be barely triclinic for both DFT and classical potential calculations.

5.3 Thermal conductivity model

A simple heat propagation model for MOFs can be derived from the thermal resistivities in the nodes and linkers, R_N and R_L. Fig. 5.1 illustrates this idea. Notice that each unit cell has four nodes and R_N corresponds to a two-node cluster and includes the bridges between the cluster and the linker on each side of it. The MIL-53 structure is approximately orthorhombic, and we shall use this approximation to describe the suggested thermal transport model. For heat to travel across one unit cell in either the [100] or [001] directions it must travel along an alternating sequence of linkers and nodes (crossing exactly two of each per unit cell). In a unit cell, the heat flow along a chain of linkers and nodes can be written as $\dot{Q} = -2C_{\text{chain}}\Delta T$, where ΔT is the temperature change along the chain, and the thermal conductance of the chain, C_{chain}, is obtained from the thermal resistance across a node and a linker

$$C_{\text{chain}} = \frac{1}{2(R_N + R_L)}. \tag{5.5}$$

Armed with the heat current along a single chain we can now determine the heat flux in any direction. For the heat flux along [100], J_{xx}, it would thus follow that

$$J_{xx} = -\frac{2C_{\text{chain}}\Delta T}{L_y L_z} = -2C_{\text{chain}}\frac{L_x}{L_y L_z}\frac{\partial T}{\partial x} = -\kappa_{xx}\frac{\partial T}{\partial x} \tag{5.6}$$

where L_x, L_y and L_z are the length of the unit cell along the x-, y- and z-directions, and κ_{xx} is the thermal conductivity along x. Using the same approach, and assuming a thermal conductance, C_{channel}, along the alternating chain of metal and oxygen atoms in the z direction, we can write the thermal conductivity tensor:

$$\kappa = 2C_{\text{chain}} \begin{pmatrix} \frac{L_x}{L_y L_z} & 0 & 0 \\ 0 & \frac{C_{\text{channel}}}{C_{\text{chain}}} \frac{L_y}{L_x L_z} & 0 \\ 0 & 0 & \frac{L_z}{L_x L_y} \end{pmatrix} \tag{5.7}$$

5.4 Computational Results and Discussion

5.4.1 Thermal conductivity simulations and model results

The values of C_{chain} and C_{channel} were obtained from the thermal conductivity calculations at 0.1 MPa, and used with the also classically obtained thermal expansion results to determine the model predicted thermal conductivities. The solid lines in Fig. 5.1 b) correspond to the expected thermal conductivity based on the model, plotted against the actual thermal conductivity values obtained. The error bars are the standard error for the thermal conductivity. We can immediately observe that the notion of a single chain resistivity to explain thermal transport along both a and c is flawed: the collective node and linker resistivity, $R_n + R_l$, is 0.083 K/W when computed with κ along a, and 0.138 if κ is along c. This results in estimated values of thermal conductivity for the open-pore MIL-53 above and below the actual values for κ along a and c, respectively (see Fig. 5.1 b)). The node resistivity is 0.015 K/W.

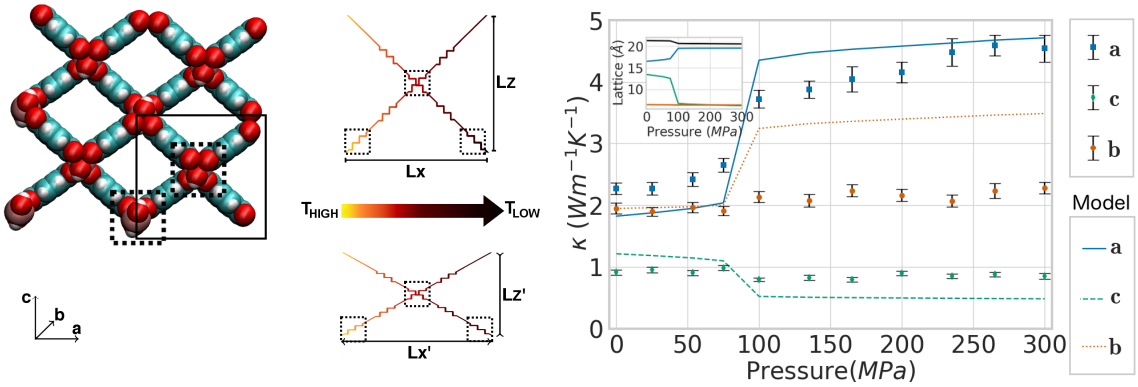

Figure 5.1: Fig. a) illustrates the scalability of the thermal conductivity tensor between breathing states in MIL-53. Fig b) are the MIL-53(Al) thermal conductivity classical potential calculations at different pressures and corresponding standard error, and expected change in thermal conductivity as predicted by the geometric model (solid lines). The inset shows the actual thermal expansion/contraction of the framework as a function of temperature, in a classical potential (the color coding is the same as for the thermal conductivity). The black line shows the deformation of the linker throughout the simulation.

Although heat is conducted along the linkers for both axes, from Fig. 5.1 b) we can observe that the thermal conductivity of the open-pore MIL-53(Al) is over twice as large along a than c. This anisotropy is in good agreement with the elastic constants in those directions, as computed by Ortiz *et al.* [446]: 90.85 GPa along a, and 33.33 GPa along c.The softer modes correspond to the deformation direction. In the closed-pore configuration, the anisotropy is accentuated as the conductivity along a doubles with the closing of the framework. The trend predicted in Fig. 5.1 b) by the geometric framework model is followed to some extent, but it fails to accurately depict the computational results. The linkers are not interconnected along the channels and, in the vacuum, heat in this direction is solely conducted through the aluminum nodes. As the pores of the MIL-53 close, the density of node arrays in the plane perpendicular to the b-axis increases. This explains the expected increase in κ along b (see dashed orange line). The actual increase in thermal

conductivity is grossly overestimated by the geometric model. A similar argument can be made for κ along a and the increase in density of linker–node chains. In this case, the model trend (see blue solid line) is in better agreement with the results. Contrary to the change along a, the plane perpendicular to c expands and the density of linkers/nodes is reduced, thus the model predicted decrease in thermal conductivity (the green dashed line). This trend is not matched by our calculations, which predict a nearly steady response to the geometric change in this direction. The geometric model does not fully capture the thermal conductivity behavior during the geometric transition. To elucidate the discrepancy between the simulation and the model results, we have computed phonon properties semi-empirically for the op and cp MIL-53(Al).

5.4.2 Features of the open- and closed-pore MIL-53(Al) dispersion relations

The phonon dispersion relations along a, b, c, and in the alternated linker–node chain direction for both the op and cp MIL-53(Al) have been calculated with tight-binding DFT (see Fig. 5.2). The group velocities along the same directions near the Γ point are also plotted (see Fig. 5.3). The full dispersion relation for the closed-pore MIL-53(Al) is barely distinguishable from that of the open-pore MIL-53(Al) (see Fig. 5.2 a)). This is unsurprising, seen as the densities of states for the conformational [387] framework isomers are nearly identical (Fig. 5.2 b)). There is a small fractional increase in the number of states in the acoustic region in the cp structure; lower frequency optical modes are also slightly more abundant in the cp structure, as are higher modes in the op MIL-53(Al). Many high-frequency modes are flat in both frameworks and therefore are not expected to carry heat.

There are, however, some lower frequency optical modes, for instance in the region shown in Figs. **??** c) and d), with a significant curvature which are thus likely to contribute towards thermal transport. A much higher number of states are available due to linker atoms than node atoms; however, they are not normalized by the number of atoms in the unit cell (68 linker atoms, and 8 node atoms).

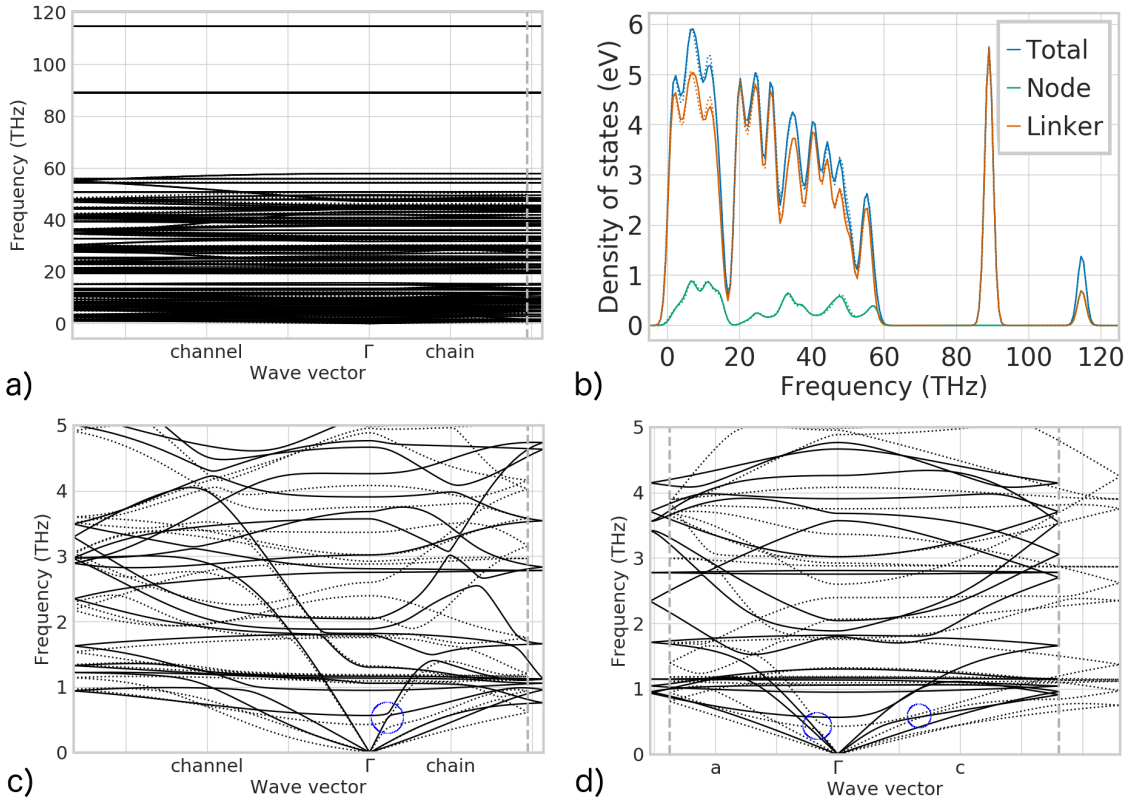

Figure 5.2: Fig. a) is the dispersion relation computed along the linker–node chain and along the aluminum nodes in the channel direction for MIL-53(Al) for the open-pore structure. In Fig. b), the total (blue) and partial density of states of MIL-53(Al) separated by the linker (orange) and node (green) contributions for the open-pore (solid lines) and the closed-pore (dashed lines) frameworks are shown. A zoom-in on the lower phonon modes of the dispersion relation in the same region given in b) for both the op (red) and cp (black) MIL-53 structures. Figure c) shows a zoom in of the dispersion relation along a and c also for the op (red) and cp (black) MIL-53.

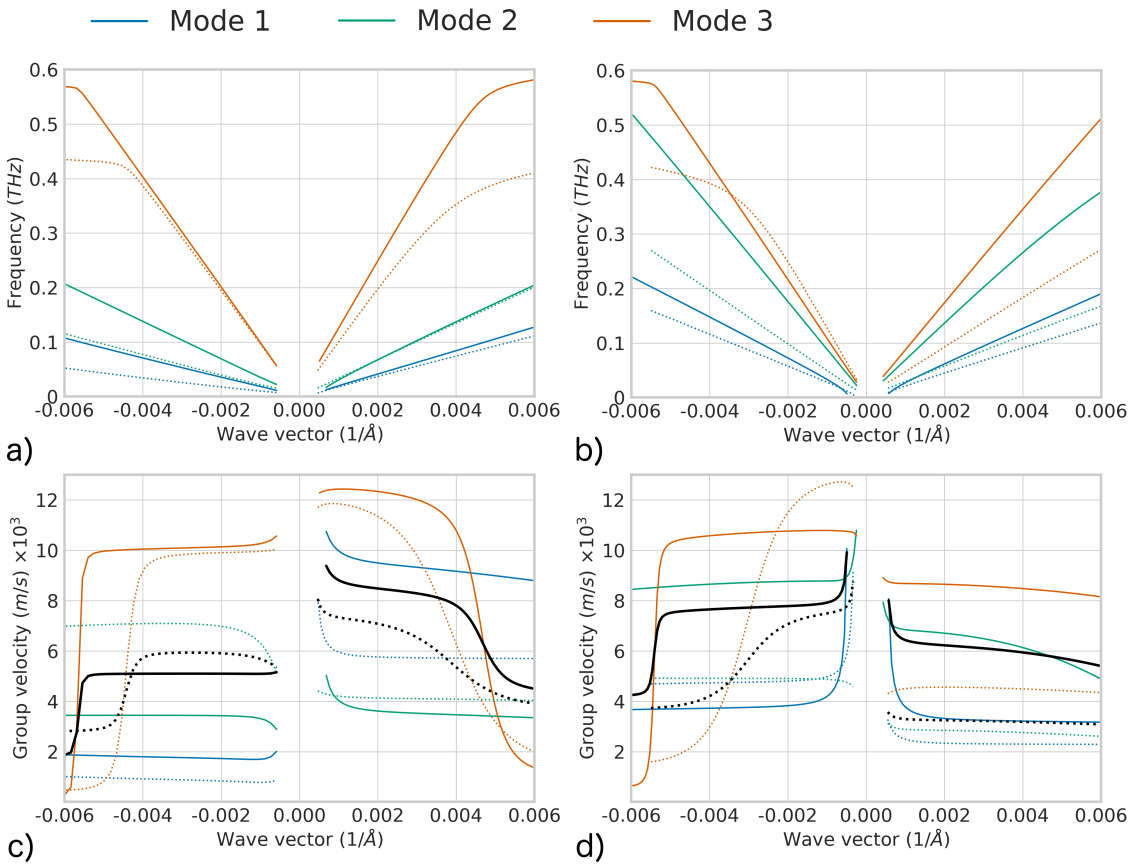

Figure 5.3: Figs. a) and b) are phonon dispersions zoomed in near the Γ point for the channel–chain and a–c directions, respectively. Figs. c) and d) are the corresponding phonon group velocities. Values at and very near the Γ point are not reliable and thus are not plotted. We found these to be slightly below zero for some modes, an indication that the framework could have been further relaxed. Modes 1–3 are labeled. Solid lines correspond to the open-pore, and dashed lines to the closed-pore frameworks. The black lines show an average of the group velocities for the three modes.

The deformation of MIL-53 is accompanied by changes in phonon group velocities in the direction of the linker. As we expected, this suggests that the lattice mode contributions to the linker resistance R_L changes as the network is deformed, and so the central premise that the linkers are independent thermal resistors does not hold. The average group velocities along the chain is less significantly altered in the "breathing" of the MIL-53 (see

Fig. 5.3 c)), where it increases, unlike along the linker, a and c. There is one caveat that needs to be drawn attention to regarding the calculations along the channel, that precludes comparisons between calculations performed with MD and dftb+: unlike in the other directions, the length of the channel increases noticeably between the open- and closed-pore configurations in dftb+, while a small decrease happens in MD. Experiments [363] suggest a small increase should be observed (see Table 5.4 in the supplementary materials).

Some abrupt changes in the group velocities and frequencies in Fig. 5.3 are due to an incomplete description of the modes, i.e. when optical modes are lower than the acoustic mode, they become entangled and while this is visually clear, it is difficult to extricate the optical modes and plot the full acoustic modes. However, mode 3 (in orange) along the chain (for both the op and cp MIL53), and mode 3 along a are effectively rapidly changing near Γ. The most significant changes to the group velocities happen along c, and to some extent a. While the lower velocity along a could explain the discrepancy between the actual thermal conductivity values and the expected value to changes in the geometry, the same justification does not hold for transport along c. A lower group velocity along c should 'push it' in the same direction as the geometric model. In other words, the changes in the group velocities do not appear to explain deviation from the model along c. One reason why we might expect the thermal conductivity to increase along c instead of decreasing, as predicted by the model, is that as the pores narrow, the corners of the linker become in contact with each other, resulting in a larger surface area for heat conduction. Even accounting for the discrepancies in channel length between dftb+ and the classical potential for the cp MIL-53, changes along b are also not seemingly justified. It would be expected that the computed

thermal conductivity along each string of aluminum nodes should remain nearly constant given the small change in channel length between the two breathing modes. Instead, we find it is kept approximately constant across the sum of the nodes, even as they become denser. Without apparent significant changes to the group velocities, it is reasonable to assume that increased phonon scattering in the cp MIL-53 could be the source of its lower-than-expected thermal conductivity.

In addition to changes in group velocity due to the non-linear behavior of some modes, such as the longitudinal mode (along a in the closed-pore MIL-53, as discussed above), other interesting features can be seen in the behavior of the group velocities. If we consider the lowest frequency mode (in blue) along the linker–node chain, upon inspection of the one-dimension dispersion plot (Figs. 5.3 a) and c)), we would expect to find the group velocities in closed- and open-pore frameworks to be much closer. Similarly, the derivative of the same mode along a (Fig. 5.3 b) and d)) would seemingly hint at a higher group velocity for the op MIL-53, yet that is not the case; conversely the first two modes of the closed pore framework in the direction of have apparent different derivatives, but very similar group velocities. The peculiar behavior of the group velocities drew our attention to the circled features in the dispersion plots in Fig. 5.2, which show a prevalence of flattened acoustic modes in the narrow pore framework. In the next section we introduce a simple model that could help explain these features.

Rattler modes

To help interpret the phonon dispersion we have developed a simple chain and spring model for an idealized framework. The model is as depicted in Fig. 5.4 b), a 2-

D network comprised of a 1-D chain of masses connected to each other by springs, and an additional spring and mass to model a rattler. The dispersion of these toy models reveals rattler behavior in which the acoustic band flattens into a *rattler mode* with zero group velocity and the trajectory of the acoustic band is picked up by an optical mode. This crossover behavior produces a band gap in the dispersion, and flattens the acoustic mode. As indicated in Fig. 5.2, the same feature shows up along the linker and the interrelated a and c directions. As the framework transitions between the open- and closed-pore structures, the linker becomes compressed (see Fig. 5.1 b), and Table 5.4). It is possible that this inhibits the rattler behavior otherwise present in the op MIL-53. Rattler modes could explain the apparent contradiction between the expected changes in thermal conductivity due to the geometry of the framework, if the heat that was previously carried by the acoustic modes becomes carried by optical modes for slightly higher wave vectors.

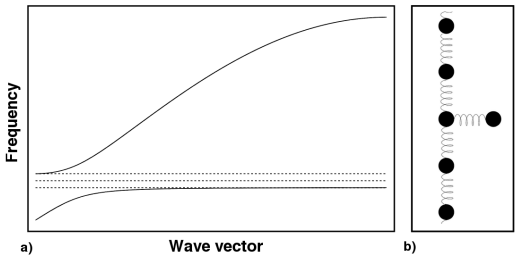

Figure 5.4: Model of a 1-d chain with a rattler, as portrayed in b), and an example, Fig. a), where its acoustic mode is dampened by the optical mode of the rattler.

Evidence of phonon focusing

The discrepancy between the group velocities and the derivative of the modes along the chain and linker directions in the closed pore framework, discussed earlier in this

work, suggests that there is a phonon-focusing effect at play, inducing the suppression of modes and correspondingly affecting the thermal conductivity of both breathing states, but particularly the compressed framework.

"In elastically anisotropic cubic crystals, the phonon flux emitted by a point heat source is focused in some direction in the crystal lattice due to non-collinearity of the phase and group phonon velocities" I think the idea is that there will be regions where the group velocity and the phase velocity (and thus k, since they point in the same direction) do not point in the same direction, and the scattering of phonons happens preferentially in one (or several) direction(s) instead of somewhat uniformly from a "heat source"

phase velocity and other characteristics of the wave are modified

for any direction in a crystal from the relation between the directions of the wave vector R, or the phase velocity V, and the corresponding directions of energy flow or group velocity V which Musgrave and Miller" have derived.

5.5 Supplementary materials

The bonds, angles and dihedrals are computed herein for the MIL-53 op and cp structures obtained with DFT, DFTB, and classically with the potential of Vanduyfhuys *et al.*. The calculation details are included in the manuscript. In Tables 5.1–5.3 the standard deviation has been included only when greater or equal to the values' significant figures (i.e. 0.01 for bond lengths, and 0.1 for angles and dihedrals).

Bond	DFTB (Å)	DFT (Å)	Potential [619] (Å)
O_l -C_1	1.31	1.26	1.27
C_1-C_2	1.49	1.48	1.50
C_2-C_3	1.40	1.39	1.40
C_3-C_3	1.39	1.38	1.39
C_3-H_l	1.10	1.10	1.08
O_1-Al	1.92	1.89	1.96 ± 0.01
O_n-Al	1.91	1.83	1.85 ± 0.01
O_n-H_n	0.96	0.97	0.91

Table 5.1: Table of bond lengths obtained for MIL-53(Al) using DFTB, DFT, and Vanduyfhuys *et al.* [619] classical potential. The subscripts n and l indicate a node and a linker atom, respectively. C_1 is the carbon linked to the linker oxygens, the C_2 atom bonds to C_1, and C_3 refers to the hydrogenated carbon atoms in the benzene rings.

Angle	DFTB (^{o})	DFT (^{o})	Potential [619] (^{o})
O_l-C_1-O_l	124.7 ± 0.1	125.6 ± 0.2	123.8 ± 0.2
C_1-C_2-C_3	120.8	119.9 ± 0.1	120.7
C_3-C_2-C_3	118.3	120.2	118.7
C_2-C_3-H_l	119.1	118.2	119.3 ± 0.1
C_3-C_3-H_l	120.0	121.9 ± 0.1	120.0 ± 0.1
C_2-C_3-C_3	120.8	119.9	120.7
C_1-C_2-O_l	117.6	117.2 ± 0.1	118.1 ± 0.3
C_1-O_l-Al	134.4 ± 0.1	133.3 ± 0.2	130.4 ± 2.2
Al-O_n-Al	128.1 ± 0.2	128.6	123.9 ± 0.3
Al-O_n-H_n	111.1	115.2	116.9 ± 0.3
O_l-Al-O_l (i)	180.0	180.0	178.4 ± 0.1
O_l-Al-O_l (ii)	89.1 ± 0.1	90.3 ± 0.8	90.3 ± 1.9
O_l-Al-O_n (i)	88.8	88.3	84.6
O_l-Al-O_n (ii)	91.2	91.7	93.0
O_n-Al-O_n	180.0	180.0	176.2 ± 0.2

Table 5.2: Table of angles for MIL-53(Al) using DFTB, DFT, and Vanduyfhuys *et al.* [619] classical potential. The subscripts n and l indicate a node and a linker atom, respectively. C_1 is the carbon linked to the linker oxygens, the C_2 atom bonds to C_1, and C_3 refers to the hydrogenated carbon atoms in the benzene rings. Angles O_l-Al-O_l, and O_l-Al-O_n are further subcategorized. In the O_l-Al-O_l angle (i) corresponds to the case where the linker oxygens belong to horizontally aligned linkers, and (ii) to the case where the linker oxygens are located in linkers perpendicular to each other. In the O_l-Al-O_n angle, in (i) the node and linker oxygens are located along the same linker direction, and in (ii) the node and linker oxygens are parallel to each other along b.

Dihedral	DFTB (^{o})	DFT (^{o})	Potential [619] (^{o})
O_l-C_1-C_2-C_3	179.7 ± 0.1	179.7 ± 0.2	178.3 ± 0.8
Al-O_l-C_1-C_2	176.5 ± 0.5	172.7 ± 0.3	162.4 ± 5.0
C_1-C_2-C_3-H_l	0.0	0.2 ± 0.2	0.2 ± 0.1
Al-O_l-C_1-O_l	4.3 ± 0.7	7.7 ± 0.3	17.6 ± 7.0
C_2-C_3-C_3-H_l	180.0	179.8 ± 0.2	179.8 ± 0.1
C_2-C_3-C_3-C_2	0.0	0.1	0.2 ± 0.1
C_3-C_2-C_3-C_3	0.0	0.1 ± 0.1	0.1 ± 0.1
H_l-C_3-C_3-H_l	0.0	0.4	0.1 ± 0.1
C_3-C_2-C_3-H_l	179.9	179.8 ± 0.1	179.8 ± 0.1
H_n-O_n-Al-O_l	[7.8, 82.87, 146.6]	[33.9, 57.7, 122.4, 146.6]	

Table 5.3: Table of dihedrals for MIL-53(Al) using DFTB, DFT, and Vanduyfhuys *et al.* [619] classical potential. The subscripts n and l indicate a node and a linker atom, respectively. C_1 is the carbon linked to the linker oxygens, the C_2 atom bonds to C_1, and C_3 refers to the hydrogenated carbon atoms in the benzene rings.

MIL-53 (Al)	Method	a ($\AA$)	b ($\AA$)	c ($\AA$)	volume ($\AA^3$)	α deg	β deg	γ deg
lp	DFTB	16.306	6.858	13.836	1,547.2	90.000	90.000	90.000
	DFT	16.466	6.602	13.007	1,414.3	90.000	90.003	90.000
	Experiment (77 K) [363]	16.913	6.624	12.671	1,419.6	90.000	90.000	90.000
	Potential [619]	16.410	6.541	13.757	1,476.6	90.062	90.000	90.007
np	DFTB	19.240	8.436	7.383	1,198.3	90.000	90.031	90.000
	DFT	19.067	7.191	6.579	902.383	90.003	89.988	90.001
	Experiment (77 K) [363]	20.824	6.871	6.607	863.9	90.000	113.949	90.000
	Potential [619] (at 300 K, 300 MPa)	19.417	6.374	6.319	782.1	89.996	90.001	89.934

Table 5.4: Table of lattice parameters for MIL-53(Al). The lattice parameters and angles described herein follow the orientation indicated in Fig. 5.1

Chapter 6

Conclusions

In this dissertation we have presented three approaches to study the fundamental thermal transport mechanism of MOFs: (shown in Fig. 1.1): (a) computing the MOFs with systematically increasing linker length in Chapter 4, (b) computing MOFs with articulated network geometry in Chapter 5 and (c) computing MOFs filled with things (MOFs and gases) in Chapter **??**. We have presented a systematic study of the interplay of MOF architecture with heat transport mechanisms. It was found that many aspects of the framework impact both the molecular-mode and lattice-mode transport processes.

In both of these cases simulations show very different dynamics in the heat current fluctuations. We thus conclude that changes to κ are buffered, because the linker mass and the O-C1-C2 angle affect the lattice and molecular modes in opposite directions. To engineer a substantial net change in κ it is necessary to identify parameters that change both heat transport mechanisms in the same direction. In this work we have found two such parameters: the node mass, and the linker arm length. The lattice-mode and molecular-

mode thermal conductivity are both reduced by increasing the mass of nodes and the lengthening linker arms.

We have presented a new approach to analyzing equilibrium molecular dynamics simulations to obtain insight into heat transport mechanisms. This approach is based on the Green-Kubo method and involves spatially decomposing the instantaneous heat current, and computing the regional autocorrelations and cross-correlations separately. The sign of the cross-correlation reveals information about heat transfer between regions.

Finally, it was found that the thermal conductivity is increased by loading MOF-5 with gas, with κ increasing with both the concentration and mass of the adsorbed gas. This result is beneficial for many gas adsorption applications where the rate of adsorption is limited by the removal of latent heat. A more complete understanding of the mechanisms of adsorbate-enhanced thermal transport will facilitate design of MOFs with desired thermal properties, and so this is an area of continued research.

Bibliography

[1] Details of this "phonon tracking" approach are described elsewhere [202] and will thus not be repeated here.

[2]

[3] Fuel cell technologies office multi-year research, development and demonstration plan, 2012.

[4] Fuel cell technologies office multi-year research, development and demonstration plan, 2012. Section 3.3 Hydrogen Storage.

[5] *Mapping thermal resistance around vacancy defects in graphite*, volume 1543, 2013.

[6] Angel Abarca, Pilar Gómez-Sal, Avelino Martín, Miguel Mena, Josep María Poblet, and Carlos Yélamos. Ammonolysis of mono(pentamethylcyclopentadienyl) titanium(IV) derivatives. *Inorg. Chem.*, 39(4):642–651, 2000.

[7] Colin D. Abernethy, Gareth M. Codd, Mark D. Spicer, and Michelle K. Taylor. A highly stable N-heterocyclic carbene complex of trichloro-oxo-vanadium(V) displaying novel Cl—C(carbene) bonding interactions. *J. Am. Chem. Soc.*, 125(5):1128–1129, 2003.

[8] S. Ahmed and K. Wallace. Evaluating a Functional Basis. In *Proceedings of the ASME Design Engineering Technical Conferences and Computers in Engineering Conference*, 2003.

[9] R. K. Ahuja, T. L. Magnanti, and J. B. Orlin. *Network Flows: Theory, Algorithms, and Applications*. Prentice Hall, Upper Saddle River, NJ, 1993.

[10] V. Akman, P.J.W. ten Haagen, and T. Tomiyama. A Fundamental and Theoretical Framework for an Intelligent CAD System. *Computer-Aided Design*, 22(6):352–368, 1990.

[11] L. Al-Hakim, A. Kusiak, and J. Mathew. A Graph-Theoretic Approach to Conceptual Design with Functional Perspectives. *Computer-Aided Design*, 32(14):867–875, 2000.

[12] B.J. Alder and T.E. Wainwright. Studies in molecular dynamics. i. general method. *Journal of Chemical Physics*, 31:459–466, 1959.

[13] B. Allen. Toolkit for decision-based design theory. *Journal of Engineering Valuation and Cost Analysis*, 3(2):85–105, 2000.

[14] M.P. Allen and D.J. Tildesley. *Computer Simulation of Liquids*. Oxford University Press, USA, 1991.

[15] Philip B. Allen and Joseph L. Feldman. Thermal conductivity of disordered harmonic solids. *Phys. Rev. B*, 48(17):12581–12588, Nov 1993.

[16] G. S. Altshuller. *Creativity as an exact science*. Gordon and Breach Publishers, Luxembourg, 1984.

[17] Neil Anderson, Achim Hartschuh, and Lukas Novotny. Chirality changes in carbon nanotubes studied with near-field raman spectroscopy. *Nano Letters*, 7(3):577–582, 2007.

[18] Eduardo Anglada, Jos?? M. Soler, Javier Junquera, and Emilio Artacho. Systematic generation of finite-range atomic basis sets for linear-scaling calculations. *Physical Review B*, 66(20):205101, November 2002.

[19] E. Antonsson and J. Cagan. *Formal Engineering Design Synthesis*. Cambridge University Press, 2001.

[20] E. Antonsson and K. Otto. Imprecision in engineering design. *Journal of Mechanical Design*, 117(B):25–32, 1995.

[21] Leah N. Appelhans, Daniele Zuccaccia, Anes Kovacevic, Anthony R. Chianese, John R. Miecznikowski, Aleco Macchioni, Eric Clot, Odile Eisenstein, and Robert H. Crabtree. An anion-dependent switch in selectivity results from a change of C—H activation mechanism in the reaction of an imidazolium salt with $IrH_5(PPh_3)_2$. *J. Am. Chem. Soc.*, 127(46):16299–16311, 2005.

[22] Balint Aradi, Ben Hourahine, and Th Frauenheim. Dftb+, a sparse matrix-based implementation of the dftb method. *The Journal of Physical Chemistry A*, 111(26):5678–5684, 2007.

[23] Anthony J. Arduengo, III, H. V. Rasika Dias, Richard L. Harlow, and Michael Kline. Electronic stabilization of nucleophilic carbenes. *J. Am. Chem. Soc.*, 114(14):5530–5534, 1992.

[24] Anthony J. Arduengo, III, Siegfried F. Gamper, Joseph C. Calabrese, and Fredric Davidson. Low-coordinate carbene complexes of nickel(0) and platinum(0). *J. Am. Chem. Soc.*, 116(10):4391–4394, 1994.

[25] J. L. Arlett, J. R. Maloney, B. Gudlewski, M. Muluneh, and M. Roukes. Self-sensing micro- and nanocantilevers with attonewton-scale force resolution. *Nano Letters*, 6(6):1000–1006, 2006.

[26] Rickard Armiento, Boris Kozinsky, Marco Fornari, and Gerbrand Ceder. Screening for high-performance piezoelectrics using high-throughput density functional theory. *Physical Review B*, 84(1):014103, July 2011.

[27] S. G. Arunajadai, R. B. Stone, and I. Y. Tumer. Failure mode identification through clustering analysis. *Quality and Reliability Engineering International Journal*, 20:511–526, 2004.

[28] V. Attaluri, D. McAdams, R. Stone, and A. De Crescenzo. Visual Representations as an Aid to Concept Generation. In *Proceedings of the ASME Design Engineering Technical Conferences and Computers in Engineering Conference*, 2006.

[29] Martin P. Attfield and Pablo Cubillas. Crystal growth of nanoporous metal organic frameworks. *Dalton Transactions*, 41(14):3869–3878, March 2012.

[30] Martin P. Attfield and Pablo Cubillas. Crystal growth of nanoporous metal organic frameworks. *Dalton Transactions*, 41(14):3869, 2012.

[31] Martin P. Attfield and Pablo Cubillas. Crystal growth of nanoporous metal organic frameworks. *Dalton Trans.*, 41:3869–3878, 2012.

[32] Hasan Babaei, Pawel Keblinski, and J. M. Khodadadi. A proof for insignificant effect of brownian motion-induced micro-convection on thermal conductivity of nanofluids by utilizing molecular dynamics simulations. *Journal of Applied Physics*, 113(8):084302, 2013.

[33] Hasan Babaei and Christopher E. Wilmer. Mechanisms of heat transfer in porous crystals containing adsorbed gases: Applications to metal-organic frameworks. *Phys. Rev. Lett.*, 116:025902, Jan 2016.

[34] B. Babić, J. Furer, S. Sahoo, Sh. Farhangfar, and C. Schönenberger. Intrinsic thermal vibrations of suspended doubly clamped singe-wall carbon nanotubes. *Nano Letters*, 3:1577–1580, 2003.

[35] Alexander A Balandin. Nanophononics: phonon engineering in nanostructures and nanodevices. *Journal of nanoscience and nanotechnology*, 5(7):1015–1022, 2005.

[36] Alexander A. Balandin. Thermal properties of graphene and nanostructured carbon materials. *Nature Materials*, 10(8):569–581, August 2011.

[37] Perla Balbuena and Jorge M. Seminario, editors. *Molecular Dynamics*. Elsevier Science, 1 edition, May 1999.

[38] Karin Barthelet, Jérôme Marrot, Didier Riou, and Gérard Férey. A breathing hybrid organic–inorganic solid with very large pores and high magnetic characteristics. *Angewandte Chemie*, 114(2):291–294, 2002.

[39] J. Barzilai. Measurement and preference function modeling. *International Transactions in Operational Research*, 12:173–183, 2001.

[40] Christina A. Bauer, Tatiana V. Timofeeva, Thomas B. Settersten, Brian D. Patterson, Vincent H. Liu, Blake A. Simmons, and Mark D. Allendorf. Influence of connectivity and porosity on ligand-based luminescence in zinc metal-organic frameworks. *Journal of the American Chemical Society*, 129(22):7136–7144, 2007. PMID: 17503820.

[41] Oren Benami and Yan Jin. Creative stimulation in conceptual design. In *Proceedings of the ASME Design Engineering Technical Conferences*, 2002.

[42] Savas Berber, Young-Kyun Kwon, and David Tománek. Unusually high thermal conductivity of carbon nanotubes. *Physical Review Letters*, 84:4613–4616, 2000.

[43] Joshua I. Bernstein. *Design methods in the aerospace industry: looking for evidence of set-based practices*. Dissertation, Massachusetts Institute of Technology, 1998.

[44] A. Bhadra and G.W. Fischer. A New GT Classification Approach: A Database with Graphical Dimensions. *Manufacturing Review*, 1(1):44–49, 1988.

[45] L. Blanchette and K. Dunbar. How analogies are generated: the roles of structural and superficial similarity. *Memory and cognition*, 28(1):108–124, 2000.

[46] L. Blanchette and K. Dunbar. Analogy use in naturalistic settings: the influence of audience, emotion, and goals. *Memory and cognition*, 29(5):730–735, 2001.

[47] C. Bliek. Set based hierarchical design: A constraint satisfaction approach. In *Proceedings of the ASME Design Engineering Technical Conferences*, 1995.

[48] Peter E Blöchl. Projector augmented-wave method. *Physical Review B*, 50(24):17953, 1994.

[49] JPL Review Board. Report on the loss of the mars polar lander and deep space 2 missions. Technical Report JPL D-18709, NASA JPL, 2000.

[50] Arun Bodapati, Patrick K. Schelling, Simon R. Phillpot, and Pawel Keblinski. Vibrations and thermal transport in nanocrystalline silicon. *Phys. Rev. B*, 74(24):245207, Dec 2006.

[51] M. Bohm, K. R. Haapala, K. Poppa, R. B. Stone, and I. Y. Tumer. Towards integrating sustainability analysis into the conceptual phase of product design. *Journal of Mechanical Design*, 132, 2010.

[52] M. Bohm, R. Stone, T. Simpson, and E. Steva. Introduction of a Data Schema: The Inner Workings of a Design Repository. In *Proceedings of the ASME Design Engineering Technical Conferences and Computers in Engineering Conference*, 2006.

[53] M. Bohm, R. Stone, and S. Szykman. Enhancing Virtual Product Representations for Advanced Design Repository Systems. *Journal of Computer and Information Science in Engineering*, 5(4):360–372, 2005.

[54] Matt R. Bohm, Robert B. Stone, Timothy W. Simpson, and Elizabeth D. Steva. Introduction of a data schema to support a design repository. *Computer-Aided Design*, 40(7):801–811, July 2008.

[55] Matt R. Bohm, Jayson P. Vucovich, and Robert B. Stone. Capturing creativity: Using a design repository to drive concept innovation. In *Proceedings of the ASME Design Engineering Technical Conferences*, 2005.

[56] Arezki Booudaoud, Yves Couder, and Martine Ben Amar. Self-adaptation in vibrating soap films. *Physical Review Letters*, 82:3847–3850, 1999.

[57] Patrice Bordat, Dirk Reith, and Florian Müller-Plathe. The influence of interaction details on the thermal diffusion in binary lennard-jones liquids. *The Journal of Chemical Physics*, 115(19):8978–8982, 2001.

[58] A. Boudaoud, Y. Couder, and M. Ben Amar. A self-adaptive oscillator. *European Physical Journal B*, 9:159–165, 1999.

[59] Donald W. Brenner, Olga A. Shenderova, Judith A. Harrison, Steven J. Stuart, and Boris Ni a nd Susan B. Sinnott. A second-generation reactive empirical bond order (rebo) poterntial energy expression for hydrocarbons. *Journal of Physics: condensed Matter*, 14:783–802, 2002.

[60] Jonathan W. Brown, Bryana L. Henderson, Matthew D. Kiesz, Adam C. Whalley, William Morris, Sergio Grunder, Hexiang Deng, Hiroyasu Furukawa, Jeffrey I. Zink, J. Fraser Stoddart, and Omar M. Yaghi. Photophysical pore control in an azobenzene-containing metal???organic framework. *Chemical Science*, 4(7):2858, 2013.

[61] Jonathan W. Brown, Bryana L. Henderson, Matthew D. Kiesz, Adam C. Whalley, William Morris, Sergio Grunder, Hexiang Deng, Hiroyasu Furukawa, Jeffrey I. Zink, J. Fraser Stoddart, and Omar M. Yaghi. Photophysical pore control in an azobenzene-containing metal-organic framework. *Chem. Sci.*, 4:2858–2864, 2013.

[62] O. Brown and P. Eremenko. Application of value-centric design to space architectures: the case of fractionated spacecraft. In *Proceedings of the American Institute of Aeronautics and Astronautics Conference*, volume AIAA Paper 2008-7869, 2008.

[63] C. Bryant. Software Evaluation of an Automated Concept Generator Design Tool. In *Proceedings of the 2006 ASEE Annual Conference*, 2006.

[64] C. Bryant, D. McAdams, R. Stone, T. Kurtoglu, and M. Campbell. A Validation Study of an Automated Concept Generator Design Tool. In *Proceedings of the ASME Design Engineering Technical Conferences and Computers in Engineering Conference*, 2006.

[65] C. Bryant, R. Stone, D. McAdams, T. Kurtoglu, and M. Campbell. Concept Generation from the Functional Basis of Design. In *Proceedings of the International Conference on Engineering Design*, 2005.

[66] C.R. Bryant, R.B. Stone, and D.A. McAdams. Automated Concept Generation from the Functional Basis of Design. *Research in Engineering Design*, Accepted for publication, 2007.

[67] M. Burgin, H. K. Lee, and N. Debnath. Software technological roles, usability, and reusability. In *IEEE International Conference on Information Reuse and Integration*, 2004.

[68] Giovanni Bussi, Davide Donadio, and Michele Parrinello. Canonical sampling through velocity rescaling. *The Journal of Chemical Physics*, 126(1):014101, 2007.

[69] J Butler, G G Jayson, and A J Swallow. The reaction between the superoxide anion radical and cytochrome c. *Biochimica et biophysica acta*, 408(3):215–222, December 1975. PMID: 60.

[70] David G. Cahill, Kenneth Goodson, and Arunava Majumdar. Thermometry and thermal transport in micro/nanoscale solid-state devices and structures. *Journal of Heat Transfer*, 124:223–241, 2002.

[71] David G. Cahill, S. K. Watson, and R. O. Pohl. Lower limit to the thermal conductivity of disordered crystals. *Physics Review B*, 46(10):6131–6139, 1992.

[72] David G. Cahill, S. K. Watson, and R. O. Pohl. Lower limit to the thermal conductivity of disordered crystals. *Phys. Rev. B*, 46:6131–6140, Sep 1992.

[73] W. Cai. Introduction to molecular simulations. February 2007.

[74] W. Cai. Introduction to statistical mechanics. March 2012.

[75] M. Campbell. Knowledge discovery in Deep Blue. *Communications of the ACM*, 42(11):65–67, 2002.

[76] M. Campbell, J. Cagan, and K. Kotovsky. Agent-based Synthesis of Electro-Mechanical Design Configurations. *Journal of Mechanical Design*, 122(1):61–69, 2000.

[77] M. Campbell, J. Cagan, and K. Kotovsky. Learning From Design Experience: Todo/Taboo Guidance. In *Proceedings of the ASME Design Engineering Technical Conferences and Computers in Engineering Conference*, 2001.

[78] Pieremanuele Canepa, Nour Nijem, Yves J. Chabal, and T. Thonhauser. Diffusion of small molecules in metal organic framework materials. *Physical Review Letters*, 110(2):026102, January 2013.

[79] Guoxin Cao, Xi Chen, and Jeffrey W. Kysar. Thermal vibration and apparent thermal contraction of single-walled carbon nanotubes. *Journal of the Mechanics and Physics of Solids*, 54(6):1206 – 1236, 2006.

[80] Rachael Carkett. 'He's different, he's got 'Star Trek' Vision': Supporting the expertise of conceptual design engineers. *Design Studies*, 25(5):459–475, 2004.

[81] Satish K. Nune Carlos A Fernandez. Synthesis, characterization, and application of metal organic framework nanostructures. *Langmuir : the ACS journal of surfaces and colloids*, 26(24):18591–4, 2010.

[82] Grace Ordaz Carole Read, George Thomas and Dr. Sunita Satyapal. U.s. department of energy's system targets for on-board vehicular hydrogen storage. *Material Matters*, 2:3, 2007.

[83] Grace Ordaz Carole Read, George Thomas and Sunita Satyapal. U.s. department of energy-s system targets for on-board vehicular hydrogen storage. *Material Matters*, 2:3, 2007.

[84] Ivano E. Castelli, Thomas Olsen, Soumendu Datta, David D. Landis, S??ren Dahl, Kristian S. Thygesen, and Karsten W. Jacobsen. Computational screening of perovskite metal oxides for optimal solar light capture. *Energy & Environmental Science*, 5(2):5814–5819, January 2012.

[85] M. Catti, G. Valerio, and R. Dovesi. Theoretical study of electronic, magnetic, and structural properties of ??-fe_{2}o_{3} (hematite). *Physical Review B*, 51(12):7441–7450, March 1995.

[86] Gerbrand Ceder. Opportunities and challenges for first-principles materials design and applications to li battery materials. *MRS Bulletin*, 35(09):693–701, January 2011.

[87] Center for History and New Media. Zotero quick start guide.

[88] C.D. Cera, W.C. Regli, I. Braude, Y. Shapirstein, and C.V. Foster. A Collaborative 3D Environment for Authoring Design Semantics. *IEEE Computer Graphics and Applications: Graphics in Advanced Computer-Aided Design*, 22(3):43–55, 2002.

[89] S. Chacko, M. Deshpande, and D. G. Kanhere. Structural and electronic properties of aluminum-based binary clusters. *Physical Review B*, 64(15):155409, October 2001.

[90] T. Chalati, P. Horcajada, R. Gref, P. Couvreur, and C. Serre. Optimisation of the synthesis of MOF nanoparticles made of flexible porous iron fumarate MIL-88A. *Journal of Materials Chemistry*, 21(7):2220–2227, February 2011.

[91] C. W. Chang, D. Okawa, H. Garcia, A. Majumdar, and A. Zettl. Breakdown of fourier's law in nanotube thermal conductors. *Physical Review Letters*, 101:075903, 2008.

[92] W. L. Chapman, A. T. Bahill, and A. W. Wymore. *Engineering modeling and design*. CRC Press, London, UK, 1996.

[93] Jianwei Che, Tahir Çagin, Weiqiao Deng, and William A. Goddard III. Thermal conductivity of diamond and related materials from molecular dynamics simulations. *The Journal of Chemical Physics*, 113(16):6888–6900, 2000.

[94] Bi Chen, Xiujian Wang, Qianfeng Zhang, Xiaoyong Xi, Jingjing Cai, Huang Qi, Si Shi, Jie Wang, Dan Yuan, and Min Fang. Synthesis and characterization of the interpenetrated mof-5. *J. Mater. Chem.*, 20:3758–3767, 2010.

[95] G. Chen. Levels of application of computer simulation in engineering disciplines education. *Education Technology and Computer (ICETC), 2010 2nd International Conference*, 2:117–120, 22-24 June 2010.

[96] W. Chen and K. Lewis. A Robust Design Approach for Achieving Flexibility in Multidisciplinary Design. *AIAA Journal*, 37(8):982–989, 1999.

[97] I. V. Chernyshova, M. F. Hochella Jr, and A. S. Madden. Size-dependent structural transformations of hematite nanoparticles. 1. phase transition. *Physical Chemistry Chemical Physics*, 9(14):1736–1750, March 2007.

[98] Dam Hieu Chi, Nguyen Thanh Cuong, Nguyen Anh Tuan, Yong-Tae Kim, Ho Tu Bao, Tadaoki Mitani, Taisuke Ozaki, and Hidemi Nagao. Electronic structures of pt clusters adsorbed on (5,5) single wall carbon nanotube. *Chemical Physics Letters*, 432(1-3):213–217, 2006.

[99] Letizia Chiodo, Juan Maria Garcia-Lastra, Amilcare Iacomino, Stefano Ossicini, Jin Zhao, Hrvoje Petek, and Angel Rubio. Self-energy and excitonic effects in the electronic and optical properties of TiO2 crystalline phases. *arXiv:1003.6010*, March 2010.

[100] Catalin Chiritescu, David G Cahill, Ngoc Nguyen, David Johnson, Arun Bodapati, Pawel Keblinski, and Paul Zschack. Ultralow thermal conductivity in disordered, layered wse2 crystals. *Science*, 315(5810):351–353, 2007.

[101] Jongweon Cho, Luis Berbil-Bautista, Ivan V. Pechenezhskiy, Niv Levy, Steven K. Meier, Varadharajan Srinivasan, Yosuke Kanai, Jeffrey C. Grossman, K. Peter C. Vollhardt, and Michael F. Crommie. Single-molecule-resolved structural changes induced by temperature and light in surface-bound organometallic molecules designed for energy storage. *ACS Nano*, 5(5):3701–3706, May 2011.

[102] J.I. Choe and B. Kim. Determination of proper time step for molecular dynamics simulation. *Korean Chemical Society*, 21(4):419–424, 2000.

[103] Byoung-Young Choi, Se-Jong Kahng, Seungchul Kim, Hajin Kim, Hyo Won Kim, Young Jae Song, Jisoon Ihm, and Young Kuk. Conformational molecular switch of the azobenzene molecule: a scanning tunneling microscopy study. *Physical review letters*, 96(15):156106, April 2006. PMID: 16712175.

[104] W. Choi, S. Hong, J. T. Abrahamson, J. H. Han, C. Song, N. Nair, S. Baik, and M. S. Strano. Chemically driven carbon-nanotube-guided thermopower waves. *Nature Materials*, 9:423–429, 2010.

[105] Henri Christiaans and Kees Venselaar. Design creativity in product innovation. *International Journal of Technology and Design Education*, 15(3):217–236, 2005.

[106] Yongchul G Chung, Jeffrey Camp, Maciej Haranczyk, Benjamin J Sikora, Wojciech Bury, Vaiva Krungleviciute, Taner Yildirim, Omar K Farha, David S Sholl, and Randall Q Snurr. Computation-ready, experimental metal–organic frameworks: A tool to enable high-throughput screening of nanoporous crystals. *Chemistry of Materials*, 26(21):6185–6192, 2014.

[107] D. Clausing. *Quality function deployment*. MIT Press, Cambridge, MA, 1994.

[108] D. Clausing. *Concurrent engineering*. ASM Handbook: Materials Selection and Design, 1997.

[109] Anne M. Coghill and Lorrin R. Garson, editors. *The ACS Style Guide*. Oxford University Press, Inc. and The American Chemical Society, New York, 3 edition, 2006.

[110] William G. Conley, Arvind Raman, Charles M. Krousgrill, and Saeed Mohammadi. Nonlinear and nonplaner dynamics of suspended nanotube and nanowire resonators. *Nano Letters*, 8:1590–1595, 2008.

[111] J. Coplien, D. Hoffman, and D. Weiss. Commonality and variability in software engineering. *IEEE Software*, 15(6):37 – 45, 1998.

[112] B. Corbett and D. W. Rosen. A configuration design based method for platform commonization for product families. *Artificial Intelligence for Engineering Design, Analysis and Manufacturing*, 18(1):21– 39, 2004.

[113] Frank Albert Cotton, Geoffrery Wilkinson, Carlos A. Murillio, and Manfred Bochmann. *Advanced Inorganic Chemistry*. Wiley, Chichester, 6 edition, 1999.

[114] D. L. Craig. *Perceptual simulation and analogical reasoning in design*. Dissertation, Georgia Institute of Technology, 2001.

[115] Nigel Cross. How creative design happens. In *Proceedings of the 12th IEEE International Requirements Engineering Conference*, 2004.

[116] Boya Cui, Cornelius O. Audu, Yijun Liao, SonBinh T. Nguyen, Omar K. Farha, Joseph T. Hupp, and Matthew Grayson. Thermal conductivity of zif-8 thin-film under ambient gas pressure. *ACS Applied Materials & Interfaces*, 9(34):28139–28143, 2017. PMID: 28791860.

[117] Stefano Curtarolo, Gus L. W. Hart, Marco Buongiorno Nardelli, Natalio Mingo, Stefano Sanvito, and Ohad Levy. The high-throughput highway to computational materials design. *Nature Materials*, 12(3):191–201, March 2013.

[118] Stefano Curtarolo, Wahyu Setyawan, Gus L.W. Hart, Michal Jahnatek, Roman V. Chepulskii, Richard H. Taylor, Shidong Wang, Junkai Xue, Kesong Yang, Ohad Levy, Michael J. Mehl, Harold T. Stokes, Denis O. Demchenko, and Dane Morgan. Aflow: An automatic framework for high-throughput materials discovery. *Computational Materials Science*, 58(0):218 – 226, 2012.

[119] Alexander U. Czaja, Natalia Trukhan, and Ulrich Meuller. Industrial applications of metal-organic frameworks. *Chemical Society Reviews*, 38(5):1284–1293, April 2009.

[120] Anne Dailly, John J. Vajo, and Channing C. Ahn. Saturation of hydrogen sorption in zn benzenedicarboxylate and zn naphthalenedicarboxylate. *The Journal of Physical Chemistry B*, 110(3):1099–1101, January 2006.

[121] Pnina Dauber-Osguthorpe, Victoria A Roberts, David J Osguthorpe, Jon Wolff, Moniqe Genest, and Arnold T Hagler. Structure and energetics of ligand binding to proteins: Escherichia coli dihydrofolate reductase-trimethoprim, a drug-receptor system. *Proteins: Structure, Function, and Bioinformatics*, 4(1):31–47, 1988.

[122] E. de Bono. *Lateral Thinking: Creativity Step by Step*. Harper and Row, 1970.

[123] Laura de Sousa Oliveira, Luping Han, Agnieszka Truszkowska, Wenxi Huang, Brady J. Gibbons, and P. Alex Greaney. Thermal conductivity transition in the breathing metal-organic-framework mil-53. *Manuscript in preparation*.

[124] Y.-M. Deng, G.A. Britton, and S.B. Tor. Constraint-based functional design verification for conceptual design. *CAD Computer Aided Design*, 32(14):889–899, 2000.

[125] D.Frenkel and B. Smit. *Understanding Molecular Simulation, Second Edition: From Algorithms to Applications*. Academic Press, 2 edition, November 2001.

[126] Davide Donadio and Giulia Galli. Thermal conductivity of isolated and interacting carbon nanotubes: Comparing results from molecular dynamics and the boltzmann transport equation. *Physical Review Letters*, 99:255502, 2007.

[127] Davide Donadio and Giulia Galli. Temperature dependence of the thermal conductivity of thin silicon nanowires. *Nano Letters*, 10(3):847–851, 2010. PMID: 20163124.

[128] J. A. Donndelinger. A decision-based perspective on the vehicle development process. In *Decision making in engineering design*, chapter 19, pages 217–225. ASME Press, 2006.

[129] K. Dorst and N. Cross. Creativity in the design process: Co-evolution of problem-solution. *Design Studies*, 22(5):425–437, 2001.

[130] F. P. Doty, C. A. Bauer, A. J. Skulan, P. G. Grant, and M. D. Allendorf. Scintillating metal-organic frameworks: A new class of radiation detection materials. *Advanced Materials*, 21(1):95–101, 2009.

[131] M. S. Dresselhaus and P. C. Eklund. Phonons in carbon nanotubes. *Advances in Physics*, 49(6):705–814, 2000.

[132] Kevin Drost. Microscale enhancement of heat and mass transfer for hydrogen energy storage, May 2014.

[133] T. Droubay, K. M. Rosso, S. M. Heald, D. E. McCready, C. M. Wang, and S. A. Chambers. Structure, magnetism, and conductivity in epitaxial ti-doped ??-fe_{2}o_{3} hematite: Experiment and density functional theory calculations. *Physical Review B*, 75(10):104412, March 2007.

[134] X. Du and W. Chen. Sequential optimization and reliability assessment method for efficient probabilistic design. *Journal of Mechanical Design*, 126(2):225–233, 2004.

[135] K. Dunbar. How scientists think: On-line creativity and conceptual change in science. In T. B. Ward, S. M. Smith, and J. Vaid, editors, *Creative Thought: An Investigation of Conceptual Structures and Processes*, pages 461–494. American Psychology Association, Washington, DC, 1997.

[136] Tina Düren and Randall Q Snurr. Assessment of isoreticular metal-organic frameworks for adsorption separations: a molecular simulation study of methane/n-butane mixtures. *The Journal of Physical Chemistry B*, 108(40):15703–15708, 2004.

[137] E. Durgun and Jeffrey C. Grossman. Photoswitchable molecular rings for solar-thermal energy storage. *The Journal of Physical Chemistry Letters*, 4(6):854–860, March 2013.

[138] Danil N. Dybtsev, Hyungphil Chun, and Kimoon Kim. Rigid and flexible: A highly porous Metal-Organic framework with unusual guest-dependent dynamic behavior. *Angewandte Chemie International Edition*, 43(38):5033–5036, 2004.

[139] Danil N. Dybtsev, Hyungphil Chun, and Kimoon Kim. Rigid and flexible: A highly porous Metal???Organic framework with unusual guest-dependent dynamic behavior. *Angewandte Chemie International Edition*, 43(38):5033???5036, 2004.

[140] Eric C. Dykeman and Otto F. Sankey. Low frequency mechanical modes of viral capsids: An atomistic approach. *Physicsl Review Letters*, 100:028101, 2008.

[141] Eric C. Dykeman and Otto F. Sankey. Vibrational energy funneling in viruses—simulations of impulsive stimulated raman scattering in m13 bacteriophage. *Journal of Physics: Condensed Matter*, 21:505102, 2009.

[142] C. L. Dym, W. H. Wood, and M. J. Scott. On the legitimacy of pairwise comparisons. In *Decision making in engineering design*, chapter 13, pages 135–143. ASME Press, 2006.

[143] Timothy L Easun, Junhua Jia, James A Calladine, Danielle L Blackmore, Christopher S Stapleton, Khuong Q Vuong, Neil R Champness, and Michael W George. Photochemistry in a 3d metal–organic framework (mof): Monitoring intermediates and reactivity of the fac-to-mer photoisomerization of re (diimine)(co) 3cl incorporated in a mof. *Inorganic chemistry*, 53(5):2606–2612, 2014.

[144] Mohamed Eddaoudi, Jaheon Kim, Nathaniel Rosi, David Vodak, Joseph Wachter, Michael O'Keeffe, and Omar M. Yaghi. Systematic design of pore size and functionality in isoreticular mofs and their application in methane storage. *Science*, 295(5554):469–472, 2002.

[145] Mohamed Eddaoudi, David B. Moler, Hailian Li, Banglin Chen, Theresa M. Reineke, Michael O'Keeffe, and Omar M. Yaghi. Modular chemistry: Secondary building units as a basis for the design of highly porous and robust metal-organic carboxylate frameworks. *Accounts of Chemical Research*, 34(4):319–330, 2001. PMID: 11308306.

[146] L. Eggli, H. Ching-yao, B.D. Bruderlin, and G. Elber. Inferring 3D Models from Freehand Sketches and Constraints. *Computer-Aided Design*, 29(2):101–112, 1997.

[147] K. L. Ekinci and M. L. Roukes. Nanoelectromechanical systems. *Review of Scientific Instruments*, 76(6):061101, 2005.

[148] Marcus Elstner, Dirk Porezag, G Jungnickel, J Elsner, M Haugk, Th Frauenheim, Sandor Suhai, and Gotthard Seifert. Self-consistent-charge density-functional tight-binding method for simulations of complex materials properties. *Physical Review B*, 58(11):7260, 1998.

[149] Roland Stote etc. Potential energy function, October 1999.

[150] Roland Stote etc. Theory of molecular dynamics simulations, October 1999.

[151] William J. Evans, Lin Hu, and Pawel Keblinski. Thermal conductivity of graphene ribbons from equilibrium molecular dynamics: Effect of ribbon width, edge roughness, and hydrogen termination. *Applied Physics Letters*, 96(20):–, 2010.

[152] D. Fairen-Jimenez, S. A. Moggach, M. T. Wharmby, P. A. Wright, S. Parsons, and T. D??ren. Opening the gate: Framework flexibility in ZIF-8 explored by experiments and simulations. *Journal of the American Chemical Society*, 133(23):8900–8902, June 2011.

[153] David Fairen-Jimenez, Raimondas Galvelis, Antonio Torrisi, Alistair D. Gellan, Michael T. Wharmby, Paul A. Wright, Caroline Mellot-Draznieks, and Tina D??ren. Flexibility and swing effect on the adsorption of energy-related gases on ZIF-8: combined experimental and simulation study. *Dalton Transactions*, 41(35):10752–10762, August 2012.

[154] G. Fantoni, C. Taviani, and R. Santoro. Design by functional synonyms and antonyms: A structured creative technique based on functional analysis. In *Proceedings of the Institution of Mechanical Engineers, Part B: Journal of Engineering Manufacture*, 2007.

[155] Omar K. Farha and Joseph T. Hupp. Rational design, synthesis, purification, and activation of Metal???Organic framework materials. *Accounts of Chemical Research*, 43(8):1166–1175, August 2010.

[156] David Farrusseng, editor. *Metal-Organic Frameworks: Applications from Catalysis to Gas Storage*. July 2011.

[157] Joseph L. Feldman, Philip B. Allen, and Scott R. Bickham. Numerical study of low-frequency vibrations in amorphous silicon. *Phys. Rev. B*, 59:3551–3559, Feb 1999.

[158] Joseph L. Feldman, Mark D. Kluge, Philip B. Allen, and Frederick Wooten. Thermal conductivity and localization in glasses: Numerical study of a model of amorphous silicon. *Phys. Rev. B*, 48(17):12589–12602, Nov 1993.

[159] Joseph L. Feldman, Mark D. Kluge, Philip B. Allen, and Frederick Wooten. Thermal conductivity and localization in glasses: Numerical study of a model of amorphous silicon. *Phys. Rev. B*, 48:12589–12602, Nov 1993.

[160] C. Feng and A. Kusiak. Constraint-based design of parts. *CAD Computer Aided Design*, 27(5):343–352, 1995.

[161] X. L. Feng, Rongrui He, Peidong Yang, and M. L. Roukes. Very high frequency silicon nanowire electromechanical resonators. *Nanoletters*, 7(7):1935–1959, 2007.

[162] Xiao Feng, Xuesong Ding, and Donglin Jiang. Covalent organic frameworks. *Chemical Society Reviews*, 41(18):6010–6022, August 2012.

[163] Gerard Férey. Hybrid porous solids: past, present, future. *Chem. Soc. Rev.*, 37:191–214, 2008.

[164] Gérard Férey and Christian Serre. Large breathing effects in three-dimensional porous hybrid matter: facts, analyses, rules and consequences. *Chem. Soc. Rev.*, 38:1380–1399, 2009.

[165] B L Feringa. In control of motion: from molecular switches to molecular motors. *Accounts of chemical research*, 34(6):504–513, June 2001. PMID: 11412087.

[166] Carlos A. Fernandez, Praveen K. Thallapally, and B. Peter McGrail. Insights into the temperature-dependent ???Breathing??? of a flexible fluorinated metal-organic framework. *ChemPhysChem*, 13(14):3275–3281, October 2012.

[167] Carlos A. Fernandez, Praveen K. Thallapally, and B. Peter McGrail. Insights into the temperature-dependent "breathing" of a flexible fluorinated metal-organic framework. *ChemPhysChem*, 13(14):3275–3281, 2012.

[168] M. French. *Conceptual design*. Springer-Verlag, London, UK, 1996.

[169] S. French. *Decision theory: An introduction to the mathematics of rationality*. Wiley, London, 1986.

[170] J Frenzel, AF Oliveira, N Jardillier, T Heine, and G Seifert. Semi-relativistic, self-consistent charge slater- koster tables for density-functional based tight-binding (dftb) for materials science simulations. *Zeolites*, 2(3):7, 2009.

[171] G??rard F??rey and Christian Serre. Large breathing effects in three-dimensional porous hybrid matter: facts, analyses, rules and consequences. *Chemical Society Reviews*, 38(5):1380–1399, April 2009.

[172] Hiroshi Fujisaki and Gerhard Stock. Dynamic treatment of vibrational energy relaxation in a heterogeneous and fluctuating environment. *The Journal of Chemical Physics*, 129(13):134110, 2008.

[173] M. Fujita, S. Sasaki, and K. Matsui. Object oriented analysis and design of hardware software codesigns with dependence analysis for design reuse. In *IEEE International Conference on Information Reuse and Integration*, 2005.

[174] Hiroyasu Furukawa, Kyle E Cordova, Michael OKeeffe, and Omar M Yaghi. The chemistry and applications of metal-organic frameworks. *Science*, 341(6149):1230444, 2013.

[175] Fei Gao, Zijing Ding, and Sheng Meng. Three-dimensional metal-intercalated covalent organic frameworks for near-ambient energy storage. *Scientific Reports*, 3, May 2013.

[176] Guanghua Gao, Tahir Çağin, and William A. Goddard III. Energetics, structure, mechanical and vibrational properties of single-walled carbon nanotubes. *Nanotechnology*, 9:184–191, 1998.

[177] D. Garcia-Sanches, A. San Paulo, M. J. Esplandiu, F. Perez-Murano, L. Forró, A. Aguasca, and A. Bachtold. Mechanical detection of carbon nanotube resonator vibrations. *Physicsl Review Letters*, 99:085501, 2007.

[178] D. Gentner. Structure-mapping: A theoretical framework for analogy. *Cognitive Science*, 7:26–36, 1983.

[179] D. Gentner, S. Brem, R. Ferguson, P. Wolff, A. B. Markman, and K. Forbus. Analogy and creativity in the works of Johannes Kepler. In T. B. Ward, S. M. Smith, and J. Vaid, editors, *Creative Thought: An Investigation of Conceptual Structures and Processes*, pages 403–460. American Psychology Association, Washington, DC, 1997.

[180] D. Gentner, K. J. Holyoak, and B Kokinov. *The Analogical Mind: Perspectives from Cognitive Science*. The MIT Press, Cambridge, MA, 2001.

[181] D. Gentner and A. B. Markman. Structural alignment in analogy and similarity. *American Psychologist*, 52:45–56, 1997.

[182] S. Gigan, H. R. Böhm, M. Paternostro, F. Blaser, G. Langer, J. B. Hertzberg, K. C. Schwab, D. Bäuerle, M. Aspelmeyer, and A. Zeilinger. Self-cooling of a micromirror by radiation preasure. *Nature*, 444:67–70, 2006.

[183] A. Girdhar and A. Mital. Expanding Group Technology Part Coding for Functionality: Part I Developing a Functional Basis for Classification. *International Journal of Industrial Engineering Applications and Practice*, 8(3):186–197, 2001.

[184] A. Girdhar and A. Mital. Expanding Group Technology Part Coding for Functionality: Part II Functional Classification of Workparts and Application to Design. *International Journal of Industrial Engineering Applications and Practice*, 8(3):198–209, 2001.

[185] J. Glover, R. Ronning, and C. Reynolds. *Handbook of Creativity*. Plenum, 1989.

[186] M. Godet. *Scenarios and Strategic Management*. Butterworth Publishers, London, UK, 1987.

[187] Ashok K. Goel. Design, analogy, and creativity. *IEEE Expert*, 12(3):62–70, 1997.

[188] Gabriela Goldschmidt and Dan Tatsa. How good are good ideas? Correlates of design creativity. *Design Studies*, 26(6):593–611, 2005.

[189] Jacob Goldsmith, Antek G. Wong-Foy, Michael J. Cafarella, and Donald J. Siegel. Theoretical limits of hydrogen storage in metal-organic frameworks: Opportunities and trade-offs. *Chemistry of Materials*, 25(16):3373–3382, 2013.

[190] Jacob Goldsmith, Antek G. Wong-Foy, Michael J. Cafarella, and Donald J. Siegel. Theoretical limits of hydrogen storage in metal-organic frameworks: Opportunities and trade-offs. *Chemistry of Materials*, 25:3373–3382, 2013.

[191] P. Gomes and C. Bento. A case similarity metric for software reuse and design. *Artificial Intelligence for Engineering Design, Analysis and Manufacturing*, 15(1):21–35, 2001.

[192] A. Gomez de Silva Garza and M.L. Maher. GENCAD: A hybrid analogical/evolutionary model of creative design. In *Proceedings of the 4th International Conference on Computational Models of Creative Design*, 2001.

[193] Xue-Qing Gong and Annabella Selloni. Reactivity of anatase TiO2 nanoparticles:??? the role of the minority (001) surface. *The Journal of Physical Chemistry B*, 109(42):19560–19562, October 2005.

[194] Xue-Qing Gong, Annabella Selloni, Matthias Batzill, and Ulrike Diebold. Steps on anatase TiO2(101). *Nature Materials*, 5(8):665–670, August 2006.

[195] J. Goodenough, A. Bruce, A. Nightingale, P. Bates, and G Budd. A unified validation methodology for system level co-design and co-implementation. In *Proceedings of the Annual IEEE International ASIC Conference and Exhibit*, 2001.

[196] E. Grabska, K. Grzesiak-Kopek, and G. Slusarczyk. Visual creative design with the assistance of curious agents. In *Lecture Notes in Computer Science; Proceedings of the 4th International Conference on Diagrammatic Representation and Inference*, volume 4045 LNAI, pages 218–220, 2006.

[197] K. Grantham-Lough, R. B. Stone, and I. Y. Tumer. Failure prevention through effective cataloguing and utilization of failure events. *Journal of Failure Analysis*, 2007. To appear.

[198] P. Alex Greaney. Exploratory calculations. Unpublished.

[199] P. Alex Greaney. Unpublished.

[200] P. Alex Greaney. Engineering smart thermal properties in metal-organic-frameworks, 2014.

[201] P. Alex Greaney and Jeffrey C. Grossman. Nanomechanical energy transfer and resonance effects in single-walled carbon nanotubes. *Phys. Rev. Lett.*, 98:125503, Mar 2007.

[202] P. Alex Greaney and Jeffrey C. Grossman. Nanomechanical energy transfer and resonance effects in single-walled carbon nanotubes. *Physical Review Letters*, 98:125503, 2007.

[203] P. Alex Greaney and Jeffrey C. Grossman. Nanomechanical resonance spectroscopy: A novel route to ultrasensitive label-free detection. *Nano Letters*, 8(9):2648–2652, 2008.

[204] P. Alex Greaney and Jeffrey C. Grossman. Nanomechanical resonance spectroscopy: A novel route to ultrasensitive label-free detection. *Nano Letters*, 8(9):2648–2652, 2008. PMID: 18707177.

[205] P. Alex Greaney and Jeffrey C. Grossman. Chapter 5 simulating thermomechanical phenomena of nanoscale systems. In *Computational Nanoscience*, pages –. The Royal Society of Chemistry, 2011.

[206] P. Alex Greaney, Jeffrey C. Grossman, and Mark D. Allendorf. *Ab initio* calculations of structural energy of irmof frameworks and framework defects. Unpublished, 2011.

[207] P. Alex Greaney, Giovanna Lani, Giancarlo Cicero, and Jeffrey C. Grossman. Anomalous dissipation in single-walled carbon nanotube resonators. *Nano Letters*, 9:3699–3703, 2009.

[208] P. Alex Greaney, Giovanna Lani, Giancarlo Cicero, and Jeffrey C. Grossman. Mpemba-like behavior in carbon nanotube resonators. *Metallurgical Transactions*, 42A:3907–3912, 2011.

[209] Jeffery A. Greathouse and Mark D. Allendorf. The interaction of water with mof-5 simulated by molecular dynamics [j. am. chem. soc. 2006, 128, 10678–10679]. *Journal of the American Chemical Society*, 128(40):13312–13312, 2006.

[210] Melville S. Green. Markoff random processes and the statistical mechanics of time-dependent phenomena. II. irreversible processes in fluids. *The Journal of Chemical Physics*, 22:398–413, 1954.

[211] Melville S. Green. Markoff random processes and the statistical mechanics of time-dependent phenomena. ii. irreversible processes in fluids. *The Journal of Chemical Physics*, 22(3):398–413, 1954.

[212] Zhixin Guo, Dier Zhang, and Xin-Gao Gong. Thermal conductivity of graphene nanoribbons. *Applied Physics Letters*, 95(16):–, 2009.

[213] Harri Haapasalo and Pekka Kess. Managing creativity: Is it possible to control the birth of innovation in product design? *International Journal of Technology Management*, 24(1):57–69, 2002.

[214] Luping Han, Makenzie Budge, and P. Alex Greaney. Thermal transport in gas laden mof-5. In preparation, 2013.

[215] Luping Han, Makenzie Budge, and P. Alex Greaney. Relationship between thermal conductivity and framework architecture in mof-5. *Computational Materials Science*, 94:292 – 297, 2014. {IWCMM23} Special Issue.

[216] Luping Han, Makenzie Budge, and P. Alex Greaney. Relationship between thermal conductivity and framework architecture in mof-5. *Computational Materials Science*, 94(0):292 – 297, 2014. {IWCMM23} Special Issue.

[217] Luping Han and P. Alex Greaney. Tbd. *Manuscript in preparation*.

[218] Luping Han and P. Alex Greaney. Tbd. *Manuscript in preparation*.

[219] J. A. Harley and T. W. Kenny. High-sensitivity piezoresistive cantilevers under 1000 åthick. *Applied Physics Letters*, 75:289–291, 1999.

[220] G. A. Hazelrigg. *System Engineering: An approach to information-based design*. Prentice Hall, 1996.

[221] G. A. Hazelrigg. A framework for decision based engineering design. *Journal of Mechanical Design*, 120:653–658, 1998.

[222] G. A. Hazelrigg. An axiomatic framework for engineering design. *Journal of Mechanical Design*, 121:342–347, 1999.

[223] Yuping He, Davide Donadio, and Giulia Galli. Heat transport in amorphous silicon: Interplay between morphology and disorder. *Applied Physics Letters*, 98(14):–, 2011.

[224] Yuping He, Davide Donadio, J-H. Lee, Jeffrey C. Grossman, and Giulia Galli. Thermal transport in nanoporoue silicon: Interplay between disorder at the mesoscopic and the atomic scale. *Unpublished*.

[225] M.A. Hearst, M.D. Gross, J.A. Landay, and T.F. Stahovich. Sketching Intelligent Systems. *EEE Intelligent Systems*, 13(3):10–19, 1998.

[226] M. Henderson and S. Musti. Automated Group Technology Part Coding from a Three-Dimensional CAD Database. *Journal of Engineering in Industry*, 110(3):278–287, 1988.

[227] W A Hendrickson and K B Ward. Atomic models for the polypeptide backbones of myohemerythrin and hemerythrin. *Biochemical and biophysical research communications*, 66(4):1349–1356, October 1975. PMID: 5.

[228] Sebastian Henke, D. C. Florian Wieland, Mikhail Meilikhov, Michael Paulus, Christian Sternemann, Kirill Yusenko, and Roland A. Fischer. Multiple phase-transitions upon selective CO2 adsorption in an alkyl ether functionalized metal???organic framework???an in situ x-ray diffraction study. *CrystEngComm*, 13(21):6399–6404, October 2011.

[229] Graeme Henkelman and Hannes J??nsson. A dimer method for finding saddle points on high dimensional potential surfaces using only first derivatives. *The Journal of Chemical Physics*, 111(15):7010–7022, October 1999.

[230] J. W. Herrmann and L. C. Schmidt. Product development and decision production systems. In *Decision making in engineering design*, chapter 20, pages 227–242. ASME Press, 2006.

[231] A.H. Heuer, T. Nakagawa, M.Z. Azar, D.B. Hovis, J.L. Smialek, B. Gleeson, N.D.M. Hine, H. Guhl, H.-S. Lee, P. Tangney, W.M.C. Foulkes, and M.W. Finnis. On the growth of Al2O3 scales. *Acta Materialia*, 61(18):6670–6683, October 2013.

[232] A.H. Heuer, T. Nakagawa, M.Z. Azar, D.B. Hovis, J.L. Smialek, B. Gleeson, N.D.M. Hine, H. Guhl, H.-S. Lee, P. Tangney, W.M.C. Foulkes, and M.W. Finnis. On the growth of Al2O3 scales. *Acta Materialia*, 61(18):6670–6683, October 2013.

[233] Thomas T. Hewett. Informing the design of computer-based environments to support creativity. *International Journal of Human Computer Studies*, 63(4-5):383–409, 2005.

[234] M. Highland, B. C. Gundrum, Yee Kan Koh, R. S. Averback, David G. Cahill, V. C. Elarde, J. J. Coleman, D. A. Walko, and E. C. Landahl. Ballistic-phonon heat conduction at the nanoscale as revealed by time-resolved x-ray diffraction and time-domain thermoreflectance. *Phys. Rev. B*, 76(7):075337, Aug 2007.

[235] J. Hirtz, R. Stone, D. McAdams, S. Szykman, and K. Wood. A Functional Basis for Engineering Design: Reconciling and Evolving Previous Efforts. *Research in Engineering Design*, 13(2):65–82, 2002.

[236] K. Holtta, E. S. Suh, and O.L. de Weck. Tradeoff between Modularity and Performance for Engineered Systems and Products. In *Proceedings of the International conference on engineering design, ICED05*, 2005.

[237] W.G. Hoover and C.G. Hoover. Nonequilibrium molecular dynamics. *Annual Review of Physical Chemistry*, 8(2(42)):1–14, 2005.

[238] Patricia Horcajada, Ruxandra Gref, Tarek Baati, Phoebe K Allan, Guillaume Maurin, Patrick Couvreur, Gérard Férey, Russell E Morris, and Christian Serre. Metal–organic frameworks in biomedicine. *Chemical reviews*, 112(2):1232–1268, 2011.

[239] Diana Horn and Gavriel Salvendy. Consumer-based assessment of product creativity: A review and reappraisal. *Human Factors and Ergonomics In Manufacturing*, 16(2):155–175, 2006.

[240] C. Hoyle, , I. Y. Tumer, , T. Kurtoglu, and W. Chen. Multi-stage uncertainty quantification for verifying the correctness of complex system designs. In *Proceedings of the ASME Design Engineering Technical Conferences*, 2011.

[241] C. Hoyle, I. Y. Tumer A. Farhang Mehr, and W. Chen. On quantifying cost-benefit of ISHM in Aero-space systems. In *Proceedings of the 2007 IEEE Aerospace Conference*, 2007.

[242] C. Hoyle, D. K. Kumar, and W. Chen. Product Attribute Function Deployment (PAFD) for decision-based conceptual design. In *Proceedings of the ASME Design Engineering Technical Conferences*, 2006.

[243] C. Hoyle, A. Farhang Mehr, I. Y. Tumer, and W. Chen. Cost-benefit of ISHM in Aerospace systems. In *Proceedings of the ASME Design Engineering Technical Conferences*, 2007.

[244] C. Hoyle, I. Y. Tumer, A. F. Mehr, and W. Chen. Health Management Allocation During Conceptual System Design. *Journal of Computing and Information Science in Engineering*, 9(2), 2009.

[245] Shih-Wen Hsiao and Jyh-Rong Chou. A creativity-based design process for innovative product design. *International Journal of Industrial Ergonomics*, 34(5):421–443, 2004.

[246] Jiuning Hu, Xiulin Ruan, and Yong P. Chen. Thermal conductivity and thermal rectification in graphene nanoribbons: A molecular dynamics study. *Nano Letters*, 9(7):2730–2735, 2009. PMID: 19499898.

[247] B.L. Huang, A.J.H. McGaughey, and M. Kaviany. Thermal conductivity of metal-organic framework 5 (mof-5): Part i. molecular dynamics simulations. *International Journal of Heat and Mass Transfer*, 50(3-4):393 – 404, 2007.

[248] B.L. Huang, A.J.H. McGaughey, and M. Kaviany. Thermal conductivity of metal-organic framework 5 (MOF-5): Part I. molecular dynamics simulations. *International Journal of Heat and Mass Transfer*, 50(3–4):393–404, 2007.

[249] BL Huang, AJH McGaughey, and M Kaviany. Thermal conductivity of metal-organic framework 5 (mof-5): Part i. molecular dynamics simulations. *International journal of heat and mass transfer*, 50(3):393–404, 2007.

[250] B.L. Huang, A.J.H. McGaughey, and M. Kaviany. Thermal conductivity of metal-organic framework 5 (MOF-5): part I. molecular dynamics simulations. *International Journal of Heat and Mass Transfer*, 50:393–404, 2007.

[251] B.L. Huang, Z. Ni, A. Millward, A.J.H. McGaughey, C. Uher, M. Kaviany, and O. Yaghi. Thermal conductivity of a metal-organic framework (MOF-5): part II. measurement. *International Journal of Heat and Mass Transfer*, 50(3-4):405–411, February 2007.

[252] B.L. Huang, Z. Ni, A. Millward, A.J.H. McGaughey, C. Uher, M. Kaviany, and O. Yaghi. Thermal conductivity of a metal-organic framework (MOF-5): Part II. measurement. *International Journal of Heat and Mass Transfer*, 50:405–411, 2007.

[253] Limin Huang, Huanting Wang, Jinxi Chen, Zhengbao Wang, Jinyu Sun, Dongyuan Zhao, and Yushan Yan. Synthesis, morphology control, and properties of porous metal-organic coordination polymers. *Microporous and Mesoporous Materials*, 58(2):105–114, March 2003.

[254] J. E. Hummel and K. J. Holyoak. Distributed representations of structure: a theory of analogical access and mapping. *Psychological Review*, 104(3):427–466, 1997.

[255] R. Hutcheson, D. A. McAdams, R. B. Stone, and I. Y. Tumer. Function-based systems engineering. In *International Conference on Engineering Design*, 2007.

[256] R. Hutcheson and I. Y. Tumer. FACEA function-based methodology for analyzing critical events. In *Proceedings of the ASME Design Engineering Technical Conferences*, 2006.

[257] Andreas K. Hüttel, Gary A. Steele, Benoit Witkamp, Menno Poot, Leo P. Kouwenhoven, and Herre S. J. van der Zant. Carbon nanotubes as ultrahigh quality factor mechanical resonators. *Nano Letters*, 9:2547–2552, 2009.

[258] Scott T. Huxtable, David Cahill, Sergei Shenogin, Liping Xue, Rahmi Ozisik, Paul Barone, Monica Usrey, Michael S. Strano, Giles Siddons, Moonsub Shim, and Pawel Keblinski. Nature materials. 2:731, 2003.

[259] T. Hwang and D. Ullman. The Design Capture System: Capturing Back-of-the-Envelope Sketches. *Journal of Engineering Design*, 1(4):339–353, 1990.

[260] B. Ilic, H. G. Craighead, S. Krylov, W. Senaratne, C. Ober, and P. Neuzil. Attogram detection using nanoelectromechanical oscillators. *Journal of Applied Physics*, 95(7):3694–3703, 2004.

[261] B. Ilic, S. Krylov, L. M. Bellan, and H. G. Craighead. Dynamic characterization of nanoelectromechanical oscillators by atomic force microscopy. *Journal of Applied Physics*, 101:044308, 2007.

[262] Stuart L. James. Metal-organic frameworks. *Chemical Society Reviews*, 32(5):276–288, August 2003.

[263] Karl K. Jeffries. Diagnosing the creativity of designers: individual feedback within mass higher education. *Design Studies*, 28(5):485–497, 2007.

[264] Monwhea Jeng. Mpemba effect: When can hot water freeze faster than cold? *American Journal of Physics*, 74:514–522, 2006.

[265] K. Jensen, Kwanpyo Kim, and A. Zettl. An atomic-resolution nanomechanical mass sensor. *Nature Nanotechnology*, 3, 2008.

[266] K. Jensen, H. B. Peng, and A. Zettl. Limits of nanomechanichal resonators. In IEEE, editor, *Nanoscience and Nanotechnology*, 2006. Cat Number 06EX411C.

[267] K. Jensen, J. Weldon, H Garcia, and A Zettl. Nanotube radio. *Nano Letters*, 7(11):3508–3511, 2007.

[268] Tae Hwa Jeon, Wonyong Choi, and Hyunwoong Park. Photoelectrochemical and photocatalytic behaviors of hematite-decorated titania nanotube arrays: Energy level mismatch versus surface specific reactivity. *The Journal of Physical Chemistry C*, 115(14):7134–7142, April 2011.

[269] Stephen Jesse, Sergei V. Kalinin, Roger Proksch, A. P. Baddorf, and B. J. Rodriguez. The band excitation method in scanning probe microscopy for rapid mapping of energy dissipation on the nanoscale. *Nanotechnology*, 18(43):435503, October 2007.

[270] H. Jiang, M.-F. Yu, B. Liu, and Y. Huang. Intrinsic energy loss mechanisms in cantilevered carbon nanotube beam oscillator. *Physical Review Letters*, 93:185501, 2004.

[271] W. Jie and S. Krishnamurty. Learning based preference modeling in engineering design decision making. *Journal of Mechanical Design*, 123(2):191–198, 2001.

[272] Y. Jin and S. C.-Y. Lu. Agent based negotiation for collaborative design decision making. *CIRP Annals- Manufacturing Technology*, 53(1):121–124, 2004.

[273] Yuhuan Jin, Shadrick I. M. Paris, and Jeffrey J. Rack. Bending materials with light: Photoreversible macroscopic deformations in a disordered polymer. *Advanced Materials*, 23(37):4312???4317, 2011.

[274] Yuhuan Jin, Shadrick I. M. Paris, and Jeffrey J. Rack. Bending materials with light: Photoreversible macroscopic deformations in a disordered polymer. *Advanced Materials*, 23(37):4312–4317, 2011.

[275] Yuhuan Jin and Jeffrey J. Rack. Molecules in motion: From sub-nanoscale to macroscale. *Israel Journal of Chemistry*, 53(5):280???287, 2013.

[276] J. E. Jones. On the determination of molecular fields. ii. from the equation of state of a gas. *Proceedings of the Royal Society of London A: Mathematical, Physical and Engineering Sciences*, 106(738):463–477, 1924.

[277] R. Jordan, M. Van Wie, R. Stone, J. Wang, and J. Terpenny. A Group Technology Based Representation for Product Portfolios. In *Proceedings of the ASME Design Engineering Technical Conferences and Computers in Engineering Conference*, 2005.

[278] K. Kalligeros and O.L. de Weck. Flexible Design of Commercial Systems Under Market Uncertainty: Framework and Application. In *Proceedings of the 10th AIAA/ISSMO Multidisciplinary Analysis and Optimization Conference*, 2004.

[279] Yosuke Kanai, Varadharajan Srinivasan, Steven K. Meier, K. Peter C. Vollhardt, and Jeffrey C. Grossman. Mechanism of thermal reversal of the (fulvalene)tetracarbonyldiruthenium photoisomerization: Toward molecular Solar???Thermal energy storage. *Angewandte Chemie International Edition*, 49(47):8926???8929, 2010.

[280] Byoungwoo Kang and Gerbrand Ceder. Battery materials for ultrafast charging and discharging. *Nature*, 458(7235):190–193, Mar 2009.

[281] Wei Kang and Mark S. Hybertsen. Quasiparticle and optical properties of rutile and anatase TiO$_{2}$. *arXiv:1006.4085*, June 2010. Physical Review B 82, 085203 (2010).

[282] P. L. KAPITZA. *Journal of Physics (USSR)*, 4:181, 1941.

[283] T.A. Kappel and A.H. Rubinstein. Failure mode identification through clustering analysis. *IEEE Transactions on Engineering Management*, 46:132–143, 1999.

[284] K. Kasmarik, W. Uther, and M.L. Maher. Motivated agents. In *Proceedings of the 19th International Joint Conference on Artificial Intelligence*, 2005.

[285] Steven S. Kaye, Anne Dailly, Omar M. Yaghi, and Jeffrey R. Long. Impact of preparation and handling on the hydrogen storage properties of Zn4O(1,4-benzenedicarboxylate)3 (MOF-5). *Journal of the American Chemical Society*, 129(46):14176–14177, November 2007.

[286] R. L. Keeney and H. Raiffa. *Decisions with multiple objectives: preferences and value tradeoffs*. Cambridge University Press, New York, NY, 1993.

[287] Ralph L. Keeney. Stimulating creative design alternatives using customer values. *IEEE Transactions on Systems, Man and Cybernetics Part C: Applications and Reviews*, 34(4):450–459, 2004.

[288] U. Kemiktarak, T. Ndukum, K. C. Schwab, and Ekinci. Radio-frequency scanning tunnelling microscopy. *Nature*, 450:85–88, 2007.

[289] R. Kicinger, T. Arciszewski, and K.A. De Jong. Evolutionary computation and structural design: a survey of the state of the art. *Computers and Structures*, 83(23-24):1943–1978, 2005.

[290] S. Killing and D. Hunter. *Yacht Design Explained: A sailor's guide to the principles and practice of design*. W.W. Norton & Company, Inc., 1998.

[291] Woochul Kima, Robert Wanga, and Arun Majumdara. Nanostructuring expands thermal limits. *Nanotoday*, 2:40–47, 2007.

[292] Albert W. King, Yuhuan Jin, James T. Engle, Christopher J. Ziegler, and Jeffrey J. Rack. Sequential picosecond isomerizations in a photochromic ruthenium sulfoxide complex triggered by pump-repump-probe spectroscopy. *Inorganic Chemistry*, 52(4):2086–2093, February 2013.

[293] Susumu Kitagawa and Kazuhiro Uemura. Dynamic porous properties of coordination polymers inspired by hydrogen bonds. *Chem. Soc. Rev.*, 34:109–119, 2005.

[294] Susumu Kitagawa and Kazuhiro Uemura. Dynamic porous properties of coordination polymers inspired by hydrogen bonds. *Chemical Society Reviews*, 34(2):109–119, 2005.

[295] Ryo Kitaura, Kenji Seki, George Akiyama, and Susumu Kitagawa. Porous coordination-polymer crystals with gated channels specific for supercritical gases. *Angewandte Chemie International Edition*, 42(4):428–431, 2003.

[296] Robert G. Knobel and Andrew N. Cleland. Nanometer-scale displacment sensing using a single electron transistor. *Nature*, 424:291–293, 2003.

[297] Yee Kan Koh and David G. Cahill. Frequency dependence of the thermal conductivity of semiconductor alloys. *Physical Review B*, 76:75207, 2007.

[298] M. Kokkolaras, R. Fellini, H. M. Kim, N. F. Michelena, and P. Y. Papalambros. Extension of the target cascading formulation to the design of product families. *Structural and Multidisciplinary Optimization*, 24(4):293 – 301, 2002.

[299] Alexie M. Kolpak and Jeffrey C. Grossman. Azobenzene-functionalized carbon nanotubes as high-energy density solar thermal fuels. *Nano Letters*, 11(8):3156–3162, August 2011.

[300] Alexie M. Kolpak and Jeffrey C. Grossman. Hybrid chromophore/template nanostructures: A customizable platform material for solar energy storage and conversion. *The Journal of Chemical Physics*, 138(3):034303–034303–6, January 2013.

[301] B. D. Kong, S. Paul, M. Buongiorno Nardelli, and K. W. Kim. First-principles analysis of lattice thermal conductivity in monolayer and bilayer graphene. *Phys. Rev. B*, 80:033406, Jul 2009.

[302] B I Korelitz and S C Sommers. Responses to drug therapy in ulcerative colitis. evaluation by rectal biopsy and histopathological changes. *The American journal of gastroenterology*, 64(5):365–370, November 1975. PMID: 2008.

[303] K. Kormann. *Numerical Methods for Quantum Molecular Dynamics*. Licentiate thesis, Department of Information Technology, Uppsala University, October 2009.

[304] J.R. Koza, M.A. Keane, M.J. Streeter, T.P. Adams, and L.W. Jones. Invention and creativity in automated design by means of genetic programming. *Artificial Intelligence for Engineering Design, Analysis and Manufacturing: AIEDAM*, 18:245–269, 2004.

[305] Lauren E Kreno, Kirsty Leong, Omar K Farha, Mark Allendorf, Richard P Van Duyne, and Joseph T Hupp. Metal–organic framework materials as chemical sensors. *Chemical Reviews*, 112(2):1105–1125, 2011.

[306] G Kresse and J Hafner. Ab initio molecular-dynamics simulation of the liquid-metal–amorphous-semiconductor transition in germanium. *Physical Review B*, 49(20):14251, 1994.

[307] Georg Kresse and Jürgen Furthmüller. Efficiency of ab-initio total energy calculations for metals and semiconductors using a plane-wave basis set. *Computational Materials Science*, 6(1):15–50, 1996.

[308] Georg Kresse and Jürgen Furthmüller. Efficient iterative schemes for ab initio total-energy calculations using a plane-wave basis set. *Physical Review B*, 54(16):11169, 1996.

[309] Georg Kresse and Jürgen Hafner. Ab initio molecular dynamics for liquid metals. *Physical Review B*, 47(1):558, 1993.

[310] Georg Kresse and D Joubert. From ultrasoft pseudopotentials to the projector augmented-wave method. *Physical Review B*, 59(3):1758, 1999.

[311] J. A. Krumhansl and J. A. D. Matthew. Scattering of long-wavelength phonons by point imperfections in crystals. *Physical Review*, 140(5A):A1812–A1817, November 1965.

[312] V.V. Kryssanov, H. Tamaki, and S. Kitamura. Understanding design fundamentals: How synthesis and analysis drive creativity, resulting in emergence. *Artificial Intelligence for Engineering*, 15(4):329–342, 2001.

[313] Ryogo Kubo. Statistical-mechanical theory of irreversible processes. i. general theory and simple applications to magnetic and conduction problems. *Journal of the Physical Society of Japan*, 12(6):570–586, 1957.

[314] Ryogo Kubo. Statistical-mechanical theory of irreversible processes. i. general theory and simple applications to magnetic and conduction problems. *Journal of the Physical Society of Japan*, 12(6):570–586, 1957.

[315] Ryogo Kubo, Mario Yokota, and Sadao Nakajima. Statistical-mechanical theory of irreversible processes. ii. response to thermal disturbance. *Journal of the Physical Society of Japan*, 12(11):1203–1211, 1957.

[316] N. Kulatilaka. The Value of Flexibility: The Case of a Dual-fuel Industrial Steam Boiler. *Financial Management*, 22(3), 1993.

[317] N. Kulatilaka. The value of flexibility: A general model of real options. In L. Trigeorgis, editor, *Real Options in Capital Investment: Models, Strategies, and Applications*. Praeger/Greenwood, Westport, 1995.

[318] J. M. Kulinski. *A model of situated analogy in design* . Dissertation, University of Sydney, Australia, 2003.

[319] Vijay Kumar and Yoshiyuki Kawazoe. Evolution of atomic and electronic structure of pt clusters: Planar, layered, pyramidal, cage, cubic, and octahedral growth. *Physical Review B*, 77(20):205418, May 2008.

[320] M.A. Kurfman, J. Rajan, R.B. Stone, K.L. Wood, and M.E. Stock. Experimental Sudies Assessing the Repeatability of a Functional Modeling Derivation Method. *Journal of Mechanical Design*, 125(4):682–693, 2002.

[321] T. Kurtoglu and M. Campbell. Automated synthesis of electromechanical design configurations from empirical analysis of function to form mapping. *Journal of Engineering Design*, 20(1), 2009.

[322] T. Kurtoglu, M. Campbell, J. Gonzalez, C. Bryant, R. Stone, and D. McAdams. Capturing Empirically Derived Design Knowledge for Creating Conceptual Design Configurations. In *Proceedings of the ASME Design Engineering Technical Conferences and Computers in Engineering Conference*, 2005.

[323] T. Kurtoglu, D. C. Jensen, and I. Y. Tumer. A functional failure reasoning methodology for evaluation of conceptual system architectures. *Research in Engineering Design*, 21, 2010.

[324] T. Kurtoglu and I. Y. Tumer. A graph-based fault identification and propagation framework for functional design of complex systems. *Journal of Mechanical Design*, 30(5), 2008.

[325] Tolga Kurtoglu and Irem Y. Tumer. A graph-based fault identification and propagation framework for functional design of complex systems. *Journal of Mechanical Design*, 130(5):051401–051401, March 2008.

[326] Young-Kyun Kwon, Savas Berber, and David Tomanek. Thermal contraction of carbon fullerenes and nanotubes. *Phys. Rev. Lett.*, 92(1):015901, Jan 2004.

[327] M. D. LaHaye, O. Buu, B. Camarota, and K. C. Schwab. Approaching the quantum limit of a nanomechanical resonator. *Science*, 304:74–77, 2004.

[328] E. S. Lamassoure, S. D. Wall, and R. W.. Easter. Model-based engineering design for trade space exploration throughout the design cycle. In *Proceedings of the Space 2004 Conference and Exhibit*, number AIAA 2004-5855, 2004.

[329] E. S. Landry, M. I. Hussein, and A. J. H. McGaughey. Complex superlattice unit cell designs for reduced thermal conductivity. *Physical Review B*, 77(18):184302, May 2008.

[330] Andrea Lang. Heat transfer and energy.

[331] B. Lassagne, D. Garcia-Sanchez, A. Aguasca, and A. Bachtold. Ultrasensitive mass sensing with a nanotube electromechanical resonator. *Nano Letters*, 8:3735–3738, 2008.

[332] Thomas J. LaTempa, Xinjian Feng, Maggie Paulose, and Craig A. Grimes. Temperature-dependent growth of self-assembled hematite (??-Fe2O3) nanotube arrays: Rapid electrochemical synthesis and photoelectrochemical properties. *The Journal of Physical Chemistry C*, 113(36):16293–16298, September 2009.

[333] Michele Lazzeri and Francesco Mauri. Coupled dynamics of electrons and phonons in metallic nanotubes: Current saturation from hot-phonon generation. *Phys. Rev. B*, 73(16):165419, Apr 2006.

[334] Michele Lazzeri, Andrea Vittadini, and Annabella Selloni. Structure and energetics of stoichiometric TiO_{2} anatase surfaces. *Physical Review B*, 63(15):155409, March 2001.

[335] Deok Yeon Lee, Dipak Vijaykumar Shinde, Seog Joon Yoon, Keum Nam Cho, Wonjoo Lee, Nabeen K. Shrestha, and Sung-Hwan Han. Cu-based metal-organic frameworks for photovoltaic application. *The Journal of Physical Chemistry C*, 0(ja):null, 0.

[336] J. Y. Lee, D. H. Olson, L. Pan, T. J. Emge, and J. Li. Microporous Metal-Organic frameworks with high gas sorption and separation capacity. *Advanced Functional Materials*, 17(8):1255–1262, 2007.

[337] Joo-Hyoung Lee, Giulia A. Galli, and Jeffrey C. Grossman. Nanoporous si as an efficient thermoelectric material. *Nano letters*, 8:3750–3754, 1008.

[338] S. Lee and W. Chen. A comparative study of uncertainty propagation methods for black-box-type problems. *Structural and Multidisciplinary Optimization*, 37(3):239–253, 2009.

[339] David M. Leitner. Energy flow in proteins. *Annual Review of Physical Chemistry*, 59(1):233–259, 2008.

[340] David M. Leitner. Frequency-resolved communication maps for proteins and other nanoscale materials. *The Journal of Chemical Physics*, 130(19):195101, 2009.

[341] Kirsty Leong, Michael E Foster, Bryan M Wong, Erik D Spoerke, Dara Van Gough, Joseph C Deaton, and Mark D Allendorf. Energy and charge transfer by donor–acceptor pairs confined in a metal–organic framework: a spectroscopic and computational investigation. *Journal of Materials Chemistry A*, 2(10):3389–3398, 2014.

[342] K. E. Lewis, W. Chen, and L. C. Schmidt. *Decision making in engineering design.* ASME Press, 2006.

[343] Deyu Li, Yiying Wu, Philip Kim, Li Shi, Peidong Yang, and Arun Majumdara). Thermal conductivity of individual silicon nanowires. *Applied Physics Letters*, 83:2934–2937, 2003.

[344] H. Li and S. Azarm. An approach to product line design selection under uncertainty and with competitive advantage. *Journal of Mechanical Design*, 122(4):411–418, 2002.

[345] Hailian Li, Mohamed Eddaoudi, M. O'Keeffe, and O. M. Yaghi. Design and synthesis of an exceptionally stable and highly porous metal-organic framework. *Nature*, 402(6759):276–279, November 1999.

[346] Jian-Rong Li, Yuguang Ma, M. Colin McCarthy, Julian Sculley, Jiamei Yu, Hae-Kwon Jeong, Perla B. Balbuena, and Hong-Cai Zhou. Carbon dioxide capture-related gas adsorption and separation in metal-organic frameworks. *Coordination Chemistry Reviews*, 255(15-16):1791 – 1823, 2011.

[347] Jian-Rong Li, Yuguang Ma, M. Colin McCarthy, Julian Sculley, Jiamei Yu, Hae-Kwon Jeong, Perla B. Balbuena, and Hong-Cai Zhou. Carbon dioxide capture-related gas adsorption and separation in metal-organic frameworks. *Coordination Chemistry Reviews*, 255(15-16):1791–1823, 2011.

[348] Jian-Rong Li, Julian Sculley, and Hong-Cai Zhou. Metal–organic frameworks for separations. *Chemical reviews*, 112(2):869–932, 2011.

[349] Yan Li, Jian Wang, Xianglong Li, and Wu Zhao. Design creativity in product innovation. *International Journal of Advanced Manufacturing Technology*, 33(3-4):213–222, 2007.

[350] Ron Lifshitz and M. L. Roukes. Thermoelastic damping in micro and nanomechanical systems. *Physical Review B*, 61:5600–5608, 2000.

[351] Si-Hyung "Shawn:" Lim, Digvijay Raorane, Srinath Satyanarayana, and Arunava Majumbar. Nano-chemo-mechanical sensor array platform for high throughput chemical analysis. *Sensors and Actuators B*, 119:466–474, 2006.

[352] Shangchao Lin and Markus J. Buehler. The effect of non-covalent functionalization on the thermal conductance of graphene/organic interfaces. *Nanotechnology*, 24(16):165702, April 2013.

[353] H. Lipson and M. Shpitalni. Conceptual Design and Analysis by Sketching. *Artificial Intelligence for Engineering Design, Analysis and Manufacturing*, 14(5):391–402, 2000.

[354] Forbes Lists. Forbes magazine. http://www.forbes.com/lists/. Accessed September 17, 2007.

[355] D. Liu, J.J. Purewal, J. Yang, A. Sudik, S. Maurer, U. Mueller, J. Ni, and D.J. Siegel. MOF-5 composites exhibiting improved thermal conductivity. *International Journal of Hydrogen Energy*, 37(7):6109–6117, April 2012.

[356] D. Liu, J.J. Purewal, J. Yang, A. Sudik, S. Maurer, U. Mueller, J. Ni, and D.J. Siegel. MOF-5 composites exhibiting improved thermal conductivity. *International Journal of Hydrogen Energy*, 37(7):6109–6117, April 2012.

[357] D. Liu, J.J. Purewal, J. Yang, A. Sudik, S. Maurer, U. Mueller, J. Ni, and D.J. Siegel. Mof-5 composites exhibiting improved thermal conductivity. *International Journal of Hydrogen Energy*, 37(7):6109–6117, Apr 2012.

[358] H. Liu and M. Tang. Evolutionary design in a multi-agent design environment. *Applied Soft Computing Journal*, 6(2):207–220, 2006.

[359] Hong Liu and Xiyu Liu. A computational approach to stimulating creativity in design. In *Lecture Notes in Computer Science; Proceedings of the 9th International Conference on Computer Supported Cooperative Work in Design*, volume 3865 LNCS, pages 344–354, 2006.

[360] Jian Liu, Praveen K. Thallapally, and Denis Strachan. Metal-organic frameworks for removal of xe and kr from nuclear fuel reprocessing plants. *Langmuir*, 28(31):11584–11589, 2012. PMID: 22799439.

[361] Jian Liu, Praveen K. Thallapally, and Denis Strachan. Metal-organic frameworks for removal of Xe and Kr from nuclear fuel reprocessing plants. *Langmuir*, 28(31):11584–11589, 2012.

[362] Yu-Tung Liu. Creativity or novelty? *Design Studies*, 21(3):261–276, 2000.

[363] Yun Liu, Jae-Hyuk Her, Anne Dailly, Anibal J Ramirez-Cuesta, Dan A Neumann, and Craig M Brown. Reversible structural transition in mil-53 with large temperature hysteresis. *Journal of the American Chemical Society*, 130(35):11813–11818, 2008.

[364] Beata M. Lobert and Dorothy G. Dologite. Measuring creativity of information system ideas: an exploratory investigation. In *Proceedings of the Hawaii International Conference on System Sciences*, 1994.

[365] Beata M. Lobert and Dorothy G. Dologite. Can we measure quality in design and do we need to? In *Proceedings of the Conference on Designing Interactive Systems: Processes, Practices, Methods, and Techniques*, 2006.

[366] Nina Lock, Mogens Christensen, Cameron J Kepert, and Bo B Iversen. Effect of gas pressure on negative thermal expansion in MOF-5. *Chemical communications (Cambridge, England)*, 49(8):789–791, January 2013. PMID: 23235693.

[367] Nina Lock, Mogens Christensen, Yue Wu, Vanessa K. Peterson, Maja K. Thomsen, Ross O. Piltz, Anibal J. Ramirez-Cuesta, Garry J. McIntyre, Katarina Noren, Ramzi Kutteh, Cameron J. Kepert, Gordon J. Kearley, and Bo B. Iversen. Scrutinizing negative thermal expansion in mof-5 by scattering techniques and ab initio calculations. *Dalton Trans.*, 42:1996–2007, 2013.

[368] Nina Lock, Mogens Christensen, Yue Wu, Vanessa K. Peterson, Maja K. Thomsen, Ross O. Piltz, Anibal J. Ramirez-Cuesta, Garry J. McIntyre, Katarina Noren, Ramzi Kutteh, Cameron J. Kepert, Gordon J. Kearley, and Bo B. Iversen. Scrutinizing negative thermal expansion in MOF-5 by scattering techniques and ab initio calculations. *Dalton Trans.*, 42:1996–2007, 2013.

[369] Nina Lock, Mogens Christensen, Yue Wu, Vanessa K. Peterson, Maja K. Thomsen, Ross O. Piltz, Anibal J. Ramirez-Cuesta, Garry J. McIntyre, Katarina Nor??n, Ramzi

Kutteh, Cameron J. Kepert, Gordon J. Kearley, and Bo B. Iversen. Scrutinizing negative thermal expansion in MOF-5 by scattering techniques and ab initio calculations. *Dalton Transactions*, 42(6):1996–2007, January 2013.

[370] Nina Lock, Yue Wu, Mogens Christensen, Lisa J. Cameron, Vanessa K. Peterson, Adam J. Bridgeman, Cameron J. Kepert, and Bo B. Iversen. Elucidating negative thermal expansion in mof-5. *The Journal of Physical Chemistry C*, 114(39):16181–16186, 2010.

[371] Nina Lock, Yue Wu, Mogens Christensen, Lisa J. Cameron, Vanessa K. Peterson, Adam J. Bridgeman, Cameron J. Kepert, and Bo B. Iversen. Elucidating negative thermal expansion in mof-5. *The Journal of Physical Chemistry C*, 114:16181–16186, 2010.

[372] Nina Lock, Yue Wu, Mogens Christensen, Lisa J. Cameron, Vanessa K. Peterson, Adam J. Bridgeman, Cameron J. Kepert, and Bo B. Iversen. Elucidating negative thermal expansion in MOF-5. *The Journal of Physical Chemistry C*, 114(39):16181–16186, October 2010.

[373] Thierry Loiseau, Christian Serre, Clarisse Huguenard, Gerhard Fink, Francis Taulelle, Marc Henry, Thierry Bataille, and Gérard Férey. A rationale for the large breathing of the porous aluminum terephthalate (mil-53) upon hydration. *Chemistry A European Journal*, 10(6):1373–1382, 2004.

[374] Giulia Lorusso, Joseph W. Sharples, Elias Palacios, Olivier Roubeau, Euan K. Brechin, Roberta Sessoli, Andrea Rossin, Floriana Tuna, Eric J. L. McInnes, David Collison, and et al. A dense metal-organic framework for enhanced magnetic refrigeration. *Advanced Materials*, 25(33):4653–4656, Sep 2013.

[375] Chun-Mei Lu, Jun Liu, Kefeng Xiao, and Andrew T. Harris. Microwave enhanced synthesis of MOF-5 and its CO2 capture ability at moderate temperatures across multiple capture and release cycles. *Chemical Engineering Journal*, 156(2):465–470, January 2010.

[376] Jennifer R. Lukes and Hongliang Zhong. Thermal conductivity of individual single-wall carbon nanotubes. *Journal of Heat Transfer*, 129(6):705, 2007.

[377] Omar M., Yaghi, Michael O'Keeffe, Nathan W. Ockwig, Hee K. Chae, Mohamed Eddaoudi, and Jaheon Kim. Reticular synthesis and the design of new materials. *Nature*, 423(6941):705–714, Jun 2003.

[378] Qintian Ma, Qingyuan Yang, Aziz Ghoufi, Gérard Férey, Chongli Zhong, and Guillaume Maurin. Guest dependent pressure behavior of the flexible mil-53 (cr): A computational exploration. *Dalton Transactions*, 41(14):3915–3919, 2012.

[379] Qintian Ma, Qingyuan Yang, Aziz Ghoufi, Ke Yang, Ming Lei, Gérard Férey, Chongli Zhong, and Guillaume Maurin. Guest-modulation of the mechanical properties of flexible porous metal–organic frameworks. *Journal of Materials Chemistry A*, 2(25):9691–9698, 2014.

[380] A. K. Mackworth. Constraint-based design of embedded intelligent systems. *Constraints*, 2(1):83–86, 1997.

[381] Mary Lou Maher. Creative design using a genetic algorithm. In *Proceedings of the 1st Congress on Computing in Civil Engineering*, volume 2, pages 2014–2021, 1994.

[382] M.L. Maher, J.S. Gero, G. Smith, and N. Gu. Cognitive agents in 3D virtual worlds. *International Journal of Design Computing*, 6, 2003.

[383] M.L. Maher and A. Gomez de Silva Garza. Adapting problem specifications and design solutions using co-evolution. *Adaptive Computing in Design and Manufacture*, V:257–271, 2002.

[384] M.L. Maher and H. Tang. Co-evolution as a computational and cognitive model of design. *Research in Engineering Design*, 2002.

[385] Tapas Kumar Maji, Ryotaro Matsuda, and Susumu Kitagawa. A flexible interpenetrating coordination framework with a bimodal porous functionality. *Nature materials*, 6(2):142–148, 2007.

[386] T. W. Mak and L. H. Shu. Abstraction of Biological Analogies for Design. *CIRP Annals*, 53(1):117–120, 2000.

[387] Trevor A Makal, Andrey A Yakovenko, and Hong-Cai Zhou. Isomerism in metal–organic frameworks:?framework isomers? *The Journal of Physical Chemistry Letters*, 2(14):1682–1689, 2011.

[388] Hegoi Manzano, Engin Durgun, Mohammed Javad Abdolhosseine Qomi, Franz-Josef Ulm, Roland. J. M. Pellenq, and Jeffrey. C. Grossman. Impact of chemical impurities on the crystalline cement clinker phases determined by atomistic simulations. *Crystal Growth & Design*, 11(7):2964–2972, 2011.

[389] A. B. Markman and D. Gentner. Structural alignment during similarity comparisons. *Cognitive Psychology*, 25(4):431–467, 1993.

[390] M. Marston, J. K. Allen, and F. Mistree. Decision Support Problem Technique: integrating descriptive and normative approaches in Decision Based Design. *Journal of Engineering Valuation and Cost Analysis*, 3(2):107–129, 2000.

[391] Michael James Martin and Brial H. Houston. Gas damping of carbon nanotube oscillators. *Applied Physics Letters*, 91:103116, 2007.

[392] Natalia Martsinovich, Daniel R. Jones, and Alessandro Troisi. Electronic structure of TiO2 surfaces and effect of molecular adsorbates using different DFT implementations. *The Journal of Physical Chemistry C*, 114(51):22659–22670, December 2010.

[393] Stephen L. Mayo, Barry D. Olafson, and William A. Goddard. Dreiding: a generic force field for molecular simulations. *The Journal of Physical Chemistry*, 94(26):8897–8909, 1990.

[394] Stephen L Mayo, Barry D Olafson, and William A Goddard. Dreiding: a generic force field for molecular simulations. *Journal of Physical Chemistry*, 94(26):8897–8909, 1990.

[395] D. A. McAdams, D. Comella, and I. Y. Tumer. Exploring effective methods for simulating dam-aged structures with geometric variation. *Journal of Applied Mechanics*, 2005. To appear.

[396] D. A. McAdams, R. B. Stone, and K. L. Wood. Interdependence and product similarity based on customer needs. *Research in Engineering Design*, 11:1–19, 1999.

[397] D. A. McAdams and I. Y. Tumer. Toward Intelligent fault detection in turbine blades: Variational vibration models of damaged pinned-pinned beams. *Journal of Vibration and Acoustics*, 127(5):467–474, 2005.

[398] D. A. McAdams and K. L. Wood. A quantitative similarity metric for design by analogy. *Journal of Mechanical Design*, 124(2):173–182, 2000.

[399] Beth Anne McClure and Jeffrey J. Rack. Isomerization in photochromic ruthenium sulfoxide complexes. *European Journal of Inorganic Chemistry*, 2010(25):3895???3904, 2010.

[400] A. J. H. McGaughey and M. Kaviany. Quantitative validation of the boltzmann transport equation phonon thermal conductivity model under the single-mode relaxation time approximation. *Physical Review B*, 69(9):094303, March 2004.

[401] A. J. H. McGaughey and M. Kaviany. Quantitative validation of the boltzmann transport equation phonon thermal conductivity model under the single-mode relaxation time approximation. *Phys. Rev. B*, 69(9):094303, Mar 2004.

[402] A.J.H. McGaughey and M. Kaviany. Thermal conductivity decomposition and analysis using molecular dynamics simulations. *International Journal of Heat and Mass Transfer*, 47(8-9):1799–1816, April 2004.

[403] A.J.H. McGaughey and M. Kaviany. Thermal conductivity decomposition and analysis using molecular dynamics simulations. part i. lennard-jones argon. *International Journal of Heat and Mass Transfer*, 47(8-9):1783–1798, April 2004.

[404] Alistair C. McKinlay, Russell E. Morris, Patricia Horcajada, Gérard Férey, Ruxandra Gref, Patrick Couvreur, and Christian Serre. Biomofs: Metal-organic frameworks for biological and medical applications. *Angewandte Chemie International Edition*, 49(36):6260–6266, 2010.

[405] D.A. McQuarrie. *Statistical Mechanics*. University Science Books, 2000.

[406] Scott T. Meek, Jeffery A. Greathouse, and Mark D. Allendorf. Metal-organic frameworks: A rapidly growing class of versatile nanoporous materials. *Advanced Materials*, 23(2):249???267, 2011.

[407] A. Farhang Mehr and I. Y. Tumer. A multidisciplinary and multiobjective system analysis and optimization methodology for embedding integrated systems health management into NASAs complex systems. In *Proceedings of the ASME Design Engineering Technical Conferences*, 2006.

[408] A. Farhang Mehr and I.Y. Tumer. Risk based decision making for managing resources during the design of complex aerospace systems. *Journal of Mechanical Design*, 128(4):1014–1022, 2006.

[409] T. Merritt. Top 10 products. CNET.

[410] Howard Middleton. Creative thinking, values and Design and Technology education. *International Journal of Technology and Design Education*, 15(1):61–71, 2005.

[411] P D Mier and J J van den Hurk. Lysosomal hydrolases of the epidermis. i. glycosidases. *The British journal of dermatology*, 93(1):1–10, July 1975. PMID: 30.

[412] N. Mingo and D. A. Broido. Length dependence of carbon nanotube thermal conductivity, and the "problem of long waves". *Nano Letters*, 7:1221–1225, 1005.

[413] Nicholas V. Mockus, Daniel Rabinovich, Jeffrey L. Petersen, and Jeffrey J. Rack. Femtosecond isomerization in a photochromic molecular switch. *Angewandte Chemie International Edition*, 47(8):1458???1461, 2008.

[414] Antje Modrow, Dordaneh Zargarani, Rainer Herges, and Norbert Stock. The first porous MOF with photoswitchable linker molecules. *Dalton Transactions*, 40(16):4217, 2011.

[415] Antje Modrow, Dordaneh Zargarani, Rainer Herges, and Norbert Stock. The first porous mof with photoswitchable linker molecules. *Dalton Trans.*, 40:4217–4222, 2011.

[416] Antje Modrow, Dordaneh Zargarani, Rainer Herges, and Norbert Stock. The first porous mof with photoswitchable linker molecules. *Dalton Transactions*, 40(16):4217–4222, 2011.

[417] Hailian Li Banglin Chen Theresa M. Reineke Michael O'Keeffe Mohamed Eddaoudi, David B. Moler and Omar M. Yaghi. Modular chemistry: Secondary building units as a basis for the design of highly porous and robust metal-organic carboxylate frameworks. *Accounts of Chemical Research*, 34(4):319–330, 2001.

[418] Nathaniel Rosi David Vodak Joseph Wachter Michael O'Keeffe Mohamed Eddaoudi, Jaheon Kim and Omar M. Yaghi. Systematic design of pore size and functionality in isoreticular mofs and their application in methane storage. *Science*, 295(5554):469–472, 2002.

[419] P. Mohanty, D. A. Harrington, K. L. Ekinci, Y. L. Yang, M. J. Murphy, and M. L. Roukes. Intrinsic dissipation in high-frequency micromechanical resonators. *Physical Review B*, 66:085416, 2002.

[420] M. Infas H. Mohideen, Bo Xiao, Paul S. Wheatley, Alistair C. McKinlay, Yang Li, Alexandra M. Z. Slawin, David W. Aldous, Naomi F. Cessford, Tina D??ren, Xuebo Zhao, Rachel Gill, K. Mark Thomas, John M. Griffin, Sharon E. Ashbrook, and Russell E. Morris. Protecting group and switchable pore-discriminating adsorption properties of a hydrophilic???hydrophobic metal???organic framework. *Nature Chemistry*, 3(4):304–310, April 2011.

[421] Hendrik J Monkhorst and James D Pack. Special points for brillouin-zone integrations. *Physical review B*, 13(12):5188, 1976.

[422] C.J. Moore, J.C. Miles, and D.W.G. Rees. Decision Support for Conceptual Bridge Design. *Artificial Intelligence in Engineering*, 11(3):259–272, 1997.

[423] Kei Moritsugu, Osamu Miyashita, and Akinori Kidera. Vibrational energy transfer in a protein molecule. *Phys. Rev. Lett.*, 85(18):3970–3973, Oct 2000.

[424] Kei Moritsugu, Osamu Miyashita, and Akinori Kidera. Vibrational energy transfer in a protein molecule. *Physical Review Letters*, 85:3970, 2000.

[425] K Moroi and T Sato. Comparison between procaine and isocarboxazid metabolism in vitro by a liver microsomal amidase-esterase. *Biochemical pharmacology*, 24(16):1517–1521, August 1975. PMID: 8.

[426] Joseph A. Morrone and Roberto Car. Nuclear quantum effects in water. *Phys. Rev. Lett.*, 101(1):017801, Jul 2008.

[427] John PS Mowat, Valerie R Seymour, John M Griffin, Stephen P Thompson, Alexandra MZ Slawin, David Fairen-Jimenez, Tina Düren, Sharon E Ashbrook, and Paul A Wright. A novel structural form of mil-53 observed for the scandium analogue and its response to temperature variation and co 2 adsorption. *Dalton Transactions*, 41(14):3937–3941, 2012.

[428] M.P. Allen. Introduction to molecular dynamics simulation. *John von Neumann Institute for Computing*, 23:1–28, 2004.

[429] E. B. Mpemba and D. G. Osborne. Cool? *Physics Education*, pages 172–175, 1969.

[430] U. Mueller, M. Schubert, F. Teich, H. Puetter, K. Schierle-Arndt, and J. Pastre. Metal-organic frameworks prospective industrial applications. *Journal of Materials Chemistry*, 16(7):626–636, February 2006.

[431] Florian Muller-Plathe. A simple nonequilibrium molecular dynamics method for calculating the thermal conductivity. *The Journal of Chemical Physics*, 106(14):6082–6085, 1997.

[432] Florian Müller-Plathe. A simple nonequilibrium molecular dynamics method for calculating the thermal conductivity. *The Journal of Chemical Physics*, 106(14):6082–6085, 1997.

[433] Florian Müller-Plathe. Reversing the perturbation in nonequilibrium molecular dynamics: An easy way to calculate the shear viscosity of fluids. *Phys. Rev. E*, 59(5):4894–4898, May 1999.

[434] Leslie J. Murray, Mircea Dinca, and Jeffrey R. Long. Hydrogen storage in metal-organic frameworks. *Chemical Society Reviews*, 38(5):1294–1314, April 2009.

[435] Y.-E. Nahm and H. Ishikawa. A new 3d-cad system for set-based parametric design. *Journal of Advanced Manufacturing Technology*, 29(1-2):137–150, 2006.

[436] W. S. Neely and V. J. Mooney III. System level design for system on a chip. *Design Automation for Embedded Systems*, 3(4):291–309, 1998.

[437] Alexander V Neimark, Francois-Xavier Coudert, Carles Triguero, Anne Boutin, Alain H Fuchs, Isabelle Beurroies, and Renaud Denoyel. Structural transitions in mil-53 (cr): View from outside and inside. *Langmuir*, 27(8):4734–4741, 2011.

[438] D. L. Nika, E. P. Pokatilov, A. S. Askerov, and A. A. Balandin. Phonon thermal conduction in graphene: Role of umklapp and edge roughness scattering. *Phys. Rev. B*, 79:155413, Apr 2009.

[439] Roberto Olivares-Amaya, Carlos Amador-Bedolla, Johannes Hachmann, Sule Atahan-Evrenk, Roel S. S??nchez-Carrera, Leslie Vogt, and Al??n Aspuru-Guzik. Accelerated computational discovery of high-performance materials for organic photovoltaics by means of cheminformatics. *Energy & Environmental Science*, 4(12):4849–4861, November 2011.

[440] S. Oman and I. Y. Tumer. The potential of creativity metrics for mechanical engineering concept design. In *International Conference on Engineering Design (In Review)*, 2009.

[441] Shyue Ping Ong, William Davidson Richards, Anubhav Jain, Geoffroy Hautier, Michael Kocher, Shreyas Cholia, Dan Gunter, Vincent L. Chevrier, Kristin A. Persson, and Gerbrand Ceder. Python materials genomics (pymatgen): A robust, open-source python library for materials analysis. *Computational Materials Science*, 68:314–319, February 2013.

[442] H. Opitz. *A Classification System to Describe Workpieces*. Pergamon Press, Ltd., 1970.

[443] H. Opitz, W. Eversheim, and H.P. Wiendahl. Workpiece Classification and its Industrial Application. *International Journal of Machine Tool Design Research*, 9:39–50, 1969.

[444] H. Opitz and H.P. Wiendahl. Group Technology and Manufacturing Systems for Small and Medium Quantity Production. *International Journal of Production Research*, 9(1):181–203, 1971.

[445] Aurélie U. Ortiz, Anne Boutin, Alain H. Fuchs, and François-Xavier Coudert. Anisotropic elastic properties of flexible metal-organic frameworks: How soft are soft porous crystals? *Phys. Rev. Lett.*, 109:195502, 2012.

[446] Aurélie U Ortiz, Anne Boutin, Alain H Fuchs, and François-Xavier Coudert. Anisotropic elastic properties of flexible metal-organic frameworks: how soft are soft porous crystals? *Physical review letters*, 109(19):195502, 2012.

[447] K. Otto and E. Antonsson. Trade-off strategies in engineering design. *Research in Engineering Design*, 3(2):87–104, 1991.

[448] K. N. Otto and K. L. Wood. Product evolution: A reverse engineering and redesign methodology. *Research in Engineering Design*, 10(4):226–243, 1999.

[449] K. N. Otto and K. L. Wood. *Product Design: Techniques in reverse engineering and new product development*. Prentice Hall, 2001.

[450] James D Pack and Hendrik J Monkhorst. " special points for brillouin-zone integrations"?a reply. *Physical Review B*, 16(4):1748, 1977.

[451] M. Padhke. *Quality engineering using robust design*. Prentice Hall, Englewood Cliffs, NJ, 1989.

[452] G. Pahl and W. Beitz. *Engineering Design: A Systematic Approach*. Springer-Verlag, June 1988.

[453] G. Pahl and W. Beitz. *Engineering Design: A Systematic Approach*. Springer-Verlag, London, UK, 1996.

[454] Long Pan, Michelle B. Sander, Xiaoying Huang, Jing Li, Milton Smith, Edward Bittner, Bradley Bockrath, and J. Karl Johnson. Microporous metal organic materials:- promising candidates as sorbents for hydrogen storage. *Journal of the American Chemical Society*, 126(5):1308–1309, February 2004.

[455] Panchal, J. and Fernandez, M. G. and Allen, J. K. and Paredis, C. J. and Mistree, F. An interval-based focalization method for decision-making in decentralized, multi-functional design. In *Proceedings of the ASME Design Engineering Technical Conferences*, 2005.

[456] B. Panella and M. Hirscher. Hydrogen physisorption in Metal-Organic porous crystals. *Advanced Materials*, 17(5):538–541, 2005.

[457] B. Panella, M. Hirscher, H. Petter, and U. Meller. Hydrogen adsorption in Metal-Organic frameworks: Cu-MOFs and zn-MOFs compared. *Advanced Functional Materials*, 16(4):520–524, 2006.

[458] Nikolaos Papakonstantinou, Seppo Sierla, David C. Jensen, and Irem Y. Tumer. Simulation of interactions and emergent failure behavior during complex system design. *Journal of Computing and Information Science in Engineering*, 12(3):031007–031007, August 2012.

[459] P. Y. Papalambros and D. Wilde. *Principles of optimal design: modeling and computation*. Cambridge University Press, 2002.

[460] B. Parks. Bottom line design awards. Buisness 2.0, http://www.cnet.com/4520-11136_1-6312246-1.html. Accessed September 17, 2007.

[461] H. B. Peng, C. W. Chang, S Aloni, T. D. Yuzvinski, and A. Zettl. Ultrahigh frequency naontube resonators. *Physical Review Letters*, 97:087203, 2006.

[462] John P. Perdew, Kieron Burke, and Matthias Ernzerhof. Generalized gradient approximation made simple. *Phys. Rev. Lett.*, 77:3865–3868, Oct 1996.

[463] John P. Perdew, Kieron Burke, and Matthias Ernzerhof. Generalized gradient approximation made simple. *Phys. Rev. Lett.*, 77:3865–3868, Oct 1996.

[464] John P Perdew and Alex Zunger. Self-interaction correction to density-functional approximations for many-electron systems. *Physical Review B*, 23(10):5048, 1981.

[465] John J. Perry IV, Jason A. Perman, and Michael J. Zaworotko. Design and synthesis of metal-organic frameworks using metal-organic polyhedra as supermolecular building blocks. *Chem. Soc. Rev.*, 38:1400–1417, 2009.

[466] John J. Perry IV, Jason A. Perman, and Michael J. Zaworotko. Design and synthesis of metal-organic frameworks using metal-organic polyhedra as supermolecular building blocks. *Chem. Soc. Rev.*, 38:1400–1417, 2009.

[467] R. Petrenko and J. Meller. Molecular dynamics. March 2010.

[468] Roman Petrenko and Jarosaaw Meller. *Molecular Dynamics*. John Wiley & Sons, Ltd, 2001.

[469] PhilipKim, Li Shi, Arun Majumdar, and Paul L. McEuen. Mesoscopic thermal transport and energy dissipation in carbon nanotubes. *Physica B*, 323:67–70, 2002.

[470] Simon R. Phillpot, Patrick K. Schelling, and Pawel Keblinski. Interfacial thermal conductivity: Insights from atomic level simulation. *Journal of Materials Science*, 40:3143–3148, 2004.

[471] Francesco Piazza and Yves-Henri Sanejouand. Long-range energy transfer in proteins. *Physical Biology*, 6(4):046014, 2009.

[472] L. A. Pinnaduwage, V. Boiadjiev, J. E. Hawk, and T. Thundat. Sensetive detection of plastic explosives with self-assembled monolayer-coated microcantilevers. *Applied Physics Letters*, 83(7):1471–3, 2003.

[473] Steve Plimpton. Fast parallel algorithms for short-range molecular dynamics. *Journal of Computaional Physics*, 117:1–19, 1995. `http://lammps.sandia.gov`.

[474] Steve Plimpton. Fast parallel algorithms for short-range molecular dynamics. *Journal of Computational Physics*, 117(1):1 – 19, 1995.

[475] Steve Plimpton. Fast parallel algorithms for short-range molecular dynamics. *Journal of Computational Physics*, 117(1):1 – 19, 1995.

[476] M. Poggio, C. L. Degen, H. J. Mamin, and D. Rugar. Feedback cooling of a cantilever's fundamental mode below 5 mk. *Physical Review Letters*, 99:017201, 2007.

[477] I. Pomeranchuk. On the thermal conductivity of dielectrics. *Physical Review*, 60:820, 1941.

[478] K. Poppa. *Theory and application of vector space similarity measures in computer assisted conceptual design* . Dissertation, Oregon State University, 2011.

[479] Dirk Porezag, Th Frauenheim, Th Köhler, Gotthard Seifert, and R Kaschner. Construction of tight-binding-like potentials on the basis of density-functional theory: Application to carbon. *Physical Review B*, 51(19):12947, 1995.

[480] Bed Poudel, Qing Hao, Yi Ma, Yucheng Lan, Austin Minnich, Bo Yu, Xiao Yan, Dezhi Wang, Andrew Muto, Daryoosh Vashaee, Xiaoyuan Chen, Junming Liu, Mildred S. Dresselhaus, Gang Chen, and Zhifeng Ren. High-thermoelectric performance of nanostructured bismuth antimony telluride bulk alloys. *Science*, 320:634–638, 2008.

[481] Zachary D. Pozun and Graeme Henkelman. Hybrid density functional theory band structure engineering in hematite. *The Journal of Chemical Physics*, 134(22):224706–224706–9, June 2011.

[482] Matej Praprotnik and Dušanka Janežič. Molecular dynamics integration meets standard theory of molecular vibrations. *Journal of Chemical Information and Modeling*, 45(6):1571–1579, 2005.

[483] S. Pugh. *Total Design*. Addison-Wesley, New York, NY, 1991.

[484] S. T. Purcell, P. Vincent, C. Journet, and Vu Thien Binh. Tuning of mechanical resonances by electric field pulling. *Physical Review Letters*, 89:276103, 2002.

[485] Justin Purewal, Dongan Liu, Andrea Sudik, Mike Veenstra, Jun Yang, Stefan Maurer, Ulrich Meuller, and Donald J. Siegel. Improved hydrogen storage and thermal conductivity in high-density mof-5 composites. *The Journal of Physical Chemistry C*, 116(38):20199–20212, 2012.

[486] Justin Purewal, Dongan Liu, Andrea Sudik, Mike Veenstra, Jun Yang, Stefan Maurer, Ulrich Müller, and Donald J. Siegel. Improved hydrogen storage and thermal conductivity in high-density mof-5 composites. *The Journal of Physical Chemistry C*, 116(38):20199–20212, Sep 2012.

[487] Justin Purewal, Dongan Liu, Andrea Sudik, Mike Veenstra, Jun Yang, Stefan Maurer, Ulrich Muller, and Donald J Siegel. Improved hydrogen storage and thermal conductivity in high-density mof-5 composites. *The Journal of Physical Chemistry C*, 116(38):20199–20212, 2012.

[488] Lena Qian and John S. Gero. Function-behavior-structure paths and their role in analogy-based design. *Artificial Intelligence for Engineering Design, Analysis and Manufacturing: AIEDAM*, 10(4):289–312, 1996.

[489] Wen Qian, Rui Hao, Jian Zhou, Micah Eastman, Beth A. Manhat, Qiang Sun, Andrea M. Goforth, and Jun Jiao. Exfoliated graphene-supported pt and pt-based alloys as electrocatalysts for direct methanol fuel cells. *Carbon*, 52:595–604, February 2013.

[490] S.F. Qin, D.K. Wright, and I.N. Jordano. From On-line Sketching to 2D and 3D Geometry: A System Based on Fuzzy Knowledge. *Computer-Aided Design*, 32(14):851–866, 2000.

[491] Lirong Qiu. A multi-agent system supporting creativity in conceptual design. In *Proceedings of the 8th International Conference on Computer Supported Cooperative Work in Design*, 2004.

[492] A. Qureshi, J. T. Murphy, B. Kuchinsky, C. C. Seepersad, and K. L. Wood. Principles of product flexibility. In *Proceedings of the ASME Design Engineering Technical Conferences*, 2006.

[493] Gordon R. Chromia evaporation in advanced ultra-supercritical steam boilers and turbines. In Juan Carlos Moreno Pirajn, editor, *Thermodynamics - Kinetics of Dynamic Systems*. InTech, September 2011.

[494] Jeffrey J. Rack. Electron transfer triggered sulfoxide isomerization in ruthenium and osmium complexes. *Coordination Chemistry Reviews*, 253(1???2):78–85, January 2009.

[495] Rajamani Raghunathan, P. Alex Greaney, and Jeffrey C. Grossman. Phonostat: Thermostatting phonons in molecular dynamics simulations. *The Journal of Chemical Physics*, 134(21):214117, 2011.

[496] H. Raiffa. *Decision Analysis: Introductory Lectures on Choices under Uncertainty*. Addison-Wesley, Reading, 1968.

[497] Martin R. Ramirez. Meaningful theory of creativity: design as knowledge: implications for engineering design. In *Proceedings of the 1994 24th Annual Conference on Frontiers in Education*, 1994.

[498] Vijaya & Rangarajan and Gopala Rangarajan. *Materials Science*. Tata McGraw-Hill Education, February 2004.

[499] D.C. Rapaport. *The Art of Molecular Dynamics Simulation*. Cambridge University Press, 2 edition, April 2004.

[500] A. K. Rappe, C. J. Casewit, K. S. Colwell, W. A. Goddard III, and W. M. Skiff. Uff, a full periodic table force field for molecular mechanics and molecular dynamics simulations. *Journal of the American Chemical Society*, 114(25):10024–10035, 1992.

[501] J. W. Rayleigh. *The Theory of Sound*. Dover Publications, New York, 1945. p. 204.

[502] Ute F. R??hrig, Leonardo Guidoni, and Ursula Rothlisberger. Solvent and protein effects on the structure and dynamics of the rhodopsin chromophore. *ChemPhysChem*, 6(9):1836???1847, 2005.

[503] Graeme Ritchie. Some empirical criteria for attributing creativity to a computer program. *Minds and Machines*, 17(1):67–99, 2007.

[504] Brett Robertson and David Radcliffe. The role of software tools in influencing creative problem solving in engineering design and education. In *Proceedings of the ASME Design Engineering Technical Conferences*, 2006.

[505] N. Patransky Robson, J. M. McCarthy, and I. Y. Tumer. The algebraic synthesis of a spatial TS chain for a prescribed acceleration task. 2006. In Review.

[506] G. Rollmann, A. Rohrbach, P. Entel, and J. Hafner. First-principles calculation of the structure and magnetic phases of hematite. *Physical Review B*, 69(16):165107, April 2004.

[507] Nathaniel L. Rosi, Juergen Eckert, Mohamed Eddaoudi, David T. Vodak, Jaheon Kim, Michael O'Keeffe, and Omar M. Yaghi. Hydrogen storage in microporous metal-organic frameworks. *Science*, 300(5622):1127–1129, May 2003. PMID: 12750515.

[508] Nathaniel L Rosi, Juergen Eckert, Mohamed Eddaoudi, David T Vodak, Jaheon Kim, Michael O'Keeffe, and Omar M Yaghi. Hydrogen storage in microporous metal-organic frameworks. *Science*, 300(5622):1127–1129, 2003.

[509] Jesse L. C. Rowsell, Andrew R. Millward, Kyo Sung Park, and Omar M. Yaghi. Hydrogen sorption in functionalized Metal-Organic frameworks. *Journal of the American Chemical Society*, 126(18):5666–5667, May 2004.

[510] Jesse L.C. Rowsell and Omar M. Yaghi. Metal-organic frameworks: a new class of porous materials. *Microporous and Mesoporous Materials*, 73(1-2):3–14, August 2004.

[511] Chris Rutherglen and Peter Burke. Carbon nanotube radio. *Nano Letters*, 7:3296–3299, 2007.

[512] D. G. Saari. *Decisions and elections: explaining the unexpected*. Cambridge University Press, New York, NY, 2001.

[513] Hector Sabelli. Arrangement, a measure of nonrandom complexity. *Systems Analysis Modelling Simulation*, 42(3):395–403, 2002.

[514] Michal Sabo, Antje Henschel, Heidrun Frede, Elias Klemm, and Stefan Kaskel. Solution infiltration of palladium into MOF-5: synthesis, physisorption and catalytic properties. *Journal of Materials Chemistry*, 17(36):3827–3832, September 2007.

[515] A.E.K. Sahraoui, M. Romdhani, A. Jeffroy, and A.A. Jerraya. Co-specification for co-design in the development of avionics systems. *Control Engineering Practice*, 4(6):871–876, 1996.

[516] Fabrice Salles, Aziz Ghoufi, Guillaume Maurin, Robert G. Bell, Caroline Mellot-Draznieks, and Gerard Ferey. Molecular dynamics simulations of breathing MOFs: structural transformations of MIL-53(Cr) upon thermal activation and CO2 adsorption. *Angewandte Chemie*, 120(44):8615–8619, 2008.

[517] Fabrice Salles, Aziz Ghoufi, Guillaume Maurin, Robert G. Bell, Caroline Mellot-Draznieks, and Gérard Férey. Molecular dynamics simulations of breathing mofs: Structural transformations of mil-53(cr) upon thermal activation and co2 adsorption. *Angewandte Chemie International Edition*, 47(44):8487–8491, 2008.

[518] Fabrice Salles, Aziz Ghoufi, Guillaume Maurin, Robert???G. Bell, Caroline Mellot-Draznieks, and G??rard F??rey. Molecular dynamics simulations of breathing MOFs: structural transformations of MIL-53(Cr) upon thermal activation and CO $_2$ adsorption. *Angewandte Chemie International Edition*, 47(44):8487–8491, October 2008.

[519] Fabrice Salles, Daniil I. Kolokolov, Herv?? Jobic, Guillaume Maurin, Philip L. Llewellyn, Thomas Devic, Christian Serre, and G??rard Ferey. Adsorption and diffusion of h2 in the MOF type systems MIL-47(V) and MIL-53(Cr): a combination of microcalorimetry and QENS experiments with molecular simulations. *The Journal of Physical Chemistry C*, 113(18):7802–7812, May 2009.

[520] Venkata Rajesh Saranam and P. Alex Greaney. Surprising behavior during dissipation and collision of flexural waves in carbon nanotubes. *Journal or Applied Physics D*, page Accepted, 2013.

[521] Rob Saunders and John S. Gero. How to Study Artificial Creativity. In *Proceedings of the Fourth Creativity and Cognition Conference*, pages 80–87, 2002.

[522] Vera Sazonova, Yuval Yalsh, Hande Üstünel, David Roundy, Tomás A. Arlas, and Paul McEuen. A tunable carbon nanotube electromechanical oscillator. *Nature*, 431:284–287, 2004.

[523] Marco Schade and Peter Hamm. Vibrational energy transport in the presence of intrasite vibrational energy redistribution. *The Journal of Chemical Physics*, 131(4):044511, 2009.

[524] Patrick K. Schelling, Simon R. Phillpot, and Pawel Keblinski. Comparison of atomic-level simulation methods for computing thermal conductivity. *Physical Review B*, 65(14):144306, April 2002.

[525] A. Schliesser, P. Del'Haye, N. Hooshi, K. J. Vahala, and T. J. Kippenberg. Radiation cooling of a micromechanical oscillator using dynamical backaction. *Physical Review Letters*, 97:243905, 2006.

[526] Burkhard Schmidt. Quantum dynamics, May 2011.

[527] L. Schmidt and J. Cagan. Recursive Annealing: A Computational Model for Machine Design. *Research in Engineering Design*, 7(2):102–105, 1995.

[528] L. Schmidt and J. Cagan. GGREADA: A Graph Grammar-Based Machine Design Algorithm. *Research in Engineering Design*, 9(4):195–213, 1997.

[529] Andreas Schneemann, Volodymyr Bon, Inke Schwedler, Irena Senkovska, Stefan Kaskel, and Roland A Fischer. Flexible metal–organic frameworks. *Chemical Society Reviews*, 43(16):6062–6096, 2014.

[530] Thorsten Schneir and John S. Gero. Learning representations for creative design using evolution. *Artificial Intelligence for Engineering Design, Analysis and Manufacturing: AIEDAM*, 10(2):175–177, 1996.

[531] K. Schwab, E.A. Henriksen, J.M. Worlock, and M.L. Roukes. Measurement of the quantum of thermal conductance. *Nature*, 404:974–977, 2000.

[532] Julian Sculley, Daqiang Yuan, and Hong-Cai Zhou. The current status of hydrogen storage in metal-organic frameworks-updated. *Energy Environ. Sci.*, 4:2721–2735, 2011.

[533] Julian Sculley, Daqiang Yuan, and Hong-Cai Zhou. The current status of hydrogen storage in metal-organic frameworks-updated. *Energy Environ. Sci.*, 4:2721–2735, 2011.

[534] G Seifert, D Porezag, and Th Frauenheim. Calculations of molecules, clusters, and solids with a simplified lcao-dft-lda scheme. *International journal of quantum chemistry*, 58(2):185–192, 1996.

[535] D. P. Sellan, E. S. Landry, J. E. Turney, A. J. H. McGaughey, and C. H. Amon. Size effects in molecular dynamics thermal conductivity predictions. *Physical Review B*, 81(21):214305, June 2010.

[536] Irena Senkovska, Frank Hoffmann, Michael Fröba, Juergen Getzschmann, Winfried Böhlmann, and Stefan Kaskel. New highly porous aluminium based metal-organic frameworks: Al(oh)(ndc) (ndc = 2,6-naphthalene dicarboxylate) and al(oh)(bpdc) (bpdc = 4,4'-biphenyl dicarboxylate). *Microporous and Mesoporous Materials*, 122:93 – 98, 2009.

[537] C. Seoánez, F. Guinea, and A. H. Castro Neto. Dissipation on graphene and nanotube resonators. *Physical Review B*, 76:125427, 2007.

[538] D. Serrano and D. Gossard. Tools and techniques for conceptual design. *Artificial intelligence in engineering design (Volume I): design representation and models of routine design*, pages 71–116, 1992.

[539] Christian Serre, Franck Millange, Christelle Thouvenot, Marc Noguès, Gérard Marsolier, Daniel Louër, and Gérard Férey. Very large breathing effect in the

first nanoporous chromium (iii)-based solids: Mil-53 or criii (oh){O2C-C6H4-CO2}{HO2C-C6H4-CO2H} x h2o y. *Journal of the American Chemical Society*, 124(45):13519–13526, 2002.

[540] Elaine Seymour. *Talking About Leaving: Why Undergraduates Leave The Sciences*. Westview Press, 2000.

[541] J. Shah and A. Bhatnagar. Group Technology Classification from Feature Based Geometric Models. *Manufacturing Review*, 2(3):204–213, 1989.

[542] J. Shah, N. Vargas-Hernandez, and S. Smith. Metrics for Measuring Ideation Effectiveness. *Design Studies*, 24:111–134, 2003.

[543] Offer Shai, Yoram Reich, and Daniel Rubin. Infused creativity: An approach to creative system design. In *Proceedings of the ASME Design Engineering Technical Conferences*, 2005.

[544] S. Shan and G.G. Wang. Space exploration and global optimization for computationally intensive design problems: A rough set based approach. *Structural and Multidisciplinary Optimization*, 28(6):427–441, 2004.

[545] J B Share. Review of drug treatment for down's syndrome persons. *American journal of mental deficiency*, 80(4):388–393, January 1976. PMID: 2011.

[546] David M. Sherman. Electronic structures of iron(III) and manganese(IV) (hydr)oxide minerals: Thermodynamics of photochemical reductive dissolution in aquatic environments. *Geochimica et Cosmochimica Acta*, 69(13):3249–3255, July 2005.

[547] Li Shi, Deyu Li, Choongho Yu, Wanyoung Jang, Dohyung Kim, Zhen Yao, Philip Kim, and Arunava Majumdar. Measuring thermal and thermoelectric properties of one-dimensional nanostructures using a microfabricated device. *Journal of Heat Transfer*, 125:881–888, 2003.

[548] Li Shi, Jianhua Zhou, Philip Kim, Adrian Bachtold, Arun Majumdar, and Paul L. McEuen. Thermal probing of energy dissipation in current-carrying carbon nanotubes. *Journal of Applied Physics*, 105:104306, 2009.

[549] George K. H. Shimizu, Ramanathan Vaidhyanathan, and Jared M. Taylor. Phosphonate and sulfonate metal organic frameworks. *Chem. Soc. Rev.*, 38:1430–1449, 2009.

[550] George K. H. Shimizu, Ramanathan Vaidhyanathan, and Jared M. Taylor. Phosphonate and sulfonate metal organic frameworks. *Chem. Soc. Rev.*, 38:1430–1449, 2009.

[551] T. Shumann, O. L. de Weck, and J. Sobieski. Integrated system-level optimization for concurrent engineering with parametric subsystem modeling. In *Proceedings of the 46th AIAA/ASME/ASCE/AHS/ASC Structures, Structural Dynamics, and Materials Conference*, number AIAA 2005-2199, 2005.

[552] C.D. Shunn, B.P. Paulus, J. Cagan, and K. Wood. Final report from the NSF Innovation and Discovery Workshop: The scientific basis on individual and team innovation and discovery. In *National Science Foundation*, 2006.

[553] J. N. Sidall. *Analytical decision-making in engineering design.* Prentice-Hall, Inc., Englewood Cliffs, NJ, 1972.

[554] A. Siddiqi. *Reconfigurability in Space Systems: Architecting Framework and Case.* Dissertation, MIT, Cambridge, 2006.

[555] M. R. Silver and O. L. de Weck. Time-Expanded Decision Network: A New Framework for Designing Evolvable Complex Systems. In *Proceedings of the 11th AIAA/ISSMO Multidisciplinary Analysis and Optimization Conference*, 2006.

[556] Siang Kok Sim and Alex H. B. Duffy. Knowledge transformers: A link between learning and creativity. *Artificial Intelligence for Engineering Design, Analysis and Manufacturing: AIEDAM*, 18(3):271–279, 2004.

[557] T. W. Simpson. Product Platform Design and Customization: Status and Promise. *Artificial Intelligence for Engineering Design, Analysis and Manufacturing*, 18(1):3–20, 2004.

[558] T. W. Simpson, J. R. A. Maier, and F. Mistree. Product platform design: Method and application. *Research in Engineering Design - Theory, Applications, and Concurrent Engineering*, 13(1):2–22, 2001.

[559] N. L. Skene and M. Bray. *Elements of yacht design.* Sheridan House, Inc., 2001.

[560] Sophia R. Sklan, P. Alex Greaney, and Jeffrey C. Grossman. Sensitivity limit of nanomechanical resonance spectroscopy. *Journal of Applied Physics*, 2013. Under review.

[561] Glen A. Slack. The thermal conductivity of nonmetallic crystals. *Solid State Physics*, 34:1 – 71, 1979.

[562] R J Smith and R G Bryant. Metal substitutions incarbonic anhydrase: a halide ion probe study. *Biochemical and biophysical research communications*, 66(4):1281–1286, October 1975. PMID: 3.

[563] D. K. Sobek. A set-based model of design. *Mechnical Engineering*, 118(7):78–81, 1996.

[564] II Sobek, Duward K. *Principles that Shape Product Development Systems: A Toyota-Chrysler Comparison.* Dissertation, University of Michigan, 1997.

[565] Jose M Soler, Emilio Artacho, Julian D Gale, Alberto Garcea, Javier Junquera, Pablo Ordejen, and Daniel Senchez-Portal. The siesta method for ab initio order- n materials simulation. *Journal of Physics: Condensed Matter*, 14(11):2745, 2002.

[566] José M Soler, Emilio Artacho, Julian D Gale, Alberto García, Javier Junquera, Pablo Ordejón, and Daniel Sánchez-Portal. The siesta method for ab initio order-n materials simulation. *Journal of Physics: Condensed Matter*, 14(11):2745, 2002.

[567] Ricardo Sosa and John S. Gero. A computational study of creativity in design: The role of society. *Artificial Intelligence for Engineering Design, Analysis and Manufacturing: AIEDAM*, 19(4):229–244, 2005.

[568] O Stamm, U Latscha, P Janecek, and A Campana. Development of a special electrode for continuous subcutaneous pH measurement in the infant scalp. *American journal of obstetrics and gynecology*, 124(2):193–195, January 1976. PMID: 2012.

[569] G. A. Steele, A. K. Huttel, B. Witkamp, M. Poot, H. B. Meerwaldt, L. P. Kouwenhoven, and H. S. J. van der Zant. Strong Coupling Between Single-Electron Tunneling and Nanomechanical Motion. *Science*, 325(5944):1103–1107, 2009.

[570] J M Stein. The effect of adrenaline and of alpha- and beta-adrenergic blocking agents on ATP concentration and on incorporation of 32Pi into ATP in rat fat cells. *Biochemical pharmacology*, 24(18):1659–1662, September 1975. PMID: 12.

[571] Mathias Steiner, Marcus Freitag, Vasili Perebeinos, James C. Tsang, Joshua P. Small, Megumi Kinoshita, Dongning Yuan, Jie Liu, and Phaedon Avouris. Phonon populations and electrical power dissipation in carbon nanotube transistors. *Nature Nanotechnology*, 4:320–323, 2009.

[572] Gerhard Stock. Classical simulation of quantum energy flow in biomolecules. *Phys. Rev. Lett.*, 102(11):118301, Mar 2009.

[573] R. B. Stone, I. Y. Tumer, and M. E. Stock. Linking product functionality to historical failures to improve failure analysis in design. *Research in Engineering Design*, 16(2):96–108, 2006.

[574] R. B. Stone, I. Y. Tumer, and M. VanWie. The Function Failure Design Method. *Journal of Mechanical Design*, 14:25–33, 2005.

[575] R. B. Stone and K. L. Wood. Development of a functional basis for design. *Journal of Mechanical Design*, 122(4):359–370, 2000.

[576] Steven J. Stuart, Alan B. Tutein, and Judith A. Harrison. A reactive potential for hydrocarbons with intermolecular interactions. *Journal of Chemical Physics*, 112:6472–86, 2000.

[577] M. Sturgill, E. Cohen, and R.F. Riesenfel. Feature-Based 3-D Sketching for Early Stage Design. In *Proceedings of the ASME Design Engineering Technical Conferences and Computers in Engineering Conference*, 1995.

[578] Masanori Sugiomoto, Koichi Hori, and Setsuo Ohsuga. Method of assisting creative design processes. *Languages of Design*, 1(4):357–367, 1993.

[579] Daofeng Sun, Yanxiong Ke, David J Collins, Gary A Lorigan, and Hong-Cai Zhou. Construction of robust open metal-organic frameworks with chiral channels and permanent porosity. *Inorganic chemistry*, 46(7):2725–2734, April 2007. PMID: 17348646.

[580] Xiuquan Sun, Collin D. Wick, Praveen. K. Thallapally, B. Peter McGrail, and Liem X. Dang. Computational study of hydrocarbon adsorption in metal-organic framework ni2(dhtp). *The Journal of Physical Chemistry B*, 115(12):2842–2849, 2011. PMID: 21384829.

[581] Xiuquan Sun, Collin D. Wick, Praveen. K. Thallapally, B. Peter McGrail, and Liem X. Dang. Computational study of hydrocarbon adsorption in metal-organic framework ni2(dhtp). *The Journal of Physical Chemistry B*, 115(12):2842–2849, 2011.

[582] V.V. Sushkov, N.J.I. Mars, and P.M. Wognum. Introduction to TIPS: A theory for creative design. *Artificial Intelligence for Engineering*, 9(3):177–189, 1995.

[583] TAMU. Making an alternate fuel usable in cars: Researcher tackles natural gas storage, April 2013.

[584] R. V. Tappeta and J. E. Renaud. Multiobjective collaborative optimization. *Journal of Mechanical Design*, 119(3):403–411, 1997.

[585] S. N. Taraskin and S. R. Elliott. Ioffe-regel crossover for plane-wave vibrational excitations in vitreous silica. *Phys. Rev. B*, 61(18):12031–12037, May 2000.

[586] Praveen K Thallapally, Carlos A Fernandez, Radha Kishan Motkuri, Satish K Nune, Jun Liu, and Charles HF Peden. Micro and mesoporous metal–organic frameworks for catalysis applications. *Dalton Transactions*, 39(7):1692–1694, 2010.

[587] Praveen K Thallapally, Jian Tian, Motkuri Radha Kishan, Carlos A Fernandez, Scott J Dalgarno, Peter B McGrail, John E Warren, and Jerry L Atwood. Flexible (breathing) interpenetrated metal-organic frameworks for CO2 separation applications. *Journal of the American Chemical Society*, 130(50):16842–16843, December 2008. PMID: 19053477.

[588] Praveen K. Thallapally, Jian Tian, Motkuri Radha Kishan, Carlos A. Fernandez, Scott J. Dalgarno, Peter B. McGrail, John E. Warren, and Jerry L. Atwood. Flexible (breathing) interpenetrated metal-organic frameworks for co2 separation applications. *Journal of the American Chemical Society*, 130(50):16842–16843, 2008.

[589] H. J. Thevenot, J. Nanda, and T. W. Simpson. A methodology to support product family redesign using a genetic algorithm and commonality indices. In *Proceedings of the ASME Design Engineering Technical Conferences*, 2005.

[590] G. Thompson and M. Lordan. Review of creativity principles applied to engineering design. In *Proceedings of the Institution of Mechanical Engineers, Part B: Journal of Engineering Manufacture*, 1999.

[591] Anna C. Thornton. Use of constraint-based design knowledge to improve the search for feasible designs. *Engineering Applications of Artificial Intelligence*, 9(4):393–402, 1996.

[592] Lukas Thulin and John Guerra. Calculations of strain-modified anatase TiO_{2} band structures. *Physical Review B*, 77(19):195112, May 2008.

[593] D. L. Thurston. A formal method for subjective design evaluation with multiple attributes. *Research in Engineering Design*, 3(2), 1991.

[594] D. L. Thurston. Real and misconceived limitations to decision based design with utility analysis. *Journal of Mechanical Design*, 123(2), 2001.

[595] Murilo L. Tiago, Sohrab Ismail-Beigi, and Steven G. Louie. Photoisomerization of azobenzene from first-principles constrained density-functional calculations. *The Journal of Chemical Physics*, 122(9):094311–094311–7, March 2005.

[596] Chang-Lin Tien. *Microscale Energy Transport (Series in Chemical and Mechanical Engineering)*. CRC Press, 1997.

[597] Atsushi Togo, Fumiyasu Oba, and Isao Tanaka. First-principles calculations of the ferroelastic transition between rutile-type and cacl 2-type sio 2 at high pressures. *Physical Review B*, 78(13):134106, 2008.

[598] Tao Tong, Yang Zhao, Lance Delzeit, Ali Kashani, M. Meyyappan, and Arun Majumdar. Dense vertically aligned multiwalled carbon nanotube arrays as thermal interface materials. *IEEE Transactions on Components and Packing Technologies*, 30:92–100, 2007.

[599] David J. Tranchemontagne, Jose L. Mendoza-Cortes, Michael O'Keeffe, and Omar M. Yaghi. Secondary building units, nets and bonding in the chemistry of metal-organic frameworks. *Chem. Soc. Rev.*, 38:1257–1283, 2009.

[600] David J. Tranchemontagne, Jose L. Mendoza-Cortes, Michael O'Keeffe, and Omar M. Yaghi. Secondary building units, nets and bonding in the chemistry of metal-organic frameworks. *Chem. Soc. Rev.*, 38:1257–1283, 2009.

[601] L. Trigeorgis. Real options: An overview. In L. Trigeorgis, editor, *Real Options in Capital Investment: Models, Strategies, and Applications*. Praeger/Greenwood, Westport, 1995.

[602] Patrick A. Truitt, Jared B. Hertzberg, C. C. Huang, Kamil L. Ekinci, and Keith C. Schwab. Efficient and sensitive capacitive readout of nanomechanical resonator arrays. *Nano Letters*, 7:120–126, 2007.

[603] Kong-Thon Tsen, Shaw-Wei D. Tsen, Q. Fu, Stuart M. Lindsay, Karen Kibler, Bert Jacobs, T-C. Wu, B. Karanam, S. Jagu, Richard B. S. Roden, Chien-Fu Hung andOtto F. Sankey, B. Ramakrishna, and Juliann G. Kiang. Photonic approach to the selective inactivation of viruses with a near-infrared subpicosecond fiber laser. *Journal of Biomedical Optics*, 14:064042–1, 2009.

[604] I. Y. Tumer. Towards ISHM Co-Design: Methods and practices for fault avoidance and management during early phase design. In *Proceedings of the 1st Integrated Systems Health Engineering and Management Forum*, 2005.

[605] I. Y. Tumer and E. M. Huff. On the Effects of Production and Maintenance Variations on Rotating Machinery Component Performance. *Journal of Quality in Maintenance and Engineering*, 8(3):226–238, 2002.

[606] I. Y. Tumer and E. M. Huff. Analysis of Triaxial Vibration Data for Health Monitoring of Helicopter Gearboxes. *Journal of Vibration and Acoustics*, 125(1):120–128, 2003.

[607] I. Y. Tumer and C.S. Smidts. Integrated design and analysis of software-driven hardware systems. *IEEE Transactions on Computers*, In Print., 2010.

[608] I. Y. Tumer and R. B. Stone. Mapping Function to Failure during High-Risk Component Development. *Research in Engineering Design*, 14:25–33, 2003.

[609] Irem Y. Tumer and Carol S. Smidts. Integrated design-stage failure analysis of software-driven hardware systems. *IEEE Transactions on Computers*, 60(8):1072–1084, 2011.

[610] Kazuhiro Uemura, Susumu Kitagawa, Mitsuru Kondo, Kôichi Fukui, Ryo Kitaura, Ho-Chol Chang, and Tadashi Mizutani. Novel flexible frameworks of porous cobalt (ii) coordination polymers that show selective guest adsorption based on the switching of hydrogen-bond pairs of amide groups. *Chemistry-A European Journal*, 8(16):3586–3600, 2002.

[611] D. G. Ullman. *The mechanical design process*. McGraw-Hill, 2003.

[612] D. G. Ullman. *Making robust decisions*. Trafford Publishing, 2006.

[613] K. Ulrich and S. Eppinger. *Product design and development*. McGraw-Hill, 1995.

[614] Naoto Umezawa and Jinhua Ye. Role of complex defects in photocatalytic activities of nitrogen-doped anatase TiO2. *Physical Chemistry Chemical Physics*, 14(17):5924–5934, April 2012.

[615] H. UstUnel, D. Roundy, and T. A. Arias. Modeling a suspended nanotube oscillator. *Nano Letters*, 5:523–526, 2005.

[616] M. Van Wie, C. Bryant, M. Bohm, D. McAdams, and R. Stone. A general model of function-based representations. *Artificial Intelligence in Engineering Design, Analysis and Manufacture*, 19(2):89–111, 2005.

[617] Niels Vandecasteele, Michele Lazzeri, and Francesco Mauri. Boosting electronic transport in carbon nanotubes by isotopic disorder. *Phys. Rev. Lett.*, 102(19):196801, May 2009.

[618] L. Vanduyfhuys, T. Verstraelen, M. Vandichel, M. Waroquier, and V. Van Speybroeck. Ab initio parametrized force field for the flexible metal-organic framework mil-53(al). *Journal of Chemical Theory and Computation*, 8(9):3217–3231, 2012.

[619] L. Vanduyfhuys, T. Verstraelen, M. Vandichel, M. Waroquier, and V. Van Speybroeck. Ab initio parametrized force field for the flexible metalorganic framework mil-53(al). *Journal of Chemical Theory and Computation*, 8(9):3217–3231, 2012.

[620] P.H.G. VanLangen, N.J.E. Wijngaards, and F.M.T. Brazier. Designing creative artificial systems. *Artificial Intelligence for Engineering Design, Analysis and Manufacturing: AIEDAM*, 18:217–225, 2004.

[621] Kirill A. Velizhanin, Chih-Chun Chien, Yonatan Dubi, and Michael Zwolak. Driving denaturation: Nanoscale thermal transport as a probe of dna melting. *Phys. Rev. E*, 83:050906, May 2011.

[622] M. Verma and W.H. Wood. A Function-Based Approach to Design for Manufacturing. In *Proceedings of the ASME Design Engineering Technical Conferences and Computers in Engineering Conference*, 2000.

[623] Willemien Visser. Two functions of analogical reasoning in design: a cognitive-psychology approach. *Design Studies*, 17(4):417–434, 1996.

[624] J. Vocovich, R. B. Stone, F. Liu, and I. Y. Tumer. Early identification of potential software failures using the software function-failure design method. 2007. In review.

[625] Christophe Volkringer, Thierry Loiseau, Nathalie Guillou, Gérard Férey, Erik Elkaïm, and Alexandre Vimont. Xrd and ir structural investigations of a particular breathing effect in the mof-type gallium terephthalate mil-53 (ga). *Dalton Transactions*, (12):2241–2249, 2009.

[626] Sebastian G. Volz and Gang Chen. Molecular-dynamics simulation of thermal conductivity of silicon crystals. *Physical Review B*, 61(4):2651–2656, January 2000.

[627] J. von Neumann and O. Morgenstern. *Theory of games and economic behavior*. Princeton University Press, Princeton, NJ, 1947.

[628] N. S.; Voros, L. Sanchez, A. Alonso, A. N. Birbas, M. Birbas, and A. Jerraya. Hardware/software co-design of complex embedded systems an approach using efficient process models, multiple formalism specification and validation via co-simulation. *Design Automation for Embedded Systems*, 8(1):5–49, 2003.

[629] J. Li W. Cai and S. Yip. Molecular dynamics. *Comprehensive Nuclear Materials*, 1:249–265, 2012.

[630] Bo Wang, Adrien P Côté, Hiroyasu Furukawa, Michael OKeeffe, and Omar M Yaghi. Colossal cages in zeolitic imidazolate frameworks as selective carbon dioxide reservoirs. *Nature*, 453(7192):207–211, 2008.

[631] Shidong Wang, Zhao Wang, Wahyu Setyawan, Natalio Mingo, and Stefano Curtarolo. Assessing the thermoelectric properties of sintered compounds via high-throughput ab-initio calculations. *Physical Review X*, 1(2):021012, November 2011.

[632] Zhenqiang Wang and Seth M. Cohen. Postsynthetic modification of metal-organic frameworks. *Chem. Soc. Rev.*, 38:1315–1329, 2009.

[633] A. Ward. *A Theory of Quantitative Inference Applied to a Mechanical Design Compiler* . Dissertation, Massachusetts Institute of Technology, 1989.

[634] A. Ward, J. K. Liker, J.J. Cristiano, and D. K. Sobek. The second toyota paradox: How delaying decisions can make better cars faster. *Sloan Management Review*, 36(3):43–61, 1995.

[635] A. Ward and W. Seering. Quantitative Inference in a Mechanical Design 'Compiler'. *Journal of Mechanical Design*, 115:29–35, 1993.

[636] T. B. Ward, S. M. Smith, and J. Vaid, editors. *Creative Thought: An Investigation of Conceptual Structures and Processes*. American Psychology Association, Washington, DC, 1997.

[637] Andrew Warr and Eamonn O'Neill. The effect of operational mechanisms on creativity in design. In *Lecture Notes in Computer Science; Proceedings of the 1st International Conference on Advanced Data Mining and Applications*, volume 3585 LNCS, pages 629–642, 2005.

[638] H. J Wassenaar and W. Chen. An approach to decision-based design. In *Proceedings of the ASME Design Engineering Technical Conferences*, pages 21–30, 2001.

[639] H. J. Wassenaar and W. Chen. An Approach to Decision-Based Design with Discrete Choice Analysis for Demand Modeling. *Transactions of the ASME: Journal of Mechanical Design*, 125(3):490–497, 2003.

[640] H. J Wassenaar, W. Chen, J. Cheng, and A. Sudjianto. Enhancing discrete choice demand modeling for decision-based design. *Journal of Mechanical Design*, 127(4):514–523, 2005.

[641] Taku Watanabe, Seda Keskin, Sankar Nair, and David S Sholl. Computational identification of a metal organic framework for high selectivity membrane-based co 2/ch 4 separations: Cu (hfipbb)(h 2 hfipbb) 0.5. *Physical Chemistry Chemical Physics*, 11(48):11389–11394, 2009.

[642] S Waxman and C Schreiber. The purification and characterization of the low molecular weight human folate binding protein using affinity chromatography. *Biochemistry*, 14(25):5422–5428, December 1975. PMID: 1084.

[643] J. Weldon, K. Jensen, and A. Zettl. Nanomechanical radio transmitter. *Physica Status Solidi (B)*, 245:2323–2325, 2008.

[644] Ma??gorzata Wierzbowska, Daniel S??nchez-Portal, and Stefano Sanvito. Different origins of the ferromagnetic order in (Ga,Mn)As and (Ga,Mn)N. *Physical Review B*, 70(23):235209, December 2004.

[645] S. Wilhelms. Function- and constraint-based conceptual design support using easily exchangeable, reusable principle solution elements. *Artificial Intelligence for Engineering Design, Analysis, and Manufacturing*, 19(3):201–219, 2005.

[646] Christopher E Wilmer, Michael Leaf, Chang Yeon Lee, Omar K Farha, Brad G Hauser, Joseph T Hupp, and Randall Q Snurr. Large-scale screening of hypothetical metal–organic frameworks. *Nature Chemistry*, 4(2):83–89, 2012.

[647] Christopher E. Wilmer, Michael Leaf, Chang Yeon Lee, Omar K. Farha, Brad G. Hauser, Joseph T. Hupp, and Randall Q. Snurr. Large-scale screening of hypothetical metal-organic frameworks. *Nature Chemistry*, 4(2):83–89, February 2012.

[648] Benoit Witkamp, Mnno Poot, and Herre S. J. van der Zant. Bending-mode vibration of a suspended nanotube resonator. *Nano Letters*, 6:2904–29–8, 2006.

[649] P. M. Wognum and I. F. C. Smith. Reuse of designs. *Knowledge-Based Systems*, 9(2):79–81, 1996.

[650] Antek G. Wong-Foy, Adam J. Matzger, and Omar M. Yaghi. Exceptional h2 saturation uptake in microporous Metal-Organic frameworks. *Journal of the American Chemical Society*, 128(11):3494–3495, March 2006.

[651] W. H. Wood and A. M. Agogino. Decision based conceptual design: Modeling and navigating heterogeneous design spaces. *Journal of Mechanical Design*, 127(1):2–11, 2005.

[652] W. H. Wood and H. Dong. Generating design alternatives across abstraction levels. In *Decision making in engineering design*, chapter 8, pages 61–72. ASME Press, 2006.

[653] Hsuan-Chung Wu, Yu-Siang Lin, and Syuan-Wei Lin. Mechanisms of visible light photocatalysis in n-doped anatase TiO2 with oxygen vacancies from GGA+U calculations. *International Journal of Photoenergy*, 2013:1–7, 2013.

[654] Hsuan-Chung Wu, Yu-Siang Lin, and Syuan-Wei Lin. Mechanisms of visible light photocatalysis in n-doped anatase TiO_2 with oxygen vacancies from GGA. *International Journal of Photoenergy*, 2013, February 2013.

[655] Hui Wu, Yong Shen Chua, Vaiva Krungleviciute, Madhusudan Tyagi, Ping Chen, Taner Yildirim, and Wei Zhou. Unusual and highly tunable missing-linker defects in zirconium Metal???Organic framework UiO-66 and their important effects on gas adsorption. *Journal of the American Chemical Society*, 135(28):10525–10532, July 2013.

[656] Qin Wu, Benjamin Kaduk, and Troy Van Voorhis. Constrained density functional theory based configuration interaction improves the prediction of reaction barrier heights. *The Journal of Chemical Physics*, 130(3):034109–034109–7, January 2009.

[657] Yabi Wu, M. K. Y. Chan, and G. Ceder. Prediction of semiconductor band edge positions in aqueous environments from first principles. *Physical Review B*, 83(23):235301, June 2011.

[658] Yabi Wu, Predrag Lazic, Geoffroy Hautier, Kristin Persson, and Gerbrand Ceder. First principles high throughput screening of oxynitrides for water-splitting photocatalysts. *Energy & Environmental Science*, 6(1):157–168, December 2012.

[659] Zhigang Wu and R. E. Cohen. More accurate generalized gradient approximation for solids. *Phys. Rev. B*, 73:235116, Jun 2006.

[660] Jian Liu Xi-Sen Wang. A porous covalent porphyrin framework with exceptional uptake capacity of saturated hydrocarbons for oil spill cleanup. *Chemical communications (Cambridge, England)*, 2013.

[661] Zhigang Xiong and Xiu Song Zhao. Nitrogen-doped titanate-anatase Core???Shell nanobelts with exposed {101} anatase facets and enhanced visible light photocatalytic activity. *Journal of the American Chemical Society*, 134(13):5754–5757, April 2012.

[662] C. Xu, J. Yang, M. Veenstra, A. Sudik, J.J. Purewal, Yang Ming, B.J. Hardy, J. Warner, S. Maurer, U. M??eller, and Donald J. Siegel. Hydrogen permeation and diffusion in densified MOF-5 pellets. *International Journal of Hydrogen Energy*, 38(8):3268–3274, March 2013.

[663] C. Xu, J. Yang, M. Veenstra, A. Sudik, J.J. Purewal, Yang Ming, B.J. Hardy, J. Warner, S. Maurer, U. Meueller, and Donald J. Siegel. Hydrogen permeation and diffusion in densified mof-5 pellets. *International Journal of Hydrogen Energy*, 38(8):3268 – 3274, 2013.

[664] Tian-hua Xu, Chen-lu Song, Yong Liu, and Gao-rong Han. Band structures of TiO2 doped with n, c and b. *Journal of Zhejiang University SCIENCE B*, 7(4):299–303, April 2006.

[665] Zhiping Xu and Markus J. Buehler. Nanoengineering heat transfer performance at carbon nanotube interfaces. *ACS Nano*, 3:2767, 2009.

[666] Zhiping Xu and Markus J. Buehler. Mechanical energy transfer and dissipation in fibrous beta-sheet-rich proteins. *Phys. Rev. E*, 81(6):061910, Jun 2010.

[667] OM Yaghi and Hailian Li. Hydrothermal synthesis of a metal-organic framework containing large rectangular channels. *Journal of the American Chemical Society*, 117(41):10401–10402, 1995.

[668] Omar M. Yaghi, Michael O'Keeffe, Nathan W. Ockwig, Hee K. Chae, Mohamed Eddaoudi, and Jaheon Kim. Reticular synthesis and the design of new materials. *Nature*, 423(6941):705–714, 2003.

[669] Omar M. Yaghi, Michael O'Keeffe, Nathan W. Ockwig, Hee K. Chae, Mohamed Eddaoudi, and Jaheon Kim. Reticular synthesis and the design of new materials. *Nature*, 423(6941):705–714, June 2003.

[670] Omar M Yaghi, Michael O'Keeffe, Nathan W Ockwig, Hee K Chae, Mohamed Eddaoudi, and Jaheon Kim. Reticular synthesis and the design of new materials. *Nature*, 423(6941):705–714, 2003.

[671] Yasuhiro Yamamoto and Kumiyo Nakakoji. Interaction design of tools for fostering creativity in the early stages of information design. *International Journal of Human Computer Studies*, 63(4-5):513–535, 2005.

[672] Yong Yan, Xiang Lin, Lin X, Alexander J Blake, Anne Dailly, Neil R Champness, Peter Hubberstey, and Martin Schroder. Exceptionally high h2 storage by a metal-organic polyhedral framework. *Chemical communications*, 7:1025–7, 2009.

[673] Yong Yan, Xiang Lin, Sihai Yang, Alexander J. Blake, Anne Dailly, Neil R. Champness, Peter Hubberstey, and Martin Schr??der. Exceptionally high h2 storage by a metal???organic polyhedral framework. *Chemical Communications*, (9):1025, 2009.

[674] Yong Yan, Xiang Lin, Sihai Yang, Alexander J. Blake, Anne Dailly, Neil R. Champness, Peter Hubberstey, and Martin Schr??der. Exceptionally high h2 storage by a metal???organic polyhedral framework. *Chemical Communications*, (9):1025–1027, 2009.

[675] Yong Yan, Xiang Lin, Sihai Yang, Alexander J. Blake, Anne Dailly, Neil R. Champness, Peter Hubberstey, and Martin Schröder. Exceptionally high H_2 storage by a metal-organic polyhedral framework. *Chemical Communications*, (9):1025, 2009.

[676] Chi Yang, Ushasree Kaipa, Qian Zhang Mather, Xiaoping Wang, Vladimir Nesterov, Augustin F. Venero, and Mohammad A. Omary. Fluorous metal-organic frameworks with superior adsorption and hydrophobic properties toward oil spill cleanup and hydrocarbon storage. *Journal of the American Chemical Society*, 133(45):18094–18097, 2011.

[677] Shaofeng Yang, John Adjaye, William C. McCaffrey, and Alan E. Nelson. Density-functional theory (DFT) study of arsenic poisoning of NiMoS. *Journal of Molecular Catalysis A: Chemical*, 321(1-2):83–91, April 2010.

[678] Y. T. Yang, C. Callegari, X. L. Feng, K. L. Ekinci, and M. L. Roukes. Zeptogram-scale nanomechanical mass sensing. *Nano Letters*, 6(4):583–586, 2006.

[679] Zhen Yao, Charles L. Kane, and Cees Dekker. High-field electrical transport in single-wall carbon nanotubes. *Phys. Rev. Lett.*, 84(13):2941–2944, Mar 2000.

[680] Wan-Jian Yin, Shiyou Chen, Ji-Hui Yang, Xin-Gao Gong, Yanfa Yan, and Su-Huai Wei. Effective band gap narrowing of anatase TiO2 by strain along a soft crystal direction. *Applied Physics Letters*, 96(22):221901–221901–3, June 2010.

[681] Minyoung Yoon, Kyungwon Suh, Srinivasan Natarajan, and Kimoon Kim. Proton conduction in metal–organic frameworks and related modularly built porous solids. *Angewandte Chemie International Edition*, 52(10):2688–2700, 2013.

[682] Pascal G Yot, Zoubeyr Boudene, Jasmine Macia, Dominique Granier, Louis Vanduyfhuys, Toon Verstraelen, Veronique Van Speybroeck, Thomas Devic, Christian Serre, Gérard Férey, et al. Metal–organic frameworks as potential shock absorbers: the case of the highly flexible mil-53 (al). *Chemical Communications*, 50(67):9462–9464, 2014.

[683] Choongho Yu, Li Shi, Zhen Yao, Deyu Li, and Arunava Majumdar. Thermal conductance and thermopower of an individual single-wall carbon nanotube. *Nano Letters*, 5, 2005.

[684] Liping Yu, Robert S. Kokenyesi, Douglas A. Keszler, and Alex Zunger. Inverse design of high absorption thin-film photovoltaic materials. *Advanced Energy Materials*, 3(1):43–48, January 2013.

[685] Xin Yu and David M. Leitner. Vibrational energy transfer and heat conduction in a protein. *The Journal of Physical Chemistry B*, 107:1698–1707, 2003.

[686] Jinsong Zhang, Timothy S. Fisher, P. Veeraraghavan Ramachandran, Jay P. Gore, and Issam Mudawar. A review of heat transfer issues in hydrogen storage technologies. *Journal of Heat Transfer*, 127(12):1391–1399, 2005.

[687] Jinsong Zhang, Timothy S. Fisher, P. Veeraraghavan Ramachandran, Jay P. Gore, and Issam Mudawar. A review of heat transfer issues in hydrogen storage technologies. *Journal of Heat Transfer*, 127(12):1391, 2005.

[688] Jinsong Zhang, Timothy S Fisher, P Veeraraghavan Ramachandran, Jay P Gore, and Issam Mudawar. A review of heat transfer issues in hydrogen storage technologies. *Journal of Heat Transfer*, 127(12):1391–1399, 2005.

[689] Zhijuan Zhang, Yonggang Zhao, Qihan Gong, Zhong Li, and Jing Li. Mofs for co2 capture and separation from flue gas mixtures: the effect of multifunctional sites on their adsorption capacity and selectivity. *Chem. Commun.*, 49:653–661, 2013.

[690] Zhijuan Zhang, Yonggang Zhao, Qihan Gong, Zhong Li, and Jing Li. Mofs for co2 capture and separation from flue gas mixtures: the effect of multifunctional sites on their adsorption capacity and selectivity. *Chem. Commun.*, 49:653–661, 2013.

[691] Zongyan Zhao and Qingju Liu. Mechanism of higher photocatalytic activity of anatase TiO $_2$ doped with nitrogen under visible-light irradiation from density functional theory calculation. *Journal of Physics D: Applied Physics*, 41(2):025105, January 2008.

[692] Zongyan Zhao and Qingju Liu. Mechanism of higher photocatalytic activity of anatase TiO2 doped with nitrogen under visible-light irradiation from density functional theory calculation. *Journal of Physics D: Applied Physics*, 41(2):025105, January 2008.

[693] Hongliang Zhong and Jennifer R. Lukes. Interfacial thermal resistance between carbon nanotubes: Molecular dynamics simulations and analytical thermal modeling. *Phys. Rev. B*, 74(12):125403, Sep 2006.

[694] Wei Zhou, Hui Wu, Michael R. Hartman, and Taner Yildirim. Hydrogen and methane adsorption in Metal-Organic frameworks: A high-pressure volumetric study. *The Journal of Physical Chemistry C*, 111(44):16131–16137, November 2007.